Automatic GPS-Based Intra-Row Weed Control System for Transplanted Row Crops

By

HAO SUN
B.S. (University of California, Davis) 2006
THESIS

Submitted in partial satisfaction of the requirements for the degree of

MASTER OF SCIENCE

in

Biological Systems Engineering

in the

OFFICE OF GRADUATE STUDIES

of the

UNIVERSITY OF CALIFORNIA

DAVIS

Approved:

---

David Slaughter, Chair

---

Shrinivasa Upadhyaya

---

Fadi Fathallah

Committee in Charge

2012





ProQuest LLC.
789 East Eisenhower Parkway
P.O. Box 1346
Ann Arbor, MI 48106 - 1346

**Table of Contents:**

## Abstract

An efficient means of weed control poses one of the greatest challenges to agricultural crop production today. The proliferation of GPS technologies has made it possible to develop automated weeding systems that utilize autoguidance, as well as a means to differentiate between crops and weeds. The aim of this study was to utilize an autoguidance system equipped with RTK GPS to map tomato transplants during planting, and subsequently remove weeds based on that plant map. In addition, the accuracy of plant map created would be compared using two different RTK GPS systems (one mounted directly on the planter and other that is a part of the tractor autoguidance system) and two additional systems one of which involved measuring the planting wheel angular position and the other utilized a light beam to detect plant. The weeding efficiency based on this plant map would also be evaluated. Close examination of the results showed that plant map creation using the planting wheel angular position had greater accuracy than the light beam sensor method. When the plant map created using transplanter GPS data along with plant detection using planting wheel angular position was compared to the actual plant location using a range pole, the average deviation between the plant map and actual location was 3.0 cm in the Easting direction, and 1.2 cm the Northing direction. However, when the tractor GPS was tested in place of the transplanter GPS, the error increased to 2.7 cm in the Northing direction and 4.1 cm in the Easting direction. Of the 503 plants detected, only 23 were killed by the knives, resulting in a survival rate of 95.4%. These promising data suggest that an automated weed removal system employing RTK GPS could be effective in weed control.

## Acknowledgements

This project has been a long and arduous ordeal, through which I have gained considerable knowledge. First and foremost, I would like to thank Professor Fadi Fathallah for inspiring me to continue my education at Davis. He has always been there to support me through my educational journey, from the very roots of my undergraduate career. Secondly, I would like to thank Professor Shrini Upadhyaya for providing guidance on this project - particularly regarding the GPS system and electronics. From the lab, I would like to thank Chris Gliever for his mentoring regarding the electrical aspects of the project. I would also like to thank Manuel Perez for his expertise on RTK GPS systems, and for his work alongside me on this challenging project. Finally, this project would not be possible without Burt Vannucci – due to his extensive knowledge of farm equipment, and ability to make anything from scratch. Thanks to his expertise, we were able to build the system from the ground up beam by beam, and bolt by bolt. Furthermore, Burt taught me how to operate nearly all of the tools in a machine shop - including welding and many aspects of mechanical design.

I have always believed I had great potential. Since the very first day I arrived at UC Davis during the Fall of 2001, Professor David Slaughter was there challenging me, and pushing me to limits I never knew I could reach. From AutoCAD in EBS 1, test reports in EBS 75 to Sensors and Controls in EBS 165, the knowledge I gained in those classes remain some of the most valuable things I've learned in college – and still apply today. I was fortunate enough to be his assistant in teaching ESB 165 - a class widely regarded as the most challenging of the entire undergraduate curriculum. Through his guidance, I obtained a deep understanding of the material, and even the skill to teach it to

others. I was fortunate enough to have the opportunity to work with Dave on the GPS Weeder project. Dave had a vision to use RTK GPS to remove weeds automatically. As a result, we developed a fully functional prototype from the ground up in less than one year. Nothing can express the sheer joy I felt when I saw our system travel down the row, and accurately opening the knives around each tomato transplant. When I complete my masters at UC Davis, it will be the greatest accomplishment in my life thus far; finishing my undergraduate degree at the top of my class comes nowhere close in comparison. When I listen to friends and coworkers talk about what they did to receive their Masters, I can't help but think that with the amount of work I put into this degree -I could easily have done their program three times over. Through this project, I applied everything I learned in my classes to develop an electro-mechanical system that was successful in proving the feasibility of automated weeding. All in all, I know I can look back on this degree and smile with the pride that comes with accomplishment.

Lastly, I would like to thank my parents for being with me every step of the way. Through their efforts in my youth, I was provided with educational opportunities that most people did not have. While we could have easily lived comfortably in a big house, they compromised with small condominium - so I could attend the best schools. They always believed in my potential, but took care to never let me be complacent. During my first quarter at UC Davis, I remember coming home proud that I had just received 2 A's and an A+. My father's reaction was, "You did ok, why didn't you get all A+'s." Regardless of my 4.0 GPA streak in the next four quarters, they always told me I could do better. I would not have had the drive to finish what I started without their love and support.

# Introduction and Background

## Significance of Weed Control

Weed control constitutes one of the biggest challenges to agricultural crop production today as it affects crop production and ultimately profit. In a recent review of weed control systems Slaughter et al. (2008) documented several studies showing how the presence of weeds can significantly reduce crop yields. Monaco et al. (1981) investigated the effect of Jimsonweed (Datura stramonium L.), tall morning glory (Ipomoea L.), common cocklebur (Xanthium strumarium L.), and large crabgrass (Digitaria sanguinalis (L.) Scop.) on tomato yield over two consecutive years. During the first year, direct-seeded tomato production decreased by 71%, 67%, 48% and 48% when Jimsonweed (Datura stramonium L.), tall morning glory (Ipomoea L.), common cocklebur (Xanthium strumarium L.), and large crabgrass (Digitaria sanguinalis (L.) Scop.) were respectively introduced in the row at a density of 11 weeds per square meter. At higher weed densities, yield was reduced by 96%, 99%, 90% and 98% respectively. Roberts et al. (1977) proposed that competition for nutrients, water and light by weed species adversely affect crop yields and showed that the season-long competition resulted in the complete loss of marketable lettuce in England. Lanine and Le Strange (1991) reported that following season long weed competition, lettuce yields in California were reduced by over 50%. The study further suggested that two weeks of weed free conditions needed to be maintained for cucumber, lettuce and cauliflower in order to achieve full yield potential. Shrefler et al. (1996) and Hodgson (1968) further added evidence that the presence of weeds reduced both lettuce and wheat production

respectively. Clearly, the effects of high weed concentrations can result in severe profit losses for farmers.

**Considerations for Weeding Research**

Significant research has been done in an effort to minimize weed concentrations, while maximizing the growth and health of crop plants. When considering weed removal methods, one must first define the region in which weeding occurs. Weeds can emerge within a crop field from three areas: (i) the area between the rows (inter-row area), (ii) the area between the crop plants within the rows (intra-row area), and (iii) the area close to and around the crop plants (close-to-crop area) (Norremark et al. 2007). Ideally, weeds need to be removed in all three areas - but in practice only the inter-row and intra-row areas are targeted to avoid damage to the crop. Automated inter-row weed control has been implemented using row-crop cultivators that randomly kill any plant matter between rows (Kepner et al. 1978). Melander (2006) describes inter-row weeding carried out with rolling cultivators and PTO-driven cultivators. Automated intra-row weeding becomes much more difficult. Heat, weed tines and herbicide are three intra-row weeding methods that have been developed that do not rely on the need to differentiate between crops and weeds. These techniques primarily rely on the crop plant being more resistant to the removal mechanism than the weed plant.

***Mechanical Weed Removal***

Mechanical methods can be used to thin weed plant material inside the row. Plant thinning and weed tines are two methods used to remove unwanted plant material within the row. Plant thinners are frequently used in the production of sugar beets, vegetables, and cotton (Kepner et al. 1978). Due to the lower emergence rate of these crops, a

common strategy is to plant excessive amounts of seed – and to thin the row to the desired stand after emergence. Random thinners remove strong and weak plants indiscriminately, producing a desired concentration of plants along the row. Among the most common low-tech implements are finger and torsion weeders, which originate from North America (Van Der Weide et al. 2008). On the other hand, selective thinners are able to thin the row removing weaker plant material. In the case of weed tines, they can be used to selectively kill weeds within a row while simultaneously saving crop plants. If weeds can be identified within a row, pneumatic or rotary knives could be positioned in and out of the seedline to physically uproot weed material.

***Heat Weed Removal***

Heat is an alternative to mechanical weed removal. Since the 1940's, a considerable amount of research using thermal weeding on cotton, corn, soybeans and grain sorghum have been conducted with varying levels of success (Kepner et al. 1978). Typically, a direct burst of flame is applied to the base of the plant to denature plant cells – resulting in death. Selective methods are commonly used to apply enough heat to damage the weeds while preserving the more resilient crop plants. Because of this, flame weeding is limited to certain crop plants; primarily the ones listed above. Although there has been much interest in flame weeding throughout the 1950's, it soon died down during the mid to late 1960's following the increased use (and effectiveness) of pre-emergence and post-emergence herbicides (Kepner et al. 1978). Recent studies have shown that hot oil that can deliver enough heat energy to kill targeted plants (Zhang et al. 2009).

***Weed Removal Using Herbicides***

Selective herbicides have been developed that target weeds while preserving crop plants. Although some herbicides are effective in selective targeting, this method has many drawbacks. Perhaps the most obvious consequence is environmental damage, including soil and ground water pollution (Nordmeyer et al. 1997, GopalaPillai et al. 1990). A total of 160,000 kg of herbicides were applied to produce processing tomatoes in California alone in 2006 (USDA, 2007). In some farms, the concentrations of harmful chemicals in ground and surface water supplies have exceeded federal health limits due to herbicide over usage (Marks and Ward 1993). Pesticide usage in California was estimated at 190 million pounds (CDPR 2007). However, these chemicals are not only damaging to the environment, but can also pose risks to the health of farm workers. Inhalation, ingestion, and absorption of chemicals are common occurrences among field workers. Exposure can result in health problems such as abdominal pain, ataxia, nausea, dizziness, vomiting, headache, cancer, sterility, blood disorders and abnormal liver and kidney functions (Mobed et al. 1992).

Concerns about possible health risks and environmental impacts of conventional food production methods (that may use pesticides, antibiotics and other chemicals in food production) have led to the popularity of organic produce (Dreezens et al. 2005; Siderer et al. 2005). It is estimated that organic sales have increased by nearly 20% annually since 1990, with consumer sales reaching $13.8 billion in 2005 (Winter 2006). By 2005, all fifty states had organic farmland with over 4 million acres dedicated to organic production (Young 2010). In one survey, the main reasons consumers purchased organic foods were: for the avoidance of pesticides (70%), for freshness (68%), for health and

nutrition (67%), and to avoid genetically modified foods (55%) (Whole Foods Market 2005). Such consumers are willing to pay the typical 10% to 40% price premium that organic products command. In organic farming, herbicides containing synthetic chemicals may not be used to control weeds; as a result, there is a reliance on manual weed removal.

***Manual Weed Removal***

With the increase in sales of organic produce also comes a corresponding increase in the cost of labor. Labor costs for farms totaled $27.4 billion in 2010 (NASS 2010). Labor costs such as those needed for manual weeding on organic farms account for the largest portion of total cost - totaling $569 million a year in the U.S. (NASS 2008). Hand hoeing, the traditional method used for centuries by farmers - has many disadvantages. For one, hand-hoeing is one of the most tedious tasks in agriculture today. Professor Roy Bainer, who was once chair of the Department of Bio and Agriculture Engineering and the first Dean of College of Engineering at the University of California Davis - describes in his memoir (Bainer 1975):

> *"This whole matter of substitution of machinery for labor, especially stoop labor, I've never felt bad about being a part of it because man was more or less created in the image of God and he shouldn't have to make his living through drudgery."*

Chandler and Cooke (1992) has also shown in the instance of cotton production that hand hoeing can be over five times more expensive than herbicide weed control. In addition, Vargas et al. (1996) found that hand-hoeing may not be very effective. In fact, hand-hoeing removes only about 65 to 85 percent of the weeds in a cotton field. This

variation was attributed to the level of supervision and similar appearance between crop and weed plants.

In addition to the cost of hand-hoeing, and the inability to control weed presence - manual weeding can also lead to long-term health problems for farm workers. It is estimated that approximately half of the world's working population (1.3 billion people) work in the agricultural sector (ISO 2003). Farm workers frequently develop musculoskeletal disorders (MSDs) because they work in a stooped position for a prolonged period of time. Research has consistently shown that MSDs are the most common of all occupational non-fatal injuries and illnesses for farm workers especially those who are involved in labor-intensive practices (Fathallah 2010, Mccurdy 2003, Villarejo 1998, Villarejo 1999). These disorders can result in crippling back pain, which accounts for 40% of absences from work in the U.S. (Guo et al. 1999). The estimated cost of back pain amounted to as much as $100 billion annually in the U.S. (Guo et al. 1999).

## Existing Machine Vision Solutions

### *Row Guidance*

For autonomous weed control systems, there must be a means by which the implement can guide itself along the row. Although there are many ways by which row guidance can be achieved, two practical methods that stand out are using machine vision and RTK GPS (Slaughter 2008). Astrand (2005) describes the following five requirements for row guidance:

1. The ability to navigate rows with an accuracy of a few centimeters.

2. The ability to control a cultivation system as well as an autonomous agricultural robot in real-time.
3. The ability to discriminate crop plants from weeds.
4. The ability to function with high weed pressures of up to 200 weeds/m^2.
5. The ability to function when crop plants are missing in the row.

Row guidance using machine vision works by detecting the crop plants and guiding the tractor along the line that connects each of them. This way, the implements that do the planting and weeding can be guided along the seedline. However, there are several problems posed to machine vision – including missing plants and false identification between weeds and plants. The Hough transform, which uses a computationally efficient procedure for detecting discontinuous lines or curves in pictures - is a common machine vision method for identifying crow rows (Hough, 1962). A study done by Marchant and Brivot (1995) using the Hough transform in real-time at 10 Hz and an equivalent travel speed of 2 m/s - determined that the method performed well. Marchant et al. (1997) performed a field test resulting in an RMS error of 20 mm in the lateral position at a travel speed of 0.7 m/s using the Hough transform in four transplanted cauliflower fields. While the Hough transform is a popular technique, Slaughter et al. (1996, 1999) developed a machine vision guidance system using real-time color segmentation of direct-seeded crops at the cotyledon to fourth leaf stages based upon the median of the spatial distribution of plants about the seedline yielding similar results.

Despite the relative success in machine vision, differences in regional environments and farming practices continue to prove challenging (Slaughter 2008). In

weed distribution, for instance -most machine vision systems assume a random spatial distribution. Unfortunately, weed distribution is hardly random. Like all plants, weeds require water, sunlight and nutrients, growing heavily in areas that have abundant sources of each. With direct-seeded tomatoes in California, farms use split-bed furrow irrigation to supply water for seed germination. In this situation, the seed line is offset to one edge of the planting bed and the applied soil moisture is not uniform. This results in a non-uniform spatial distribution of weeds with respect to the seed line (Slaughter 2008). If pre-emergence herbicides are used, another problem arises. Along the outer edges of the herbicide strip, weeds will tend to accumulate. This accumulated growth can confuse the machine vision system when weeds outnumber crop plants, and even cause the system to believe the weed row is actually the crop row. In some regions of the world, center pivot irrigation systems are used. Therefore, the adjusted seed line is curved instead of being linear. Since machine vision systems are designed for straight rows, they encounter problems near the center – where the radius of curvature is smaller.

A typical machine vision system, such as the CLAAS CAM PILOT cultivator guidance system, uses a digital camera that takes 25 pictures/s of the crop row. These pictures are processed by a computer to determine the row centerline (Fennimore 2010). As the row centerline shifts, the computer signals a control valve to move a hydraulic cylinder horizontally - to keep the cultivator centered over the row. Fennimore showed that the CLAAS CAM PILOT system can reduce the width of the uncultivated area around the row from 5 to 3 inches. Weeding costs were reduced by 10% to 35%, and 40% less herbicide was used on the 3-inch band.

***Plant Differentiation***

In addition to guidance, machine vision can also gather data to differentiate between crop plant and weed. A machine vision system using a combination of three methods - biological morphology, spectral characteristics and visual texture – can be used to distinguish plants from weeds.

Classification between crop plant and weed using biological morphology is based upon the differences in shape and structure of the plant, and its parts. In image processing, basic operations are applied to an image to differentiate between weed and crop. Until recently, the processing power available was too slow to process advanced classification algorithms.

A number of studies have been conducted using biological morphology to distinguish between crops and weeds. Chi et al. (2002) demonstrated a 95.1% classification rate for four vegetable seedlings. Woebbecke et al. (1995b) studied roundness, aspect, perimeter thickness, elongatedness and seven invariant central moments to distinguish between plants. Similarly, Yonekawa et al. (1996) used image

analysis based on simple dimensionless shape factors to distinguish between plant types. Despite promising results, these classifications fail when the plant or leaf is not well displayed (e.g., damaged leaf, overlapping of leaves, missing structures). Franze et al. (1991a) and Lee (1998) suggest that if the leaf is oriented away from horizontal, this could add another issue with classification using biological morphology. Sogaard (2005) developed a method to compare plants to a database with shape models for 19 important weed species found in Danish agricultural fields. The results showed an accurate classification rate from 65 to 90 percent depending on weed species. A recent study by Kishore and colleagues has shown that 90% of nightshade plants were correctly identified using the automated active shape matching system (Kishore et al. 2011).

Essentially, machine vision is designed to mimic the human ability to decipher weeds from crops using biological morphology. Machine vision systems suffer from occlusion because they cannot re-orientate their field of vision to observe the plant. Concurrent Solutions (2004) has attempted to use multiple camera views to get around this problem of occlusion. Although many machine vision systems work well under ideal conditions, they fail to function when subjected to leaf occlusion, leaf damage, twisting in the wind, insect damage, and splashing by wetted soil.

Another method of machine vision uses spectral characteristics to distinguish between crops and weeds. Two main advantages of using this method are that pixel based color, or hyperspectral classifiers - are resistant to partial occlusions and less computationally demanding than shape-based techniques. Woebbecke et. al. (1995a) looked at the use of color and chromaticity values to distinguish between crop plants and weeds. They determined that using these traits alone did not provide a robust classifier.

Franz et al. (1991b) investigated the broadband reflectance in the visible and near infrared on different green house plants and found that a 94% identification accuracy was achieved when leaf orientation was controlled. When leaf orientation was not controlled, the accuracy dropped to 76%. Slaughter et al. (2004) showed narrowband hyperspectral models in the near infrared region provided the best results (100%) followed by narrowband hyperspectral models in the visible region (95%) and finally broadband color-based models were the least accurate (75%). Astrand and Baerveldt (2002) developed an autonomous robot to achieve a 91% classification accuracy when distinguishing weed plants from sugar beets.

In recent years, hyperspectral machine vision systems have been evaluated for automated weed detection. Zhang (2011a, b) showed that when a global calibration method was utilized to account for temperature effects and sunlight effects, the system was able to achieve an overall classification rate of over 90%. Staab et al. (2009) showed a 95% success rate in distinguishing processing tomato from weeds when using a hyperspectral system. Slaughter et al. (2008) achieved an average crop vs weed classification accuracy of 90.3%.

Robocrop is a commercially available machine guided cultivator system that is able to take images of frontal row and use computer processing to determine the locations of each crop plant in the row. The computer system then synchronizes the rotation of a cyclical cultivating disc to hoe between plants within the row (Tillett and Hague Technology LtD., 2012). The Robocrop system can cultivate both inter-row and intra-row at a speed of two crop plants per second. The Robocrop system can be expanded to simultaneously cultivate 9 rows at once.

Two of the main drawbacks of machine vision detection systems are the limitations on traveling speed, and the necessity of classifier data over multiple planting seasons which can be used to distinguish between crops and weeds. As computer processing technology advances, machine vision systems will be able to operate at faster speeds. However, that boon does not extend to the collection of classifier training data, which must be painstakingly collected for each crop/weed pair. An alternative to plant classification is using location data, which is becoming more realistic due to the development of GPS technology.

**GPS Background**

The Global Navigation Satellite System (GNSS)– with full worldwide coverage has revolutionized how humans work, travel and interact with their surroundings. Global Positioning System (GPS) by US and GLONASS by Russia are two systems with GNSS capabilities. Although the use of GPS receivers have exploded in recent years, satellite based positioning concept has been in existence for over 50 years. When Sputnik 1, the first man-made satellite to be put into earth's orbit, was launched in 1957, Dr. Frank T. McClure of the Applied Physics Laboratory at Johns Hopkins University proposed that if the orbit of the satellite was known, it may be possible to locate a user based on the distance between the user and the satellite (Bowditch 2002) using the Doppler shift in the signal sent from the satellite. GPS technology was born with the transit system of the 1960's and then followed by the United State's Department of Defense development of GPS technology for military purposes in the early 1970's. Today, the DOD's GPS system is open to both military and civilian use (FRP, U.S. Federal Radio navigation Plan

2001). This access has led to the application of GPS technology for mobile navigation, surveying, construction, agricultural and many other applications. Recent advances in GPS, specifically Real Time Kinematic GPS - has allowed accuracies on the order of one centimeter (Trimble 2010).

***Signal Triangulation***

The basic idea behind GPS is to use the location of three points, and their respective distances – to triangulate an unknown position within that area. If a GPS signal is transmitted from a known location (point A) and a GPS receiver is located at point P (unknown location), then the location of point B must fall on the surface of the sphere represented in Figure 1. If the location of A was known to be 10 meters away from B, then the receiver must have coordinates on the surface of the sphere with a radius of 10 meters centered at point A. If the distance between a GPS receiver located at unknown point P and two GPS signals located at known points A and B then location P must fall on the circle representing the intersection of the two spheres shown in Figure 2. As shown in figure 3, if there are three transmitting signals, the location of the GPS receiver can be narrowed down to one of the two points which is described by the intersection of all three spheres (Langley 1991a). Most of the time, the location of one of the two points would be in space so it can easily be discarded.

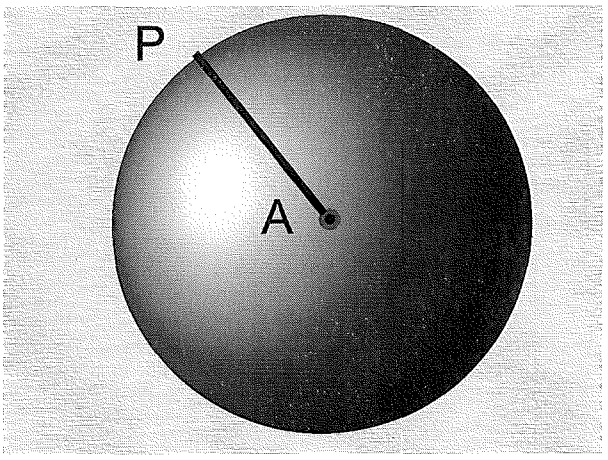


Figure 1. If the location of point A is known and point P is known to be 10 meters away, then the location of point P is on the surface of a sphere centered at point A with radius 10 meters.

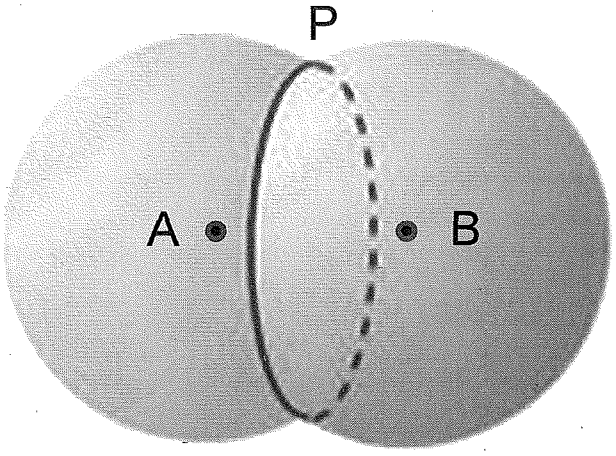


Figure 2. Points A and B represent the centers of two spheres with known radii. Point P falls on the circle representing the intersection of spheres centered at A and B.

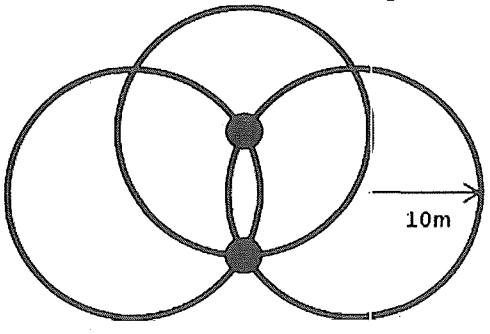


Figure 3. Effect of three transmitting signals. The receiver location is one of the two points of intersection of the three spheres centered by the three transmitting signals.

In reality, the GPS transmitters are located on satellites orbiting roughly 14,000 miles away in Earth's exosphere. There are more than 24 GPS satellites (24 operational + some spares) orbiting the Earth (Hoffmann-Wellenhof et al. 2001). The reason there are so many operational satellites is so that at any given moment in time at a given location, there will always be enough satellites detectable by the receiver to triangulate its location anywhere on earth (i.e., worldwide coverage). Although three satellites are needed to locate an object in 3-D space, a fourth satellite can be used to compensate for the receiver clock offset – otherwise known as the difference between the receiver clock and the GPS time (Kaplan and Hegarty 2006). When four or more satellites are in view, the remaining satellites will help improve the accuracy of the position.

***Determining Satellite Receiver Distance***

The distance between satellite and receiver is determined by comparing two radio signals; one sent from the satellite the same time the identical signal is produced on the receiver. Pseudorandom and carrier signals are two such radio waveforms that can be matched up to determine the time of flight from the satellite to the receiver. When this time of flight is multiplied by the speed of light, the distance between the GPS satellite and the GPS receiver can be obtained. Two identical square waves are produced from the satellites and the receiver at the same instance in time. Figure 4 shows how the time delays of the same signals are compared in order to determine the signal flight time between the GPS receiver and satellite (Trimble 2010). More accurate position can be achieved by using receivers that measure phase of the carrier waves. The carrier signals L1 and L2 are normal sine waves with frequencies of 1575.42 MHz and 1227.6 MHz, respectively. These translate into wavelengths of 19 and 24.4 cm for the L1 and L2

signals, respectively (Hoffmann-Wellenhof et al. 2001). Carrier phase measurement involves measuring a fraction of the wave or phase arriving at a receiver and then tracking the satellite to resolve "integer ambiguity" using an optimization scheme. This technique requires a local (i.e., physical base station within a few km) or virtual base station that tracks the same satellites as the rover mounted on a tractor. Once the integer ambiguity is resolved, very accurate position determination on the order of a few mm becomes possible. However, if a satellite goes out of the view, there can be a temporary signal loss (Hoffmann-Wellenhof et al. 2001).

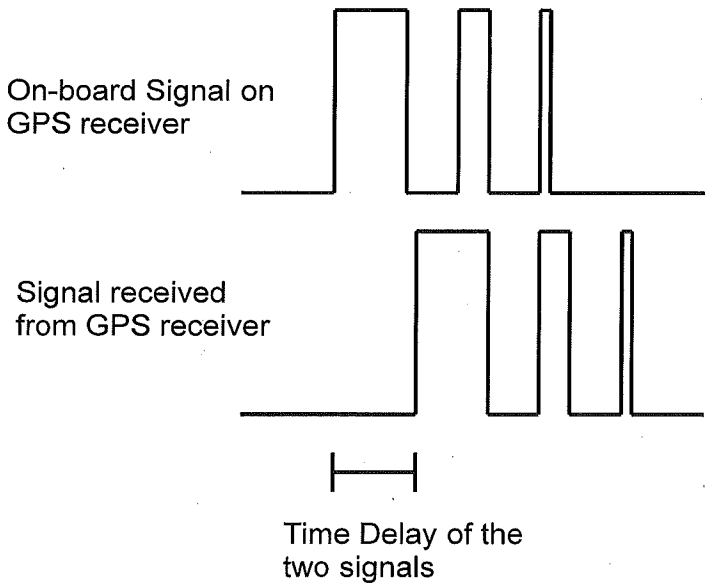


Figure 4. Comparison between the pseudorandom signal produced on the GPS receiver and the same signal received from a GPS satellite. The time delay of the two signals can be multiplied by the speed of light to determine the distance between the receiver and the GPS satellite.

Since the satellite is about 14,000 miles away, it takes a fraction of a second for the signal to travel to the receiver. With highly accurate atomic clocks aboard each of the satellites, one can determine the timing offset between the signal transmitted by the

satellite, and the signal produced by the receiver (Langley 1991b). Atomic clocks using Cesium are the most accurate clocks developed thus far. Cesium clocks work by counting the oscillations of an atom of Cesium as it transitions back and forth between two energy levels, much like the oscillations of a pendulum inside a grandfather clock. The oscillation is extremely consistent, and can be used to determine an accurate time difference that can ultimately be used to determine the distance between the GPS satellite and the GPS receiver. The triangulation of these distances can be used to calculate the location of the GPS receiver.

### *Sources of GPS Error*

There are three places where error could arise: at the satellites, receiver, or during signal transmission through the atmosphere (Kleusberg and Langley 1990). Combined, these sources of error can lead to discrepancies between the actual location and the location determined by the global positioning system.

#### *Satellite Error*

Initial errors can originate at the GPS satellite itself, due to a deviation from the predicted orbit. This is known as ephemeris error in which the gravity of the moon or other planets cause the satellite to deviate from the orbit. To correct for this error, the DOD has advanced radar stations on the surface of the earth that can measure the exact altitude, location and speed of the satellites. This information is then transmitted to the Master Control Station where the data gets processed and ephemeris error is determined. This information is then uploaded to satellites by the upload stations and the error is corrected. Another source of error at the satellite is due to the atomic clocks, which vary

from about 8.64 ns to 17.28 ns per day. This time error translates into a distance of 2.59 meters to 5.18 meters (Langley 1991b). Unlike the others, SA is a type of error purposely programmed by the United States government for national security reasons. The SA error can be as high as 100 meters in the horizontal direction, and 156 meters in the vertical direction (Georgiadou and Doucet 1990). However, SA error is no longer relevant to GPS accuracy, as it was removed by the United States Government on May 2, 2000 (Shaw et al. 2000). The number of satellites in view and their distribution also affects measurement error. This is usually represented as dilution of precision (DOP).

***Atmosphere Error***

Because radio waves have to travel through the Earth's atmosphere, they tend to become distorted by the fluctuating electron densities in the ionosphere. This results in a bent GPS signal whose speed has been altered (Hoffmann-Wellenhof et al. 2001). In turn, it takes longer for the signal to arrive at the receiver – causing a false distance measurement that prevents accurate triangulation. Modeling and differencing techniques are used to minimize this error. Newer satellites have L2CM and L2CL (L2 Civilian Medium and L2 Civilian Long) to help in getting rid of many of the errors.

Another source of atmospheric error is the troposphere, which constantly experiences changes in temperature, pressure, and humidity that interfere with signal frequency. Fortunately, mathematical models have been developed to minimize this error (Leick 2004).

***Receiver Error***

In addition to satellite and atmospheric errors, the receiver can be a source of error as well. Multipath error is a common phenomenon caused by signal reflectance off objects surrounding the receiver.

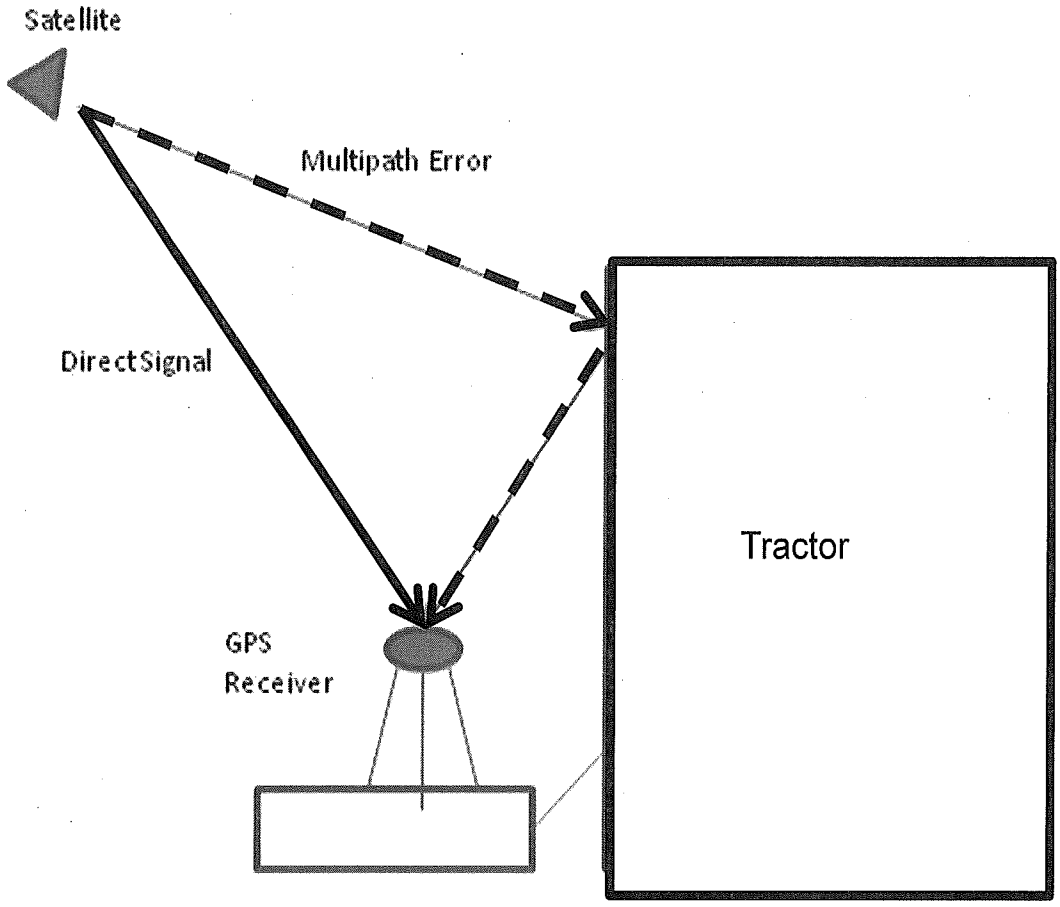


Figure 5. Graphical representation of multipath error (dashed line).

In figure 5, the signal that is reflected off the tractor takes longer to travel to the GPS receiver than the direct signal. This type of error affects both the pseudorandom and the carrier phase measurement. Therefore, in this study, the receiver was placed at a height greater than the tractor to avoid any objects from interfering with the GPS signal.

A second source of receiver error is the phase-center error, which occurs when the location of the received signal and middle of the antenna do not align. Since the GPS antenna is usually a few cm across and deep, there can be upwards of a few centimeters of phase-center error (Kleusberg and Langley 1990). With proper design of the GPS receiver, one can disregard this error. A third source of error is the receiver timing error due to the use of crystal clocks which are less costly and less accurate than the atomic clocks used on the satellites.

To improve error corrections, a second stationary GPS receiver located at a known or reference point (say a coastguard beacon) can be used to help correct much of the error discussed previously. The stationary GPS represents a true location by using an average over time. Most of the errors affecting the moving receiver will affect the stationary receiver as well if they are in close proximity. Therefore, if the rover receives the correction signals from a nearby (less than 150 km) beacon, then many of the errors associated with the satellites and atmosphere can be eliminated. This type of GPS is called differential GPS or DGPS. Although coastguard beacon is one such system, there are wide area satellite based correction systems that use a network of reference stations distributed over a wide area, compute the error for a receiver located within that area and send it to the receiver using geostationary satellites). Both WAAS (Wide Area Augmentation System) and Omnistar (a division of Trimble Navigation Ltd.) provide such corrections. While WAAS is available free in the United States, Omnistar is a for-fee commercial vendor.

### *Types of GPS*

While a low cost GPS system can have errors measured in meters, there are many different GPS technologies that can be used to reduce the three types of errors described above to a variance of approximately one centimeter.

#### *Classical GPS*

The classical low-cost GPS system described above determines the distance between each satellite and the receiver by utilizing the C/A code on the L1 carrier wave and triangulation process described earlier. This is known as pseudoranging. The standard deviation can reach 10 meters in the horizontal direction and 19 m in the vertical direction (Hoffmann-Wellenhof et al. 2001).

#### *Precision Point Positioning GPS*

The next type of GPS system is Precise Point Positioning, commonly known as PPP GPS. It is crucial to note that the PPP does not suffer from the previously mentioned SA error. PPP GPS also uses the P-code L1 and L2 carrier signals to correct for ionospheric delay. Unfortunately, PPP is not available for civilian use. Only authorized users such as department of defense (DOD) has access to these signals.

#### *Post Processing GPS*

Post processing GPS stores GPS data for correction at a later date. Post processing can achieve centimeter accuracy. The disadvantage of this type of GPS is that operations cannot be done in real-time (El-Rabbany 2006).

***Differential GPS***

Currently, many government agencies and private firms provide correction signals. DGPS can successfully reduce ephemeris error, clock error, ionospheric error and tropospheric error. The resulting coordinates can have accuracy ranging from less than one meter to nearly five meters (Hoffmann-Wellenhof et al. 2001). Even at this accuracy, it is unrealistic for crop plants such as tomatoes, which are planted a mere 46 centimeters apart.

***RTK GPS***

Real Time Kinematic GPS, or RTK GPS - is the method used to obtain centimeter level accuracies in real-time. It is used primarily to survey a large number of points close to the base station. Because RTK uses a radio antenna to communicate between the base station and the rover, it is only applicable when the rover is within a short distance from the base unless a satellite based virtual reference station (VRS) network is employed. With a correction signal, accuracies about 1 cm in the horizontal direction and 1.5 cm in the vertical direction can be obtained with RTK GPS (El-Rabbany 2006). GPS coordinates are associated with a timing pulse per second (PPS). The PPS is commonly used because it takes time for the base station to do the calculations to provide a correction for the rover. Since it takes 100 milliseconds to communicate with the base station and do calculations, RTK GPS is usually output at once per second and require interpolation when used in kinetic applications.

### *RTK GPS as an Alternative to Machine Vision*

As the limitations of machine vision approaches, a system that uses RTK GPS technology could be a feasible alternative. Instead of using machine vision to identify a row of crop plants and then guide a tractor along that row, RTK GPS can be used to create the bed in the first place and later guide the tractor along the original route. RTK GPS location methods can also replace machine vision plant classification methods. If the GPS locations of each crop plant are logged, the tractor can be guided along the same row directly above the plant and perform weeding (Upadhyaya 2003).

#### *Row Guidance*

Advances in RTK GPS technology have provided an alternative solution to machine vision for row guidance (Slaughter 2008). Leer and Lowenberg-DeBoer (2004) showed that RTK GPS is able to provide steering accuracies of 25 mm from pass to pass in a row crop. Stoll and Kutzach (2000) reported a standard deviation of steering better than 100 mm. Nagasaka et al. (2004) reported a standard deviation of 55 mm at a travel speed of 0.7 m/s using RTK GPS in combination with fiber optic gyroscope sensors to correct for tilt. Kise et al. (2002) showed that a tractor following a sinusoidal path with a 2.5 m amplitude and 30 m wavelength at 6.5 km/h had a 6 cm RMS error with a 13 cm maximum error. Abidine et al. (2004) also demonstrated the feasibility of an RTK GPS system for planting and subsequent weeding of processing tomato transplants. All of the aforementioned studies prove that RTK GPS is capable of automatically guiding a tractor along a preprogrammed row.

***Plant Map Determination***

In addition to using RTK GPS to automatically guide the tractor, it can also be used to tag the location of each crop plant as it is planted into the bed. A map of each plant location can be compiled to pinpoint the location of each plant (Norremark et al. 2007, Upadhyaya 2003). Ehsani et al. (2004) proposed that it could eventually facilitate plant-specific farming techniques, by combining an accurate seed map with a machine vision sensor – which would produce a less computationally-demanding algorithm for weed detection. This vision system would classify any plant material outside the crop map locations as weeds.

Since RTK GPS coordinates are outputted once a second, linear regression can be used along with odometry data to find true GPS coordinates of each plant. Ehsani et al. (2004) defined $(X_i^a, Y_i^a)$ to be an RTK GPS (Fixed quality) antenna position and $\Delta_I$ to be the corresponding transplanter odometry value. The heading angle ($\phi$) was determined by linear regression between $X_i^a$ and $Y_i^a$ for a set of consecutive positions. Once $\phi$ was known, the offset in Easting and Northing at the ground surface (due to pitch and roll of the transplanter at position i) was determined and used to provide an inclination corrected position $(X_i, Y_i)$. Utilizing three consecutive inclination corrected positions - i, j, k, and their corresponding odometry values - the following models were defined:

$$x_m = a\delta_m \quad (1)$$

$$y_m = b\delta_m \quad (2)$$

where $x_m$, $y_m$ and $\delta_m$ were the mean centered values for the three positions. Using the sum of squared errors minimization technique modified for odometry, Ehsani et al. (2004) determined parameters a and b by regression as follows:

$$a = \frac{\sum_m x_m \delta_m}{\sum_m \delta_m^2} \quad (3)$$

$$b = \frac{\sum_m y_m \delta_m}{\sum_m \delta_m^2} \quad (4)$$

Ehsani et al. (2004) then determined the geo-spatial location values semi-automatically using a program written in Visual Basic (Microsoft Corp., Redmond, WA). To find the three position values bounding a planter wheel/optical sensor, they developed a macro that would first search the plant event database. Secondly, equations 3 and 4 were used to determine the associated regression coefficients, while equations 1 and 2 predicted geo-spatial positioning.

Upadhyaya et al. (2003) and Ehsani et al. (2004) tested the accuracy of seed mapping with maize seeds in an agricultural field using this method. On average, it was found that seeds were mapped within 34 mm of a crop plant after germination. In a similar study, Griepentrog et al. (2005) showed that the precision of mapping sugar beets ranged from 16 to 43 mm, depending on seed spacing and vehicle travel speed. Sogaard and Norremark (2004) and Bak and Jakobsen (2004) decided to investigate the capabilities of an RTK GPS controlled autonomous robot in detecting sugar beet crop

plants - using an automatically generated planted map to 16 mm. Sun et al. (2010) developed an RTK GPS guided tomato transplanter that was able to accurately provide centimeter accuracy mapping of tomato transplants. Perez-Ruiz et al. (2012) furthered the development of the transplanter to build a system for geospatial mapping of crop plants using an RTK GPS auto-guidance system mounted on the tractor.

***RTK GPS Advantages/Disadvantages***

RTK GPS is a position technology that can solve many of the issues associated with machine vision. While it does not require a visual guidance directrix it requires an unobstructed view of the sky from all parts of the field. Unlike machine vision which only provides relative positioning based on local landmarks, RTK GPS provides absolute global positioning of the system. Since RTK GPS does not depend on the visual appearance of the crop, it is not limited by weed density, shadows, missing plants or other conditions that degrade the performance of machine vision systems. Perhaps the biggest advantage of RTK GPS systems is that they do not rely on classification between weeds and crop plants. Unlike machine vision systems that rely on classifier data to distinguish between weed and crop plant, RTK GPS systems purely use the location of the crop plant to make the distinction. Thus, this technology can be applied to any crop plant and weed pairing. Finally, the RTK GPS row guidance systems can easily be programmed to follow curved rows. Despite their overwhelming advantage over machine vision systems, the RTK GPS does have its drawbacks. First, the crop must be planted using an RTK GPS guided planting system – and the GPS base station should be within 6 miles of the rover. However, with VRS, the proximity of the rover to the base station is not as important. There are many systems designed for automated weed control (Bakker 2009,

Christensen et al. 2009, Comba et al. 2010). Bakker et al. (2011) developed an autonomous navigating robot platform incorporating RTK-DGPS with machine vision that has achieved a standard deviation of 1.6 cm, which corresponds to the accuracy of the RTK-DGPS system. Other robotic systems have been developed with onboard servers to store plant maps (Bochtis et al. 2011).

## Intra-Row Weed Removal Mechanisms

Once a plant has been successfully verified as a weed, one must decide on a method of killing or removing it. The development of precision planters in the 1960s inspired the concept of automatic thinning machines over the next twenty years (Inman 1968). Mechanical, chemical, thermal and electrical methods are four types of mechanisms that show promising compatibility with selective in-row weed control systems (Kepner et al. 1978). Slaughter et al. (2008) summarize the many methods of weed removal in their review of autonomous robotic weed control systems.

### *Mechanical Weed Removal*

Mechanical methods of plant removal were commonly used for thinning in the 1960s. Garrett (1966a, b) studied the accuracy of a mechanical thinning tool to remove excess plant material. His studies on sugar beet, cotton, tomato, lettuce, broccoli and melon showed that performance was largely a function of the spacing between the plants, and the distance the tool travels between initiation and the first cut into the row.

Selective mechanical methods of weed removal include positioning weed knives within the soil to cut away any unwanted plant material. These knives can then be positioned in the seed line to kill the target plants. Figure 22 demonstrates when the

knives open and close around a crop plant saving it while killing the unwanted weeds in the field. In the open position, the knife edges avoid any plant roots so they pass by the plants without killing them. When the knives are positioned in the seed line, the cut is made at any roots that obstruct the path. Prior to reaching the crop plants, the knives open thereby avoiding damage to the root structure of the crop plants. In addition to pneumatic knives that open and close around the crop plant, other mechanical methods such as the tine-rotor method (Norremark et al. 2008) or the cycloid hoe (Griepentrog et al. 2006) have been demonstrated to show good results. A fourth method of mechanical weed removal used a rotating hoe that could be adjusted vertically to selectively remove plants (Astrand and Baerveldt 2002). However, the energy required to overcome the inertia when operating the knives ultimately limits the travel speed at which these methods can still operate effectively (Tillett et al. 2008). At high travel speeds, the rapidly-spinning hoe blades can push the soil outwards due to the force of entry and exit into the seed line. Depending on the shape and size of the knives, it is possible to expose the root structure of the crop plant – which can result in irreparable damage.

Tillet et al. (2008) described a novel approach which uses a rotating disk with a quadrant cut-out that is powered by a hydraulic motor. As the disk travels along the seed line, it will cut through any weeds. Once the disk reaches a crop plant however, a proportional valve controls the rotation timing so that the crop plant passes through the cut-out portion of the disk unharmed. In theory, the continuous rotation of the disk – and the resistance required to make minor adjustments - allow the disk to travel along the row at a speed only limited by the accuracy of the controller.

The cycloid hoe is another advanced device for intra-row cultivation. It was developed for weed control in corn by the University of Osnabruck, Germany (Kielhorn et al. 2000). A cylindrical rotor works as actuator and contains eight tines placed around a vertical axis. The tines rotate in a circular motion at a rotational diameter of 0.234 m (Griepentrog et al. 2006). The cyclic movement of the tines can control translation speed of the implement, and rotational speed of the tines. Griepentrog et al. (2007) and Gobor (2007) have since conducted promising results using his type of hoe.

Pinpoint GPS location of the crop plant is crucial when positioning the knives for killing weeds – while simultaneously sparing crop plants. Factors that may affect the accuracy are travel speed, precision of row guidance, proper height adjustment of the knives in the soil, and the relative distance between the disk knives and crop plant. Proper soil conditions may also affect the performance of mechanical knives as well. An additional limitation of mechanical weed removal systems is the age of the weed. Older weeds are much more firmly rooted, which makes it difficult for the mechanical knives to cut through the weeds.

***Weed Removal Using Herbicides***

In the late 1960's, McLean (1969) suggested using a targeted stream of herbicide to remove weeds. He argued that using precision spraying minimized the physical disturbance of the crop plant and surrounding soil - thereby improving the chances of its survival. A precision spray system was developed by Lee et al. (1999) for use with robotic weed control systems in conjunction with a machine vision system. Eight spray ports were installed to each spray a cell 0.63 x 1.25 cm in size. Each of these spray ports were positioned 15 cm above the seed line, and a micro-controller activated each of the

associated solenoid valves to allow individual cells to be sprayed. When a region contained a weed leaf, a 10ms pulse of herbicide would be sprayed on to each cell containing the leaf. Due to inaccuracies, a 1 cell buffer was introduced around each sprayed cell to protect neighboring plants from splash damage. The advantage of using this method is that one does not have to be selective with the type of herbicide. However, splashing can potentially damage neighboring crop plants. Due to damage by splashing, Giles et al. (2004) recommended a bias towards conservative protection of crop in order to maximize yields. Downey et al. (2004a, b) investigated the effect of splashing from this micro-drift and found that this issue can be minimized by using a surfactant.

***Thermal Weed Removal***

A favorable alternative to spraying herbicides is the use of heat to kill weeds. Hot liquid weed control methods boast the organic benefits of mechanical weed removal, as well as the minimal soil disturbance of precision herbicide spraying systems. Daar (1994) used hot water spot treatment to successfully kill young weeds. Daniell et al. (1969) and Levitt (1980) have shown that higher temperatures are more effective for thermal weed control. Due to the thermal energy cap of hot water, Giles et al. (2005) modified the precision spray system used by Lee et al. (1999) for the application of hot oil, which can reach temperatures of 200 degrees Celsius. The thermal energy stored by the oil at 177 degrees Celsius killed virtually all weeds studied. Giles also showed that efficacy decreased with lower temperatures, and that 150 degrees Celsius was the minimum temperature at which efficacy was reliable. Staab et al. (2009) and Zhang et al. (2009) reported similar success in using hot oil to kill weeds. Other thermal weed removal systems have used flame to destroy weeds. However, this technology is limited to use on

heat-resistant plants, and requires much more costly fuel (Ascard, 1998; Lague et al., 2001).

### *Electrical Weed Removal*

Slaughter et al. (2008) describes a fourth method of weed removal by delivering a large burst of energy to the weed. The voltage discharge varies from 15 to 60kV (Diprose and Benson, 1984). Obvious advantages of electrocution include minimal soil disturbance, and a lack of toxic herbicides being released into the environment. Unfortunately, electrocution requires electrical probes to make physical contact, or be within a range of 2 cm in order to be effective. It also has trouble eliminating weeds that are close to the soil because the uneven soil and dirt clods can directly short the probes to ground. Additional problems arise if the soil moisture is not correct – which can cause contact damage without actually killing the weeds. Ultimately, electrocution becomes impractical for weed species that grow close to the ground. The effectiveness of electrocution varies from 50% to slightly over 90%. Another downfall of electrocution as shown by Blasco et al. (2002) is that 200ms of contact per weed is required to deliver enough energy to kill the weeds. Since this time does not including any sensing or positioning time, the feasibility of using electrocution in automated weeding systems decreases.

## Electronic Sensors and Controls Background

Sensors are important in the world we live in because they enable us to perceive and detect the world around us. For example, nerve endings in a human hand can be considered a sensor. When nerve cells are stimulated – for instance, a hand touching

scalding hot water - a signal of pain is sent to the brain. Likewise, an accelerometer can detect if a car is approaching an accident, thus deploying the airbags in response. A sensor has a broad definition that can be classified as any device that can respond to a signal or stimulus. Electrical sensors are specific types of sensors that are able to convert pressure, temperature, acceleration among other inputs into an electrical output. Once calibrated, the electrical output of the sensor can be measured to quantify the property being measured. This information from the sensor can then be used to monitor or control other devices such as a switch to deploy airbags. For this reason, sensors play an important role in controlling electrical systems.

***Sensor Classification***

Sensors can range in properties and complexities. A common way to classify sensors is passive vs active. Passive sensors are like thermocouples, which do not require an external energy source other than the environment to operate. Active sensors require external power and operate by modifying the excitation signal to produce the final output. A thermistor is an example of an active temperature sensor. The second classification is absolute vs relative sensors. Absolute sensors require a stimulus, which is referenced against an absolute physical scale free of measurement conditions. Relative sensors, on the other hand – output a signal that relate to some special case. Thermistors are examples of absolute sensors, where electrical resistance directly relates to the absolute temperature scale of Kelvin.

In addition to the two classifications described above, sensors can be described by many other properties. There are many types of sensors that can be used to measure the same input signal, using different methods of sensing - each with their advantages and

disadvantages. Temperature sensors can utilize resistive, thermoelectric, semiconductive, optical, acoustic, or piezoelectric properties to measure temperature (Fraden 2010). For instance, examine a normal mercury thermometer in comparison to a thermocouple. While both can be used to measure temperature, they vary greatly in properties such as accuracy, operation range and cost.

***Accuracy***

Perhaps one of the greatest concerns in choosing the right sensor is accuracy. The temperature sensor used to control a sensitive bio-fermentation process is very different than one used to control a home air conditioning unit where an error of a few degrees may be acceptable. The accuracy of a sensor can be determined by many factors such as physical property, cost and calibration.

A thermistor utilizing resistive properties is typically more accurate than a mercury thermometer using thermal expansion as a means to sense temperature. Despite their accuracy, they can also be much more expensive. Because of material variations, workmanship, design errors, manufacturing tolerances, and other limitations - sensors tested under identical conditions can vary in performance. For example, manufacturers of thermistors can trim the body to a required dimension that directly controls the nominal value of resistance at a set temperature. Increased performance frequently leads to higher prices. While it is generally more expensive, platinum RTDs (Resistance Temperature Detector) are generally accepted as the best temperature sensor for most temperature ranges. One alternative approach to improve a sensor's accuracy (but not its precision) is through calibration.

***Calibration***

Calibration results in a transfer function that represents the relationship between a stimulus and a response electrical signal produced by the sensor (Fraden 2010). The accelerometer used to deploy airbags, as mentioned above – is an example of a sensor that contains calibration information. The accelerometer must be calibrated to determine the electrical output at known accelerations. These data can then be used to determine the relationship between acceleration and the electrical output. Let's say an airbag deploys at 20 g's, which corresponds to an accelerometer output of 3 volts. As the car is monitoring the accelerometer, it recognizes that the output of the sensor has surpassed the threshold of 3 volts, and deploys the airbags.

One of the most common ways to calibrate an electrical sensor is to measure the electrical output at several sample points that are generated by a known reference source. In the calibration of a temperature sensor for example, reference points such as the boiling point and freezing point of water can be used to calibrate the sensor assuming the sensor is linear or the exact transfer function is known and has two or fewer parameters. The purpose of the calibration is to calculate the unknown coefficients of the inverted transfer function, so that it can be used to compute any points in the desirable range (Fraden 2010). Since many factors such as design, manufacturing variations and tolerances can affect the accuracy of a sensor, the conversion from the specifications may not include errors. One can typically improve the accuracy of the purchased sensor by performing a calibration. When a sensor is calibrated, the input and output values are plugged into the inverted transfer function to compute its coefficients. Once a sensor has been calibrated, it is ready to be used.

***Error***

The ideal sensor has perfect accuracy, has no effect on the medium being measured, responds instantly and has an easily conditioned output (Fraden 2010). Response time is one of the most important properties to consider when choosing the right sensor. Different sensors will have different response times depending on the design and the methods of sensing. First-order sensors have time independent responses, and incorporate energy storage components such as the RTD. They are temperature sensors that are typically larger in mass and encased in metal. These sensors have a slower response time because temperature sensing is not accurate until heat has transferred through to the sensing element. On the other hand, a thermocouple reacts very quickly due to its small mass. A second-order sensor has two energy storage components such as an accelerometer that incorporates an inertial mass and a spring. Second-order sensors take time to reach the steady state signal, but can also incorporate a rate of change component. In choosing the best sensor for the desired application, one must take response time into consideration because the electrical output may correspond to an input that occurred many seconds in the past. If the tilt at a specific instance is required, the sensor chosen needs to output a value that reflects the true tilt at the moment being measured - not the tilt in the past few seconds.

Hysteresis is the source of error resulting in deviation of the sensor's output at a specific point of the input signal when it is approached from opposite directions (Fraden 2010). For example, an angular displacement sensor may produce slight differences in voltage output if it is approached from either the clockwise or counterclockwise

directions. Typical causes for hysteresis are friction, structural changes in materials and geometry of the design.

***Range and Linearity***

Every sensor has a range in which it can accurately produce output. A bucket can be considered a sensor that measures collected rainfall if the water level is checked after set time intervals. One can determine the rate of daily rainfall if he/she checks the water level before it becomes full. If the bucket becomes full, it will not be able to indicate the true amount of rainfall. A charge coupled device (CCD) is a light sensor common in digital cameras. Light intensities beyond a certain saturation point will result in a picture that is either washed out or fully exposed. A sensor whose output is mostly linear loses its linearity once it goes beyond the saturation point.

Linearity of a sensor is an important factor, even when the signal has not yet reached its saturation point. While many sensors can be calibrated to follow a mostly linear line with a slope b, the resulting transfer function is an approximation of the true response of the sensor. Even if a sensor is able to consistently measure the known value of two terminal reference points, the true transfer function is likely not a straight line through the two points. When multiple points are measured during the calibration of a sensor, the $R^2$ value is a good indicator of linearity of the transfer function.

***Resolution***

Resolution, which is the smallest increment of stimulus that can be sensed – is yet another property that affects the accuracy of the signal being measured. A regular ruler can make accurate measurements to the millimeter, while micrometers have much higher

resolutions - making length measurements accurate to the $1/1000^{th}$ of a millimeter. Because of this, using a ruler to measure tight tolerances on mechanical components is inappropriate. Optical encoders are another example of sensors where resolution can play a big role in determining the accuracy of measured input. A 4-bit absolute rotary angle encoder would only have a resolution of 22.5 degrees - compared to a resolution of 1.4 degrees and 0.09 degrees for an 8-bit and 12-bit absolute encoder, respectively. This can make a huge difference in applications where precise angular positioning is required.

***Noise***

One of the most important factors that affect accuracy of a sensor is noise. Any sensor, regardless of design and manufacture - can never produce an electric signal that is a perfect representation of the input stimulus. Noise can arise from within the circuit, and interference picked up from the environment. Power supply transients, magnetic, electrostatic, radiofrequency EM fields, thermal variations, gravitational force, acceleration, humidity, ionization radiation and chemical agents can all be sources of noise. Both sensor and the attached circuit can act as receivers for the interferences. Filtering and shielding are two methods that can significantly reduce the noise picked up by sensors. For example, if noise from an external 60 Hz power supply is introduced into the sensor, filtering can be employed to remove any noise at that frequency, assuming the signal does not share a similar frequency range. Likewise, shielding can be used to prevent most external noise from reaching the sensor and circuitry. If noise is not reduced, it can greatly distort the output - especially if the inherent output signal is weak and requires amplification.

***Output Format***

Output format is important to consider when describing sensors. The output characteristics include voltage, current, charge, frequency, amplitude, phase, polarity, shape of a signal, time delay and digital code (Fraden 2010). Three of the most common forms of output from electrical sensors include analog, digital, and pulse signals. Different instrumentation is required in the control system to read these outputs.

Analog outputs are very common for electrical circuits. Commercial sensors outputting an analog signal typically have an output range from 0 to 5 volts – or from 0 to 24 volts where they correspond to the range of the input being measured. Instrumentation required to read an analog signal consists of a signal and ground input. The output of the analog sensor will be read as a difference in potential of these two signals, and are rarely able to connect directly to monitoring or recording circuitry. In most cases, the output signal of these sensors transmits a signal that is either too weak, too noisy, or containing undesirable components. In the case of a high speed video signal, electromagnetic radiation from the environment can cause artifacts in the image by introducing noise to the video signal. While noise is relatively small, many cases have been found where the sensor output is also low. As a result, amplification of the output signal is required in order for detection by controller circuitry to occur. While the signal can be amplified by a large magnitude for detection purposes, this same amplification will increase noise from the environment. In such instances, active filters are used to boost the signal as well as filtering and reducing unwanted noise. Signal to noise ratio is an important concept for analog signals. The stronger the output of the sensor is the better

the clarity at which it is interpreted. Despite being susceptible to noise and distortion of the output of analog signals, they are commonly used in control systems.

Digital sensors with built-in error checking produce signals that are resistant to transmission noise that is common in analog outputs over long distances, particularly for small voltages. Many sensors convert the output to a digital signal prior to being detected by a controller system. Because the signal is changed from a number such as 0.2761 into an array of 0 and 1's, it is more resistant to external noise. The number of bits of a digital output describes the resolution of the ultimate output. A one bit output can be described as a light bulb that can only be switched on or off. A 12 bit output would have 4096 different permutations. Take a sensor that can measure a range between 0 and 1 cm. If the sensor is actually measuring a length of 0.2761 cm, the one bit digital sensor would output a value of 0 since it can only be zero or one. A 12 bit digital output can increment by 0.0002 cm - the same signal would be represented as 0.2760 cm. This is far more representative of the actual value. Each bit of a digital sensor is read by an individual input on the controller circuitry. The difference between a vinyl record and a compact disk demonstrates the inherent differences between analog signals. A vinyl record has an engraved groove that mirrors the original sound's waveform. The groove represents an analog signal that can reproduce the sound, as well as broadcast it into a sound wave. However, any dust or damage to the surface will result in static noise. On the other hand, compact discs are read through microscopic bumps on the surface of the CD, which represent digital signals that are either true or false. Digital recordings do not degrade over time, and if the recording contains silence, there will be no noise.

A pulse is the third type of output commonly emitted from electronic sensors. Unlike digital or analog signals, a pulse output is in the form of a square wave with a certain width. In the case of a rotary encoder sensor, the amount the shaft rotates will translate into a number of pulses that can be detected by the controller circuitry. For example, if each 1 degree turn of the encoder outputs one pulse and 180 pulses are detected, the circuitry knows that the shaft has just rotated 180 degrees. When the width of a pulse signal is very small, the circuitry may not be able to read quickly enough - and instead interpret multiple pulses as a single pulse.

### *Types of Sensors*

#### *Rotary Encoders*

A rotary encoder is an electro-mechanical sensor that converts angular position or motion to a digital or analog signal. The output of an incremental encoder can provide information on angular displacement, velocity and acceleration. Incremental encoders are used in applications that require the detection of rotation such as in automobiles, and even rotational knobs on stereo systems. Incremental encoders can output as many as 10,000 counts per revolution of the shaft. By counting the number of pulses in the sensor output in a certain amount of time, the angular displacement, velocity and acceleration can be determined. Optical encoders are used in applications where higher RPMs are encountered or higher degree of precision is required. The concept of a quadrature output (dual outputs that are 90 degrees out of phase) arises when direction is required as well. By employing these two signals, the sensor is able to give an up count or down count, which can help determine the direction of travel.

***Absolute Encoders***

Absolute encoders are special encoders that can indicate the current position of the shaft, as well as displacement. These encoders are used in industries such as robotics where understanding of shaft position is required as well. An optical absolute encoder consists of a disk with both transparent and opaque areas. A photo detector and light source is combined to read the optical pattern that result from the disc's position at any given time. This pattern can then be translated into an absolute angle of the shaft.

***Light Beam Sensors***

Light beam sensors are sensors that can detect the passing of an object. They typically employ a light emitter that is lined up with a photo detector. The photo detector will continue to detect the light from the emitter, unless a conflicting object passes through the stream of photons. They are commonly used at the entrances to small businesses in order to detect when a customer has just entered the store. In more precise applications, a special emitter of infrared light at a specific wavelength is paired with a detector of that signal. This is used in many outdoor applications so that sunlight or other sources of light do not affect the photo detector. Light beam sensors can also be made more robust by installation of aperture kits designed to detect certain objects. For example, in applications where detection of a skinny object such as a plant stem is required, the installation of an aperture kit with a small slit on both the emitter and detector would make the detection of the thin stem more robust.

***Tilt Sensors***

Tilt sensors are sensors used to measure orientation with respect to a reference position. Many handheld devices such as cellular phones, tablets and digital cameras currently employ tilt sensors to determine orientation. In mobile devices, tilt sensors are used to sense orientation when taking pictures and also for many mobile games. Accelerometers and gyroscopes are two examples of electronic sensors that can determine tilt.

An accelerometer is a sensor that measures acceleration relative to a frame of reference. In the case of multi-axial accelerometers (i.e. more than one accelerometer), measurement of magnitude and direction of the acceleration can be determined, and can be used to sense the orientation of the device. Accelerometers measure acceleration by measuring force exerted on a known mass. Acceleration experienced by the mass is proportional to the force exerted on it. When standing still on a flat surface, an accelerometer should experience zero G of force. However, a falling accelerometer will experience 1G of force, since it is moving with gravity. In instances where the sensor is tilted in a stationary position, the deviation away from 1G of force can be translated into a tilt angle. While the sensor is in motion, the output represents the acceleration due to gravity, plus the acceleration of the device itself relative to its rest frame. When an accelerometer experiences vibration, steady-state tilt output errors may occur. In such cases, filtering must be employed to reduce this high frequency noise. A gyroscope can be used to measure or maintain the orientation of a device. Unlike an accelerometer, which measures the linear acceleration of the device -a gyroscope measures the orientation directly.

***Solenoids***

A solenoid is a device used to produce a magnetic field. They are commonly used to electrically control a switch or valve. Solenoids operate by streaming current through wire coiled around a movable metal core. As a result, a magnetic force is generated at the center by the current wrapped around it. The center core is typically spring loaded so that when current is not flowing through the coiled wire, the core is retracted to its original position. Solenoids are used in applications such as triggering, locking, and latching. They are found in copy machines, washing machines, car doors, audio speakers and air valves.

## Objectives of this Project

The goal of this project was to develop a RTK GPS guided transplanter that would create a real-time crop plant map, and automatically guide knives to kill weeds while sparing crop plants. The specific objectives of this project were to:

- Retrofit a transplanter with a RTK GPS system, sensors and controlling circuitry that can be used to collect transplanter odometry, GPS location data, tilt, and plant stem locator.
- Create a program that can collect all the sensor data in real-time so that the Easting and Northing values of each transplant could be estimated offline.
- Collect the actual GPS location of each tomato transplant and determine the accuracy of the mapping system.
- Retrofit an implement with a mechanical weed removal system.
- Create a program that could determine the implement's current location and after comparison with the plant map, remove all weeds in a predefined zone in between each of the crop plants.
- Determine the accuracy of the automatic weeding system in removing weed plants while sparing tomato plants using video.

## Design and Equipment

The automatic weed removal system used in this study contained two main subsystems: (i) plant mapping, and (ii) real-time weed removal system. Figures 6 and 7 illustrate a design platform that facilitated both aims. Plant mapping was achieved using sensors placed on a tomato transplanter that recorded geoposition data each time a tomato transplant was put into the ground. These data were used offline to calculate the Northing and Easting coordinates of each tomato transplant. Once mapping was completed, the same sled was modified to hold a set of pneumatic powered weed removal knives. The plant map was downloaded into an onboard control system, and GPS and odometry sensors helped the control system determine when to move the knives in a diamond shape pattern around a crop plant as it passed by.

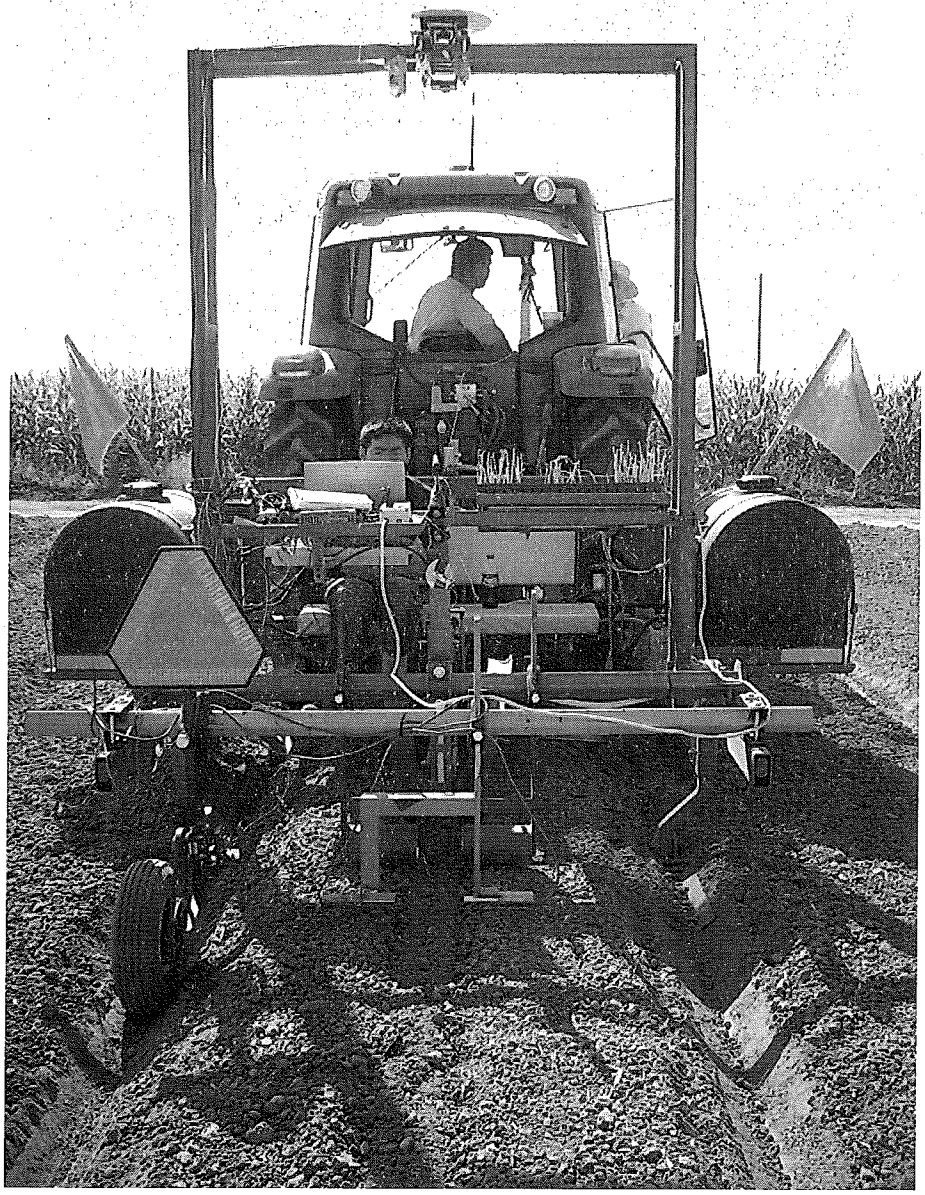

Figure 6. Picture showing the tractor and transplanting sled as they traveled down a row during a field test.

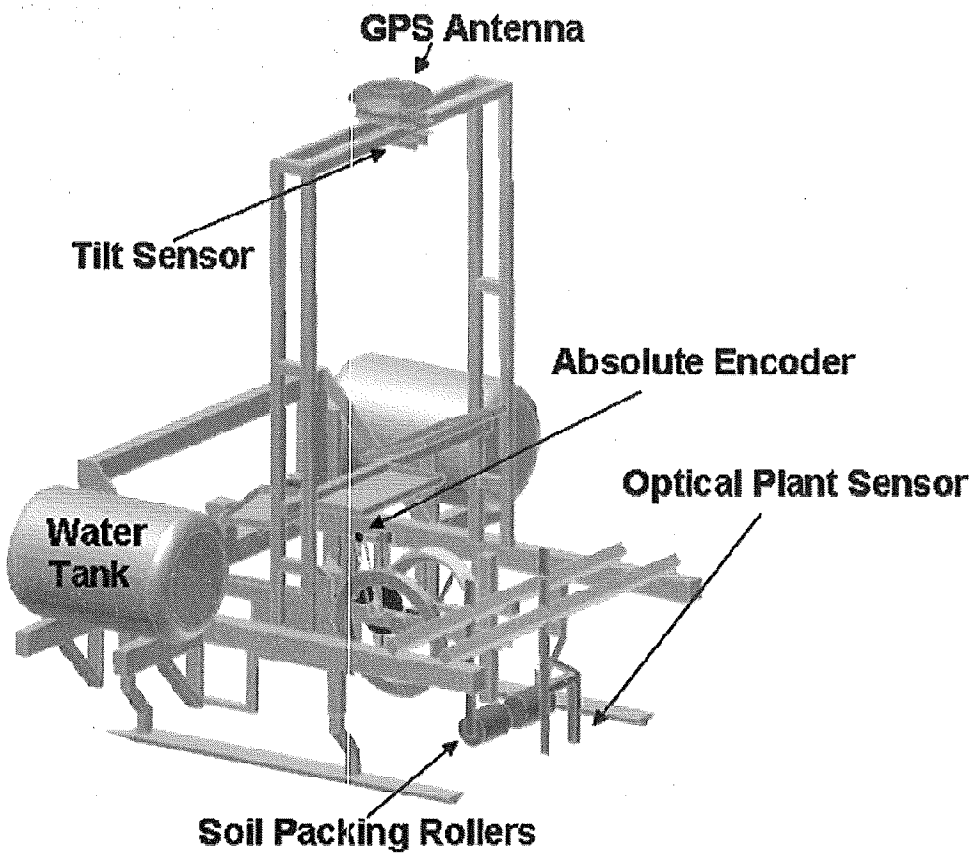


Figure 7. CAD model showing the GPS antenna, tilt sensor, absolute encoder, optical sensor packing roller and the water tanks located on the transplanting implement.

**Row Guidance**

Row Guidance was achieved using the GPS autopilot system on the tractor. All seedbed preparation operations were conducted with a tractor steered by GPS autoguidance using a common set of GPS AB line coordinates for all tillage and planting operations. The transplanter and weeding sled was pulled behind a tractor steered by an RTK GPS autoguidance system (model EZ-Guide 500, Trimble Navigation Ltd., Sunnyvale, CA, USA) that followed the same AB line.

**Plant Mapping**

The second critical step of GPS weeding is determining the plant map. For tasks such as automated weeding, a 1 cm range of geo-position accuracy and precision is required. Fortunately, the RTK GPS system was suitable for this study, due to its accuracy. Figure 8 below shows a flowchart of the events both in real-time and offline in map creation.

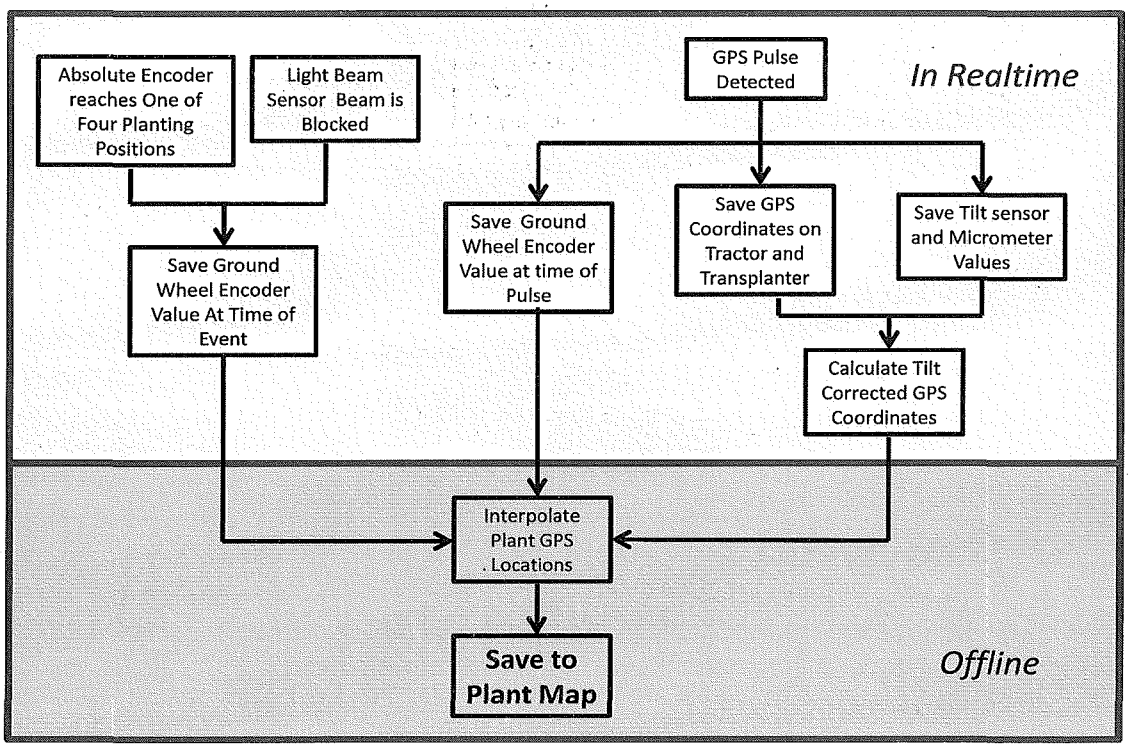


Figure 8. Flowchart describing the steps required for map determination and when they take place.

### *Transplanter Sled Design*

A transplanting sled was built and retrofitted with machinery to simultaneously place transplants in the soil while acquiring tilt, odometry, GPS, and crop plant stem location detection data. All of the aforementioned information was stored in order to create the crop plant map at a later time. In this study, the two methods of plant detection used included an absolute encoder, and lightbeam sensor. GPS data were collected from two rover RTK receivers located on the transplanter directly above the planting wheel and the roof of the tractor. Data for both GPS units and plant detection methods were collected simultaneously to compare the difference in accuracies when: (i) the GPS was placed on the tractor, or (ii) directly over the transplanting location. Some shared components between the transplanter and weeding systems included the sled, tilt sensor, micrometer, GPS systems, controller system, and odometry system. The tomato transplanter, absolute encoder system, lightbeam sensor, dirt clod rollers and watering system were used for the mapping portion - while the pneumatic knives and air compressor were used solely for the weed removal portion of the design.

### *Transplanter*

A positive-placement row-crop transplanter (model 1600, Holland Transplanter Co., Holland MI, USA) was mounted on a transplanting sled (SWEMEC Woodland, CA) that was modified for RTK GPS capability. The long support skis on the sled transplanter act as mechanical dampeners to both stabilize the transplanter, and to reduce along and cross track error by distributing the weight of the transplanter along the full length of the skis. A sturdy support frame was added to the transplanter in order to mount the transplanter GPS at a height of 3 meters above the soil. At this height, the

rover GPS antenna was located at the same level as the roof of the tractor, thereby greatly reducing the multipath error from the tractor.

***Tilt Correction***

Even though elevating the GPS antenna nearly eliminated the multipath error from the tractor, any changes to the pitch and roll of the implement could lead to a large error in the transplanter GPS data due to the height of the antenna and because the transplanter GPS was not compensated for tilt. To compensate, a 0.25 Hz dual-axis inclinometer (Accustar II/DAS 20, Schaevitz Sensors) was installed directly below the transplanter GPS antenna to minimize this error. The tilt sensor was capable of measuring pitch and roll with a resolution of 0.00017 radians, which corresponded to a 0.5 mm resolution parallel and perpendicular to the direction of travel at a height of 3 meters. The sensor provided offset correction of GPS data at the soil elevation due to implement tilt caused by the unevenness of the field. In order to calibrate the tilt sensor, a plumbob was suspended from the tilt sensor to determine the relationship between voltage value and deviation of the plumbob – all the while when the transplanter was tilted using a jack (Figure 9). This relationship was then used to determine the tilt offset in both the Northing and Easting directions. A separate tilt sensor was not required for the GPS system mounted on the tractor because it had tilt correction built in by the manufacturer.

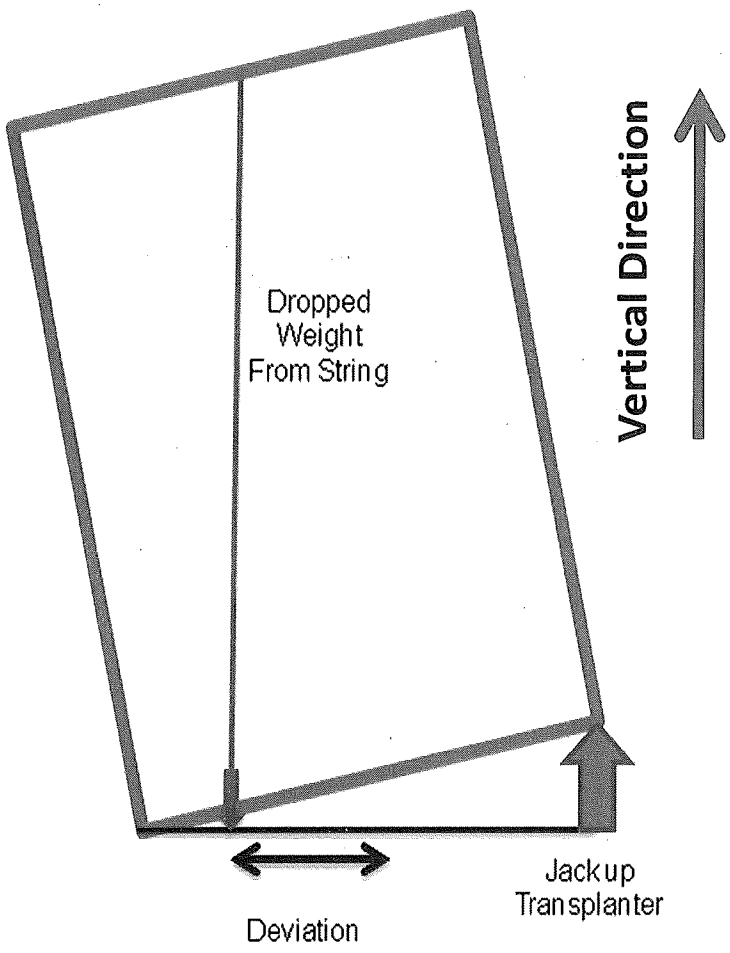


Figure 9. Description of how the tilt sensor was calibrated by jacking up the transplanter and relating the deviation from center of the plumbob to the voltage output of the tilt sensor.

***Micrometer***

The transplanter was connected to the tractor via a standard three-point hitch linkage. A micrometer was used to measure the yaw between the tractor and transplanter so that the tractor GPS antennae could be related to the position of the transplanter position. A micrometer with a travel length of 10 cm, and resolution of 0.01 mm (TD590M-D-100, Transducers Direct, Miamiville, OH) was used to provide the yaw correction signal for motion between the tractor GPS and the transplanter GPS. Figure 10 illustrates the operation of the micrometer, which was bolted to a cantilevered beam

extending backwards from the rear of the tractor. A return spring was added to the micrometer to ensure it would always make contact with the backing plate mounted on the transplanter. This backing plate was welded to the transplanter so that its surface was perpendicular to the rod extending from the micrometer and in a vertical plane parallel to the direction of travel. As the transplanter pivoted with respect to the tractor, the backing plate on the transplanter pushed or released the spring rod on the micrometer. The micrometer was powered by a reference voltage of 5 volts. Calibration was achieved by relating the voltage output to the deviation from center as the transplanter was forced to rotate as seen in figure 11.

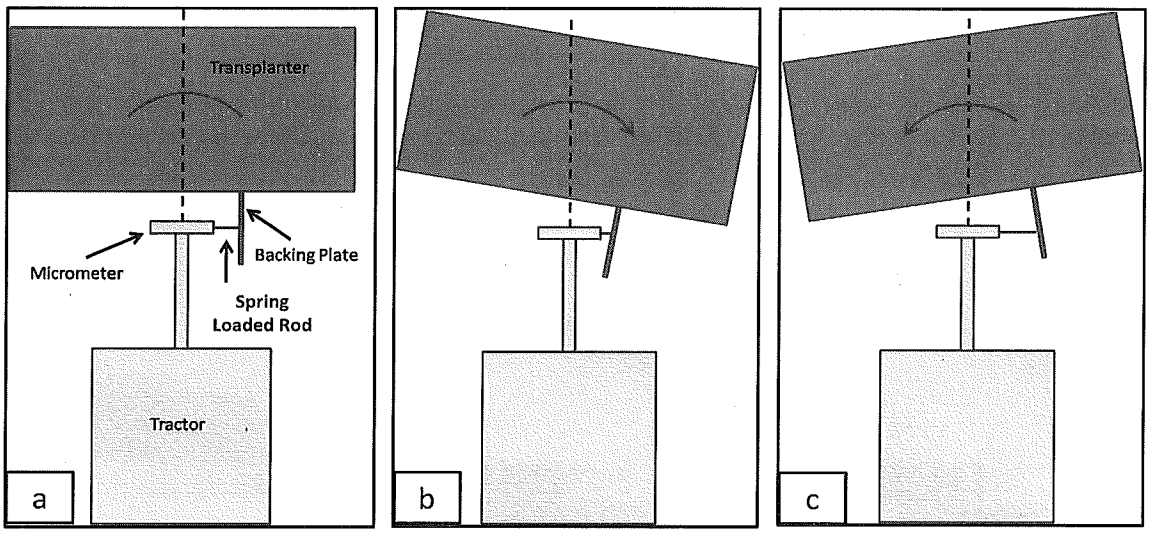


Figure 10. Micrometer (yaw sensor) design; (a) All components of the micrometer (yaw sensor) design. Notice the neutral of the spring rod as it held against the backing plate. (b) and (c) Show the spring rod being pushed in and being extended out away from the neutral position by the back plate depending on the orientation of the transplanter with respect to the tractor. The red arc is an exaggerated depiction of the location of the GPS receiver as it is rotated from side to side. In this study, it is assumed that since the radius of the arc is small, the forward and reverse error is negligible.

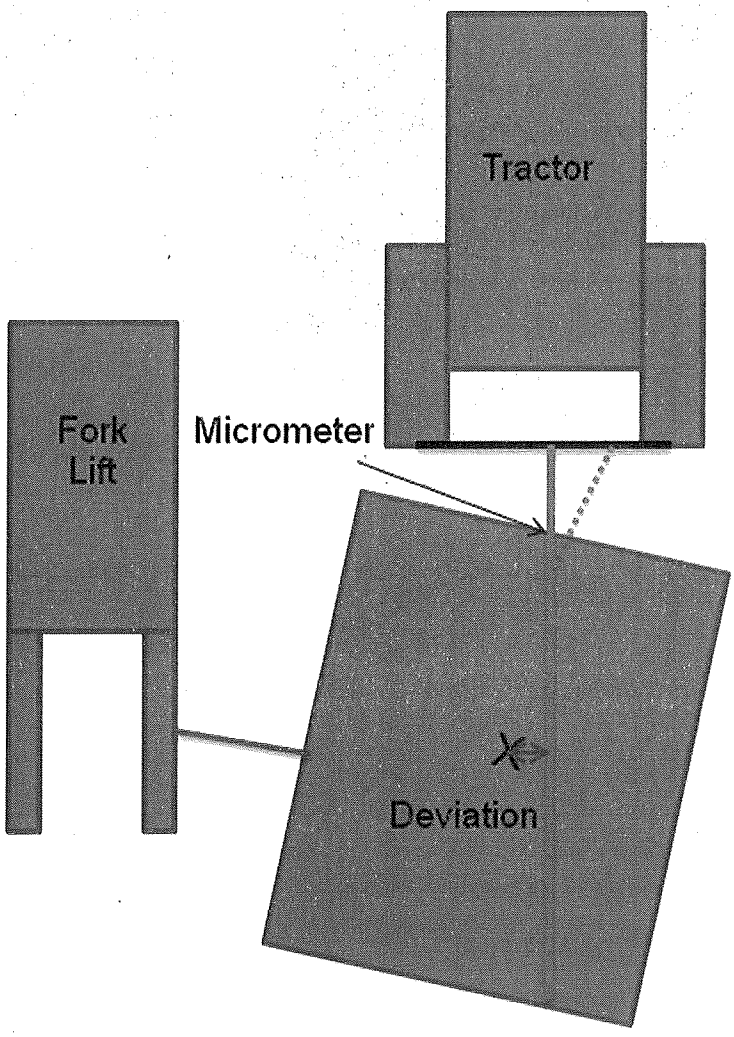


Figure 11. Description of how the micrometer was calibrated by forcing the transplanter to one side with respect to the tractor and relating the deviation from center to the voltage output.

***Planting wheel***

A Holland brand transplanter was chosen due to its popularity for planting processing tomato planting in California. It features the ability to consistently place transplants of non-uniform plant sizes, on top of being cost-effective. The transplanter's planting wheel was fitted with four planting arms and configured to plant each tomato transplant approximately 46 cm apart (Figure 12). This distance was carefully selected to

allow for large plant spacing while still falling within the recommended plant distance (30 – 46 cm) for processing that would maximize productivity. This larger spacing was chosen to deal with knife inertia at high travel speeds, and to use a plant spacing where the rate of the GPS error to plant spacing was small enough to make the GPS system feasible. Ultimately, by maximizing these three factors - the system should be able to offer the best compromise between travel speed and data accuracy.

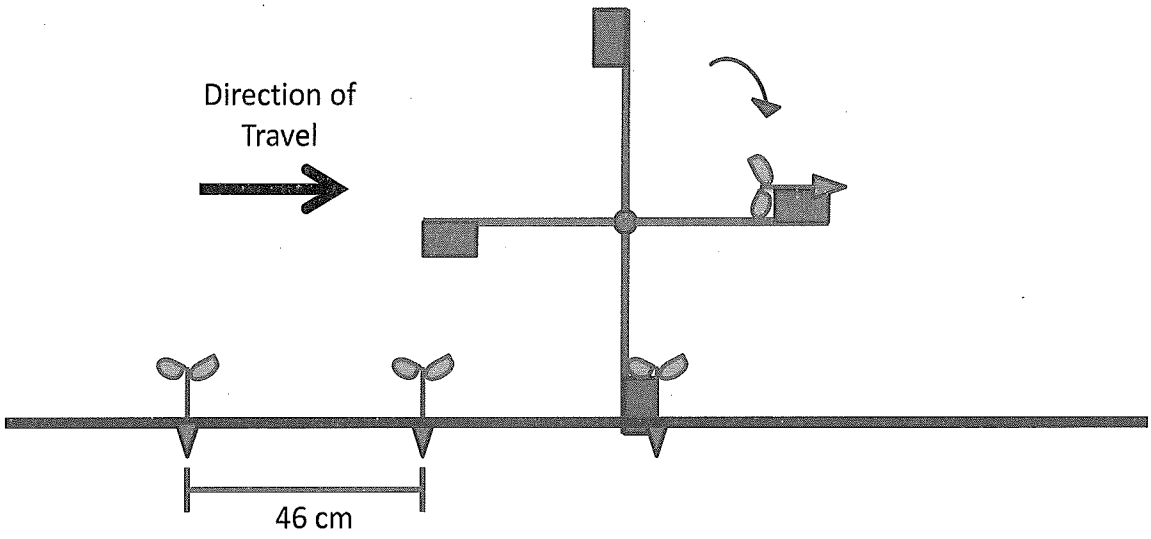


Figure 12. Depiction of how the planting wheel places the tomato transplants in the row and the ultimate spacing between each plant.

***Odometry System***

Transplanter odometry was monitored by using a ground driven wheel that rotated as the transplanter traveled along the row. An optical shaft encoder (model 0622 Grayhill, Inc., IL, USA) was interfaced to this unpowered ground wheel at the rear of the transplanter to provide a resolution of 0.6 mm in the direction of travel (Figure 13). The output of the optical encoder was connected to a quadrature converter circuit which improved the resolution of each pulse. By keeping track of the total number of pulses detected, the distance traveled along the row could be calculated. These data would

ultimately be useful in interpolating plant locations from GPS data and plant detection sensors to create a crop plant map.

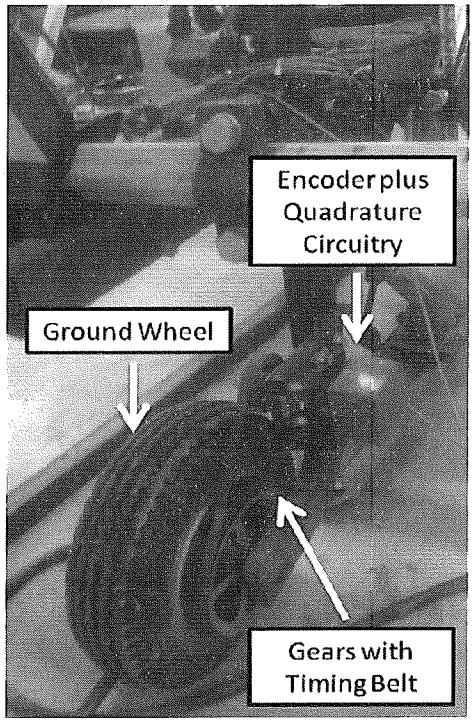


Figure 13. Ground wheel with encoder circuitry.

***Watering System***

In fields where transplants are placed, the temperatures are often warm (~30°C - 35°C) with low to moderate soil moisture levels. To increase survival rate of the transplants, water is distributed among the soil surrounding the plants at transplanting. This was accomplished by using two 55-gallon water tanks, positioned on each side of the transplanter, and as the transplanter planted tomatoes along the row, gravity feed caused water to flow to the plants in order to increase the survival rate. Tubing (1/2" ID) was used to direct sufficient amounts of water to the soil, without flooding the field.

***Data Acquisition Hardware***

Controlling hardware and software required seamless real-time integration to accurately manage the data collection and decision making that is crucial for the project. A National Instruments compact RIO system with field programmable gate array (FPGA) capabilities along with their Labview software was chosen to accomplish this. The FPGA system was able to simultaneously perform multiple parallel processes in real-time to synchronize all the data collection and controlling processes. Three computing systems were simultaneously used in the plant mapping portion of the study. Figure 14 shows how the three systems communicated and how the sensors were connected to each module.

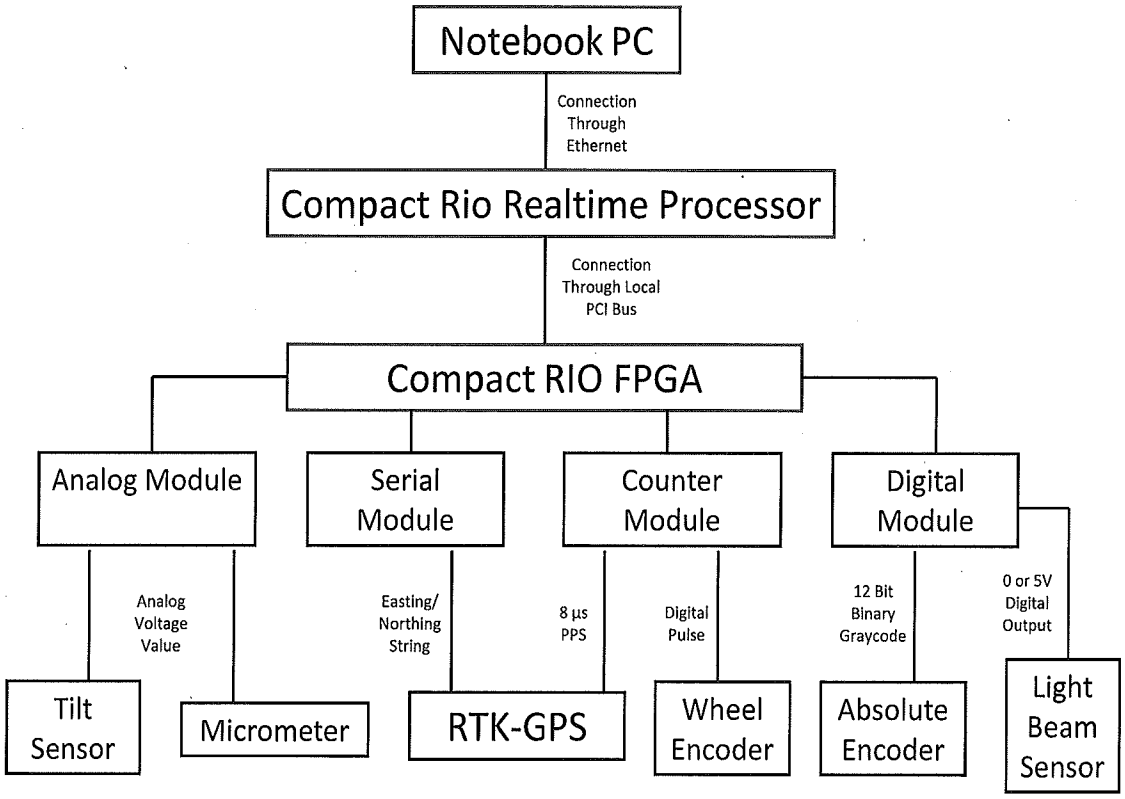


Figure 14. Flowchart describing how the three hardware systems (in red) communicated, and their connections to each module. This also shows the data output of each sensor.

The details of the controller hardware are described below:

- Labview programming was compiled on a laptop computer (Dell D600) where it communicated with a rugged, real-time, embedded controller (cRIO-9004, National Instruments, Austin, TX, USA) through an Ethernet cable.
- The laptop computer allowed access to cRIO status information and access to logged data (via an on-board FTP server). This embedded controller had a low-power CPU (195 MHz Pentium, Intel, Santa Clara, CA, USA) and 512 MB of nonvolatile flash memory storage. The embedded controller was capable of executing deterministic control loops at update rates exceeding 1 kHz.
- The embedded controller was interfaced (via a local PCI bus) to a field programmable gate array (FPGA; cRIO-9104, National Instruments, Austin, TX, USA) which provided truly parallel sensor monitoring capability in real-time (25 ns resolution). The FPGA contained a matrix of 3 million reconfigurable logic gates for parallel processing applications. The processing power of the FPGA was necessary in order to sync the collection of data from all the sensors in real-time.
- The FPGA had 8 expansion ports that allowed for the flexibility of additional data acquisition and controller modules. In this study, the cRIO was upgraded with four data acquisition modules.
- Analog sensor input data were digitized at a 12-bit resolution with a real-time rate of 500 k-samples/s using an input module (NI 9201, National Instruments, Austin, TX, USA) interfaced directly to the FPGA. This analog module included inputs from the tilt sensor as well as from the micrometer.

- An I/O TTL digital module (NI 9403, National Instruments, Austin, TX, USA) was used to input data from the 12 bit absolute encoder as well as the light beam sensor. Since the short 8 microsecond pulse per second (PPS) from the GPS was at the limit in which the digital module could detect a pulse, an additional high-speed pulse detection module (NI 9411, National Instruments, Austin, TX, USA) was used to detect the GPS PPS pulse to ensure it would not be missed. Since this module had two counting inputs, the second input was also used to detect the pulse output of the encoder wheel.
- The cRIO-9104 came with one serial connection. Each of the two GPS systems used required its own serial port so a RS-232 module was used to collect both GPS strings in real-time ((NI 9870, National Instruments, Austin, TX, USA).

***Data Acquisition Software***

All data collection software was written in the G programming language (LabVIEW™ version 8.5, National Instruments, Austin, TX). At run time, the graphical code was automatically translated into text-based VHDL code. The VHDL code was then compiled (ISE Design Suite, Xilinx Inc. San Jose, CA) into a hardware circuit realization and used to reconfigure the FPGA gate array logic. The FPGA was configured to continuously run five simultaneous (i.e. truly parallel) data monitoring tasks in real-time (100 kHz) in order to store instantaneous timing, transplanter odometry, inclination, planter wheel position, GPS PPS and optical sensor (i.e., plant presence) events. The rotation of the planter wheel to a planting position, the presence of a GPS PPS, or the optical sensor blocked by the stem of a plant, would trigger a data archival

event where time, transplanter odometry and pertinent sensor data were written to three respective data files on the nonvolatile flash memory.

### *Global Positioning System Base Station*

RTK GPS requires the presence of a correction signal within a few kilometers of the rover GPS unless there is VRS available. The GPS base station (Trimble model 4700, Trimble Navigation Ltd., Sunnyvale, CA, USA) was placed on the roof of the Western Center for Agriculture Equipment (WCAE) at the University of California, Davis (Latitude: 38.53894946 N , Longitude: 121.7751468 W) to acquire the GPS correction signal necessary for RTK Fixed quality location information. This correction signal was transmitted to the GPS receiver (Model 4700) through a radio antenna (AgGPS 115). An 8 μs duration GPS clock reference pulse (called PPS, for pulse per second) was produced by the GPS receiver in order to synchronize all the connected GPS systems. RTK GPS Fixed quality was achieved for all antenna positions recorded during planting. Fortunately, since the test field was only a few hundred meters away from the base station, an accurate correction signal was obtained.

### *Transplanter GPS*

A GPS receiver was placed directly above the point at which a plant was dropped into the row by the transplanter, minimizing any possible translational errors. The system is comprised of a rover RTK GPS (model MS750, Trimble Navigation Ltd., Sunnyvale, CA, USA), with the GPS mounted 3 m above the planting wheel. Contrary to previous GPS seed planter designs, which mounted the GPS antenna 1 m above ground (Norremark et al., 2007, Ehsani et al., 2004), this mounting position provided a clear

view of the entire sky, unobstructed by tractor or transplanter. As a result, it maximized the potential for utilizing high quality satellite geometries. In addition, the 3 m antenna height also minimized the potential for GPS multipath error. The GPS was configured to output the "NMEA-0183 PTNL, PJK" string which contained the UTM coordinates (Easting and Northing) approximately 100 microseconds after the 8 μs reference pulse - via an RS-232 serial connection.

***Tractor GPS***

The constraint of an additional GPS antenna on the implement would significantly increase the overall cost of the weeding system. Since tractors with high precision GPS systems are becoming more common, the success of this study using the tractor GPS receiver would greatly reduce expenses, while simultaneously improving cost-effectiveness of this system in the field. Unlike the transplanter GPS receiver which was placed directly above the planting location, a second RTK GPS system with console (AgGPS EZ-Guide 500) and GPS (Navcontroller II) was installed on the tractor to compare the difference in performance. The RTK GPS system on the tractor had its own pitch and roll correction, therefore eliminating the need for a tilt sensor on the tractor.

***Plant Detection using Absolute Encoder***

The time of transplant can be determined by measuring the angular position of the planting wheel. The angular position of the planting wheel was monitored using an absolute shaft encoder (12-bit Gray code, ARS 20 Sick Stegmann, Inc., OH, USA) to provide an angular resolution of 0.00154 radians (or about 0.45 mm of travel along the row). The two were connected using a timing belt with a 1:1 gear ratio as depicted in

Figure 15. An absolute encoder provided a unique 12-bit "identification" value for each of the four planting arms when they were correctly positioned to place a transplant into the soil. For instance, the data acquisition hardware would know that a transplant was planted into the bed the moment the encoder value exceeded 1, 1024, 2048 or 3072 (Figure 16). An encoder with binary gray code was preferred over a traditional binary output because any subsequent change in encoder shaft location would only change one bit at a time (Figure 17).

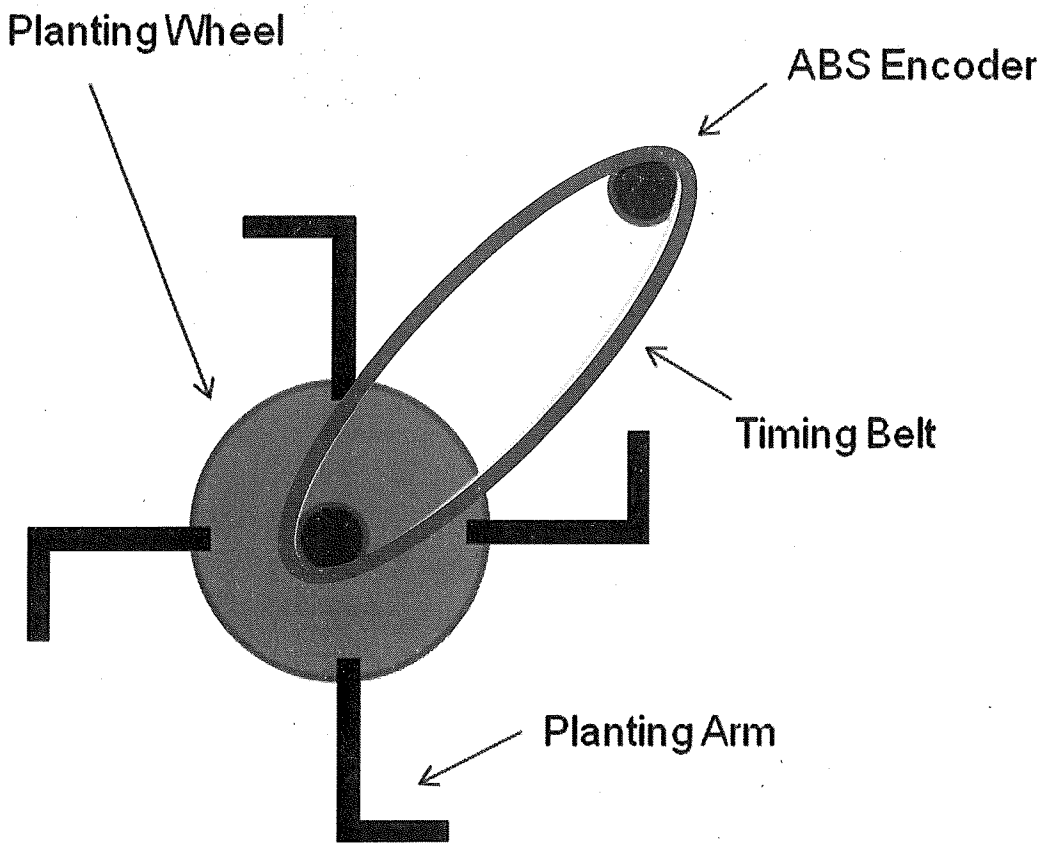


Figure 15. Depiction of how the absolute encoder was attached to the planting wheel through a timing belt connecting two identical gears.

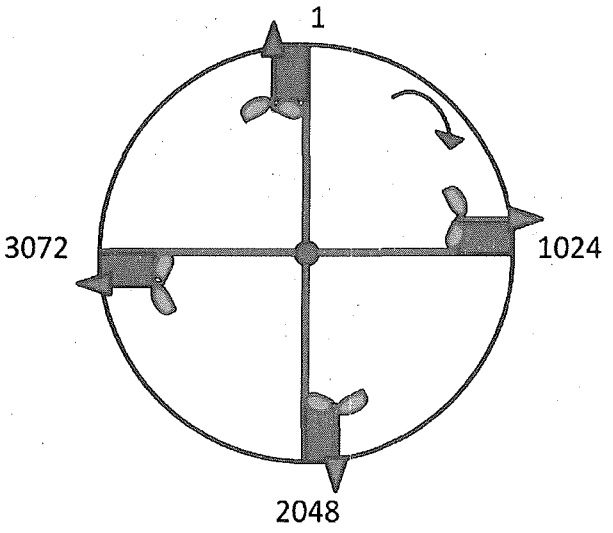


Figure 16. Depiction of how the system would know a plant was just placed in the ground when the absolute encoder value was equal to 1, 1024, 2048 or 3072.

| Integer | Binary Code | Gray Code |
|---|---|---|
| 0 | 0 0 0 | 0 0 0 |
| 1 | 0 0 1 | 0 0 1 |
| 2 | 0 1 0 | 0 1 1 |
| 3 | 0 1 1 | 0 1 0 |
| 4 | 1 0 0 | 1 1 0 |
| 5 | 1 0 1 | 1 0 0 |
| 6 | 1 1 0 | 1 0 1 |
| 7 | 1 1 1 | 1 1 1 |

Figure 17. Comparison of the representation of the integers between 0 and 7 in traditional binary code and gray code. A transition between the integer values of 3 and 4 results in all three binary bits to change while any increment in integer value will only change one bit at a time when represented in gray code. By using gray code, the system becomes much more robust in the event there is a miscommunication between the sensor and the controller.

***Plant Detection using Light Beam Sensor***

A second plant monitoring system, based upon an infrared (880 nm), opposed-mode, optical light beam-based sensor (Mini-Beam models SM31E/SM31R Banner Engineering Corp., Minneapolis, MN) was also evaluated (Figure 18). This sensor was configured to output a TTL pulse when the infrared beam was blocked by the passage of the plant stem. The beam would be positioned approximately 6 cm above the soil, and 1.035 m behind the GPS antenna – to allow the motion of the transplant to stabilize before passing between the sensor's emitter/detector pair. Figure 19 illustrates the voltage signal the light beam sensor outputs during plant detection - and also the absence of said plant. In order to minimize false detection of soil clods, two rollers were installed between the transplanter and the optical sensor to flatten the soil on both sides of the seed line (Figure 20). Furthermore, aluminum casings were built to protect the light beam sensors from dirt clods. To increase their sensitivity to thin objects, a 0.5 mm vertical aperture kit was used.

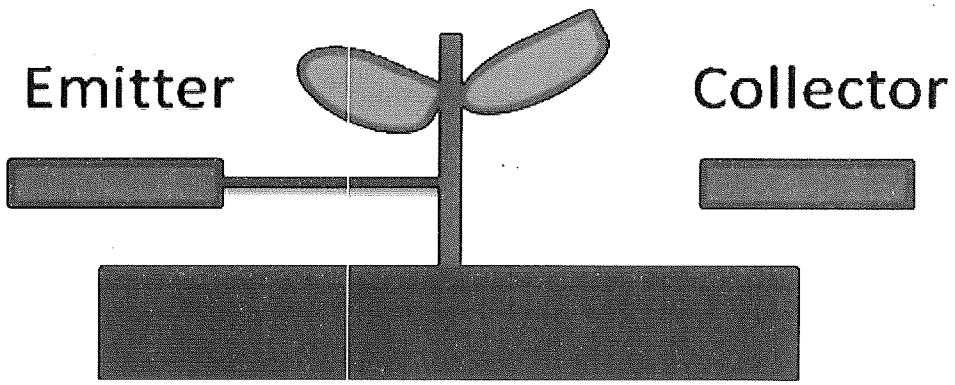


Figure 18. Depiction of how the presence of a plant stem blocks infrared light originating from the emitter to the collector.

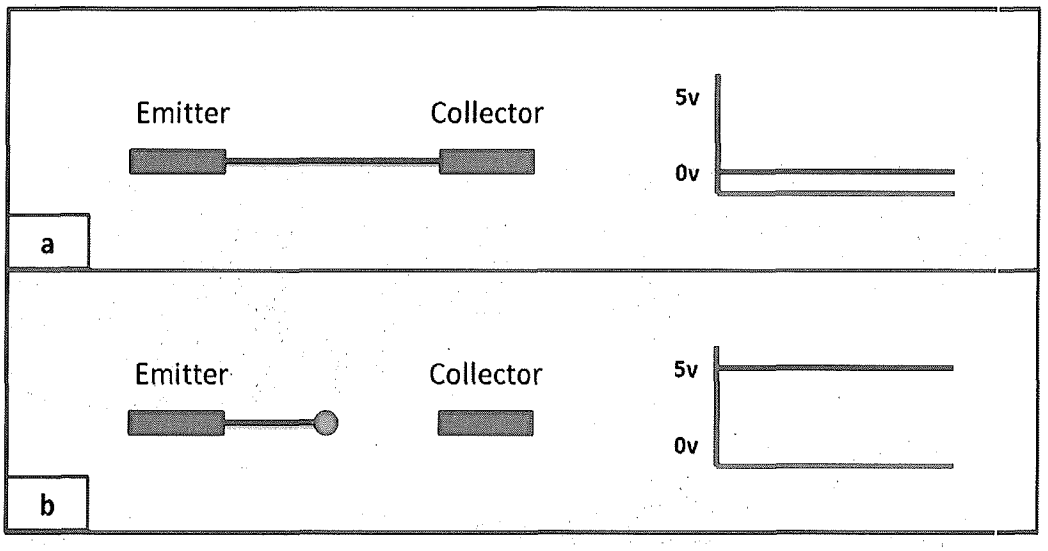


Figure 19. Depiction of how the voltage signal the light beam sensor outputs during plant detection and when there is no plant.

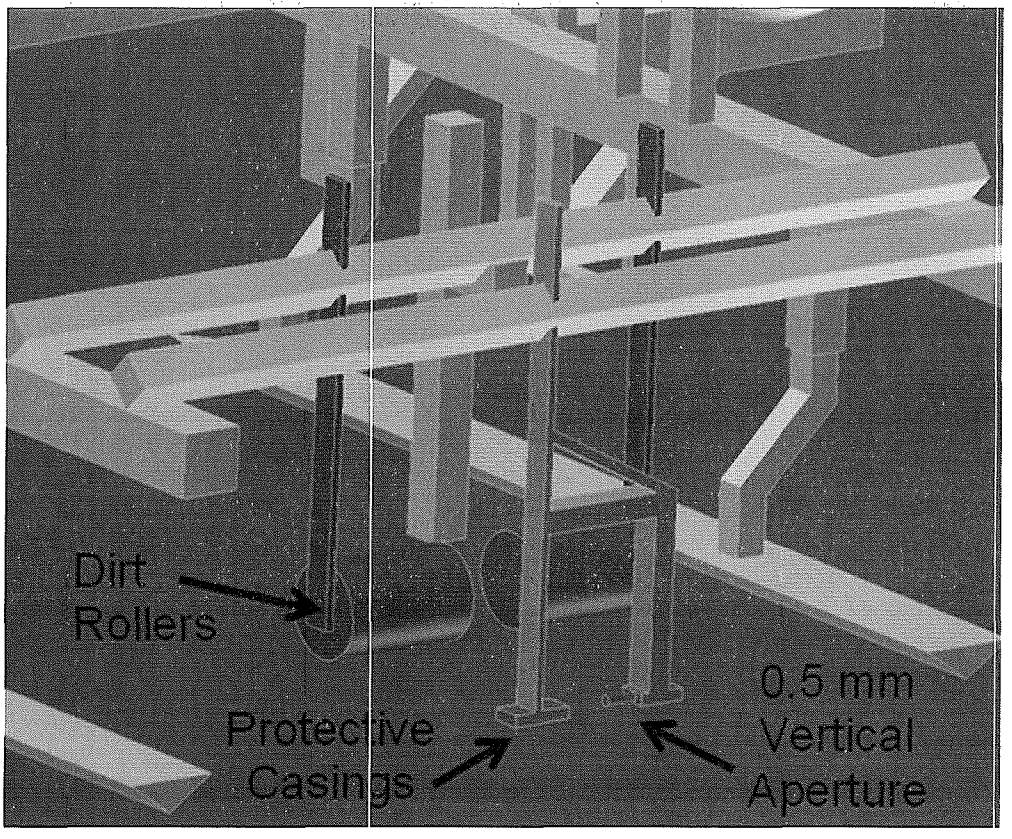


Figure 20. Model showing the location of the dirt rollers with respect to the light beam sensor as well as the protective casing and the 0.5 mm aperture kit used to help with plant detection.

**Weed Removal System**

The automatic within-row weed removal system use a crop plant map for real-time weed knife control. The location of each plant was pre-determined before weeding. Once the plant map was loaded into the weeding system, GPS data were compared in real-time to the location of each plant to determine when to open and close the knives. The weeding implement used the same sled that originally housed the transplanter. In place of the transplanter, pneumatic knives were mounted directly below the transplanter GPS. Auto-guidance was used to ensure the knives traveled along the seed line. Opening and closing the pneumatic weed knives 6.4 cm away from the crop plant was chosen as a compromise between the shortest distance the knives need to travel (to go between open and close configurations), and the widest distance (to minimize crop damage in the event the knives deviated from the seed line). Figure 21 describes the flow chart of the weeding portion of the study. Figure 22 demonstrates how using the plant map to control the knife actuation will (assuming a constant knife speed) create a diamond shape around the transplant, sparing the crop while eliminating all in-row weeds in between crop plants.

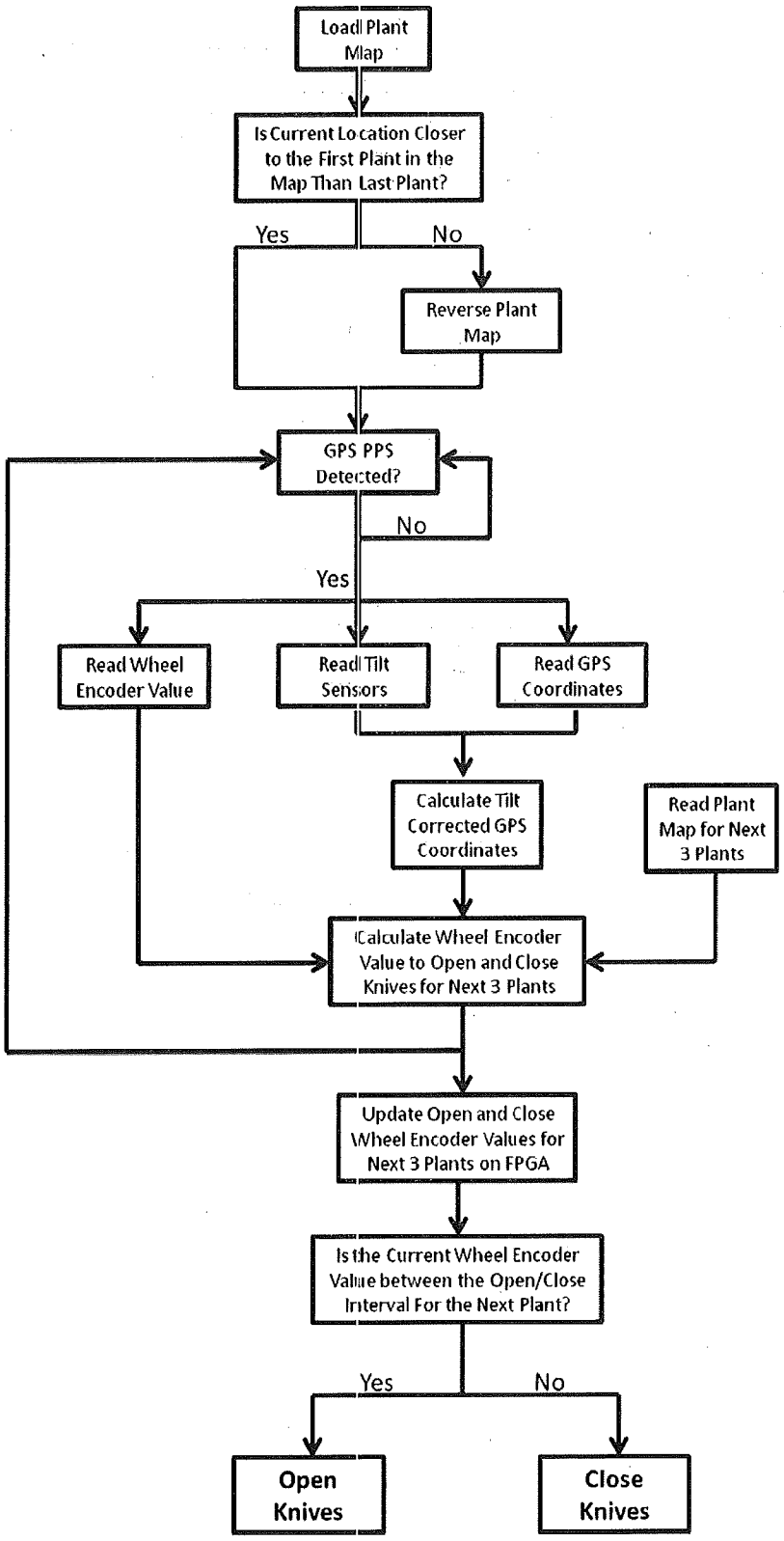


Figure 21. Flowchart of the weeding portion of the study.

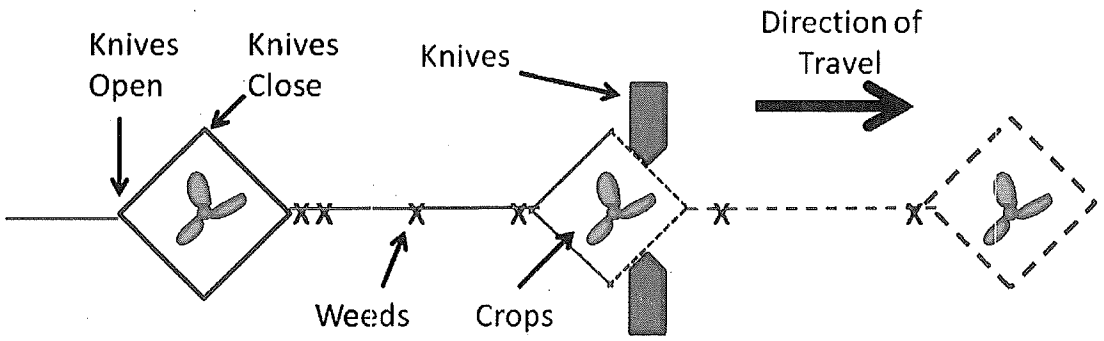


Figure 22. Concept of knives opening before the plant, and closing after it has passed by - creating a diamond around the plant while sparing the transplant. This also shows how the weeds (red X's) in the seedline would be cut while the knives are in the closed position. Also shown is at what point knives open and at what point knives close.

***System of Knives***

Pneumatic powered control systems were used as the method for knife control in this study. The knives were positioned just below ground so that as they traveled along the row in the closed position, they would cut the roots of any plants that obstructed their path. In this study, as the sled traveled away from the beginning of the row, the skis would dig into the row thereby lowering the knives further into the ground. A compressed air tank was attached to provide the pneumatic power to operate the knives. To ensure that the pressure was kept at a minimum of 620 kPa and a nominal of 689 kPa, an air compressor was used to repressurize the tank. The air flow was controlled by solenoid valves (Flow-Tite Model LR 51090, Lumberton, NC) that were controlled by the digital module on the cRIO controller via a relay circuit (Figure 23). The relay circuit consisted of a 5V control signal from the cRIO connected to a solid state relay, which in turn was linked to a mechanical relay (Omron My 2) that controlled a 24V signal. Two pneumatic cylinders (Speedaire Model 1A428, Grainger, Lake Forest, IL) were

connected to the knife linkage that moved the knives either to the open or closed positions (Figure 24). Upon activation by the solenoid valve, the knife took 34 milliseconds to fully open and close. The knife blades were 7.5 cm apart when in the open configuration, and subsequently touching each other when in the closed position.

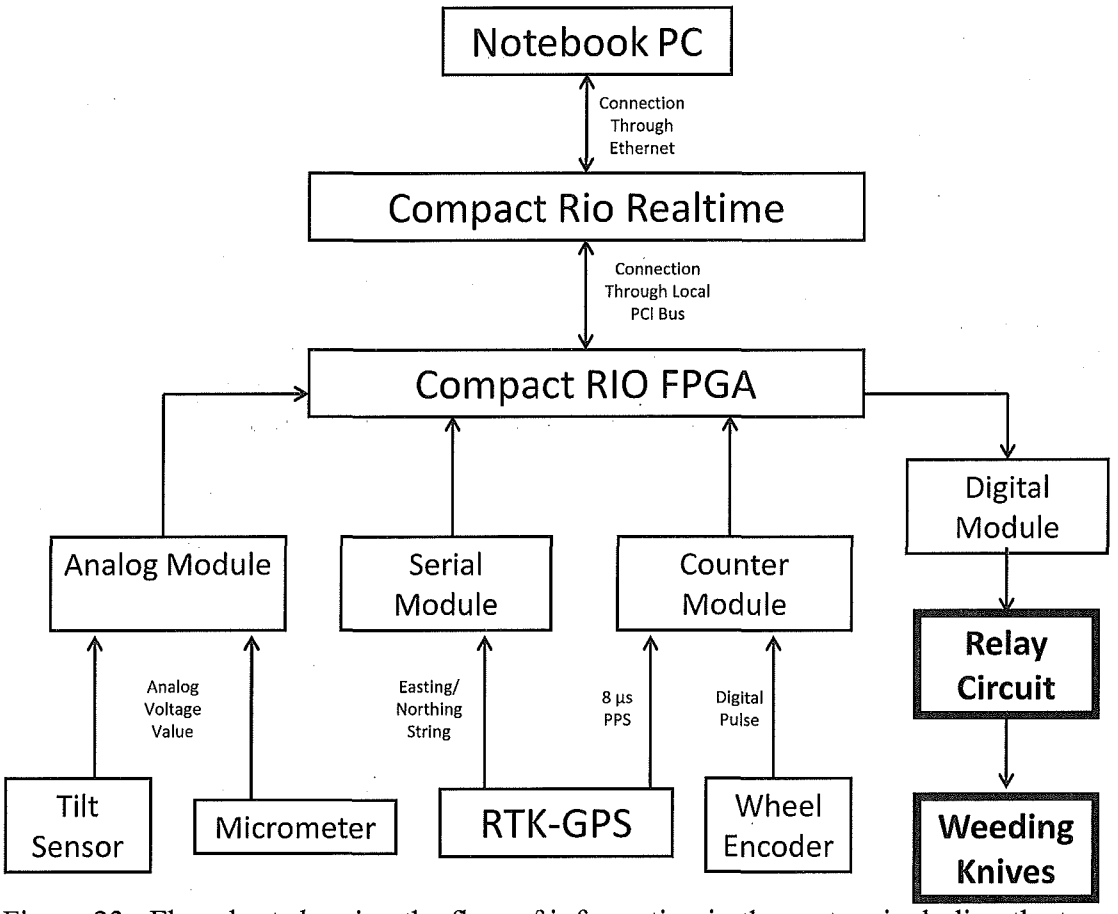


Figure 23. Flowchart showing the flow of information in the system including the type of data and the direction of information flow. Bold items depict those that were added to the original mapping system for weed removal.

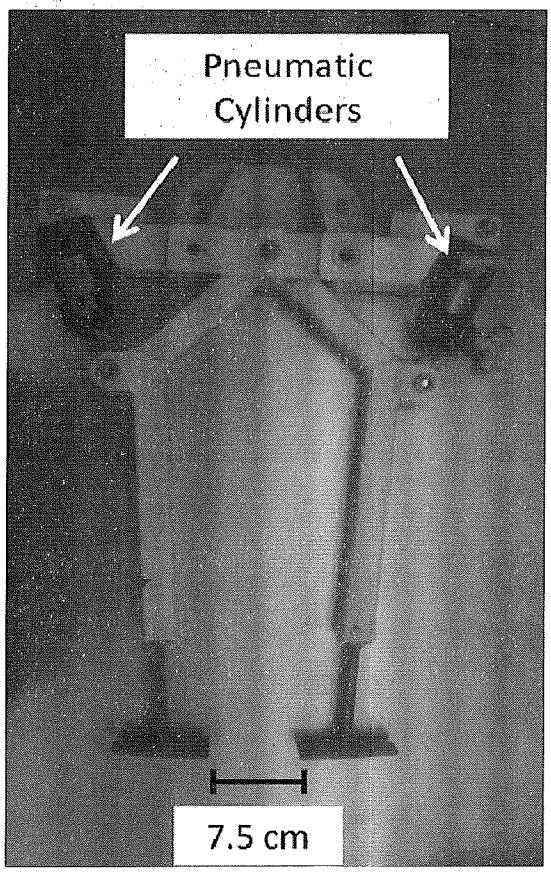


Figure 24. Pneumatic knife linkage showing an open distance of 7.5 cm.

***Plant Map Storage***

A GPS crop plant map, created at planting, was stored onboard the mobile platform for real-time access. A tab deliminated text file was created with a column for both Easting and Northing locations of each plant in the row, and downloaded onto the cRIO flash memory. Prior to each weeding pass, the plant map was loaded into an array in the Labview weeding program. Based on the current location of the weeder, the program would determine in which direction the tractor was traveling by its proximity to the first and last plants in the array. In the event the weeding direction was opposite that of the planting direction, the array would then be reversed so that the first plant switched positions with the last, and vice versa.

### *Current Location Determination*

While the mapping portion of the study could utilize offline GPS data processing to determine the plant locations, the weeding segment required a constant fix on the current GPS location of the system and required real-time processing to determine positioning in real-time. A loop was set up on the FPGA running at a speed of 100 kHz, to monitor the current GPS location. Once the 8 microsecond wide PPS was detected, the loop would wait approximately 80 milliseconds for the GPS data string to come. The end of the GPS string would be indicated by the carriage return. Once this string was read by the FPGA, a program running on the cRIO would parse out the Easting and Northing components from the GPS string.

### *Determining when Knives Open and Close*

Once the current location of the knife was determined, the distance between the next plant in the map and the knives would be calculated. As the ground wheel moved along the row, a second while loop running at 100 kHz on the FPGA would increase the wheel encoder count in relation to the total distance traveled. The difference between the current location and the next plant was then converted into wheel encoder counts, allowing the system to gauge the precise distance at which to open and close the knives. This was accomplished by multiplying the difference in meters by a simple ratio to determine the distance away in wheel encoder counts. By adding this count to the total of the wheel encoder, the controller would know at what ground wheel pulse count the knives would reach the next plant. In the same manner, the pulse count that corresponded to the next two plants would also be calculated and sent to the FPGA. The same loop that read the pulse count conveniently compared the current location to the

position of the next plant. At a distance of 6.4 centimeters before the plant, the knives would open. Likewise, when the program has detected that the knives had passed 6.4 centimeters beyond the plant, the knives would close. After each successive cut, the weeding program would recalculate the plant index and start monitoring the next plant in the row. Upon receiving the current GPS coordinates every second, the cRIO program would send the updated opening and closing ground wheel pulse counts to the FPGA. The cRIO program was also designed with a feedback loop that had the following function: once per second, it would cross-reference the current GPS location with that of the nearest plant, and update the plant number if it had determined that a plant had been skipped. This was required because at the time the tilt sensor was not properly setup and could cause distance calculation errors which resulted in plants being skipped. Essentially, the controller constantly compares the current wheel encoder value to the value at which to open and close the knives. Assuming the total count fell between these saved values, the knives would open.

## Methodology Field Experiments and Data Analysis

### Plant Mapping

Field tests were conducted during the summer of 2008 using processing tomato transplants as the target crop. The field site was located at the Western Center for Agriculture Equipment (WCAE) at the University of California, Davis (Latitude: 38.53894946 N, Longitude: 121.7751468 W). In this test, seven rows were planted (single crop row/bed, 1.5 m bed spacing) with the GPS Transplanter to evaluate the performance of the transplant mapping system. The field layout was such that the rows

faced predominantly in the East-West direction. Each row was planted at a travel speed of 1.6 km/h. The transplanter sled was pulled behind a tractor equipped with an RTK GPS auto guidance system (model EZ-Guide 500, Trimble Navigation Ltd., Sunnyvale, CA, USA). All seedbed preparation operations were also conducted with the same tractor using a common set of GPS AB line coordinates for all tillage and planting operations.

After planting, the actual geo-spatial location of each transplant in a 350 $m^2$ section of the field was estimated using a RTK GPS surveying system (shown as the "real" plant location in Figure 26). For each plant, the bottom tip of the GPS antenna range pole was placed against the plant stem at the soil surface, and held vertical using the aid of a bubble level. The absolute encoder identification values corresponding to the planting positions of the planting wheel were determined by using a subset of 15 plants in rows 1 and 5 as a calibration set. These offset values were then applied to the remaining plants in the study. The performance of the GPS transplant mapping system was evaluated by calculating the geometric distances (Easting and Northing) between the locations mapped by the transplanter and surveyed plant positions. Data were analyzed using typical statistical methods for mean and standard deviation.

***Data Processing***

To estimate the geo spatial location of each transplant, a linear regression technique (based on Ehsani et al., (2004) and modified for transplanter odometry) was employed. This step was required because planting events and GPS signals were asynchronous as shown in figure 25.

The geo-spatial location values were determined offline semi-automatically using a program (written in Visual Basic and implemented in Excel, Microsoft Corp., Redmond, WA) designed to search the plant event database. Once activated, it would find the three position values bounding a planter wheel or optical (light beam) sensor event, match the associated regression coefficients, and finally - calculated the predicted geo-spatial location.

### *Actual Plant Location Determination*

After planting, the actual location of each transplant could be determined by using a handheld control unit (Trimble model TCS1) interfaced to a rover RTK GPS (Trimble model 4700) - and configured for surveying with the GPS antenna mounted on a 2 m range pole. All of the aforementioned was achieved by placing the lower tip of the range pole against the transplant stem at the soil surface, while the pole was held vertical by aid of a bubble level. The NAD 83 (Conus) Datum was used during and after planting for all RTK GPS measurements.

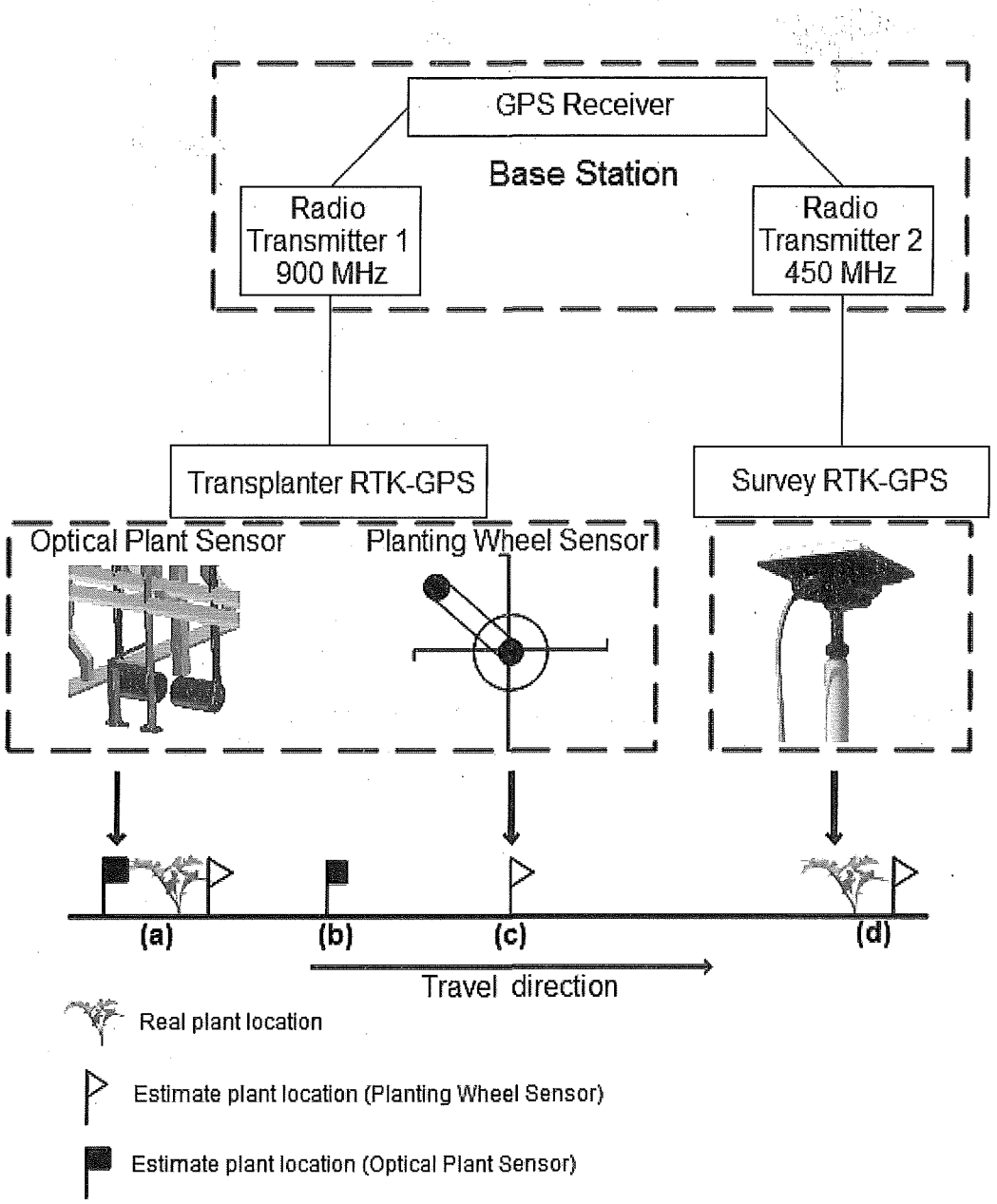


Figure 25. Schematic diagram of the GPS mapping and surveying systems created by Manuel Perez-Ruiz illustrating the asynchronous relationship between GPS data events and plant location.

**Weeding Experiment**

To ensure the efficacy (in terms of seedling survival) and accuracy of the RTK GPS transplant map, a weeding experiment was conducted the day following the transplant experiment. The tractor auto-guidance during weeding was programmed with

the same AB line used in planting and bed creation and the tractor was operated at a 1.6 km per hour travel speed. The weeding program was loaded onto the FPGA along with the plant map with all the GPS coordinates of each plant in the row. In order to determine the accuracy of the knife's cutting mechanisms, a digital video camera (DCR HC96, Sony Corporation, Japan) was attached to the device and used to record the position of the knife with respect to the plant as it passed along the row - at 30 frames per second.

As the knives were opening and closing, camera video was taken and analyzed offline to observe the distance of the blade from the plant – and the efficiency of the weeding system. Once the digital video recording was started, a tape measure was laid down on the soil for distance calibration. The image of the tape measure was used to determine the width in centimeters on the surface of the plant bed corresponding to each pixel on the video image. These procedures were repeated six times for the other six rows.

### *Measuring the Accuracy of the Knife Mechanism*

The effectiveness of weeding can be gauged by the distance between knife and plant at the moment the knives opened and closed. As the blades open while approaching - and close after passing the plant - an area of immunity was created. Regardless of being a transplant or weed, any plant in this diamond-shaped zone will remain intact. Adobe Premier 6.0 software (Adobe, San Jose, CA) was used to export the subset of image frames corresponding to the instant the knives opened and closed. Figure 26 shows a sample frame used to calculate the distance between the knives and the plant during the approach, while Figure 27 shows a sample frame used when the knives closed. At the

beginning of each row, a frame showing the tape measure on the ground was loaded into Image J (National Institutes of Health, Bethesda, Maryland). A line was drawn on the image between the two inch markers on the tape measure that were farthest apart. The length of this line was calculated by converting the number of pixels into a standard measurement unit (using a ratio). The performance of the weeding system was determined by measuring the distance between the leading edge of the knives and the plant upon opening and the trailing edge of the knives to the plant on closing.

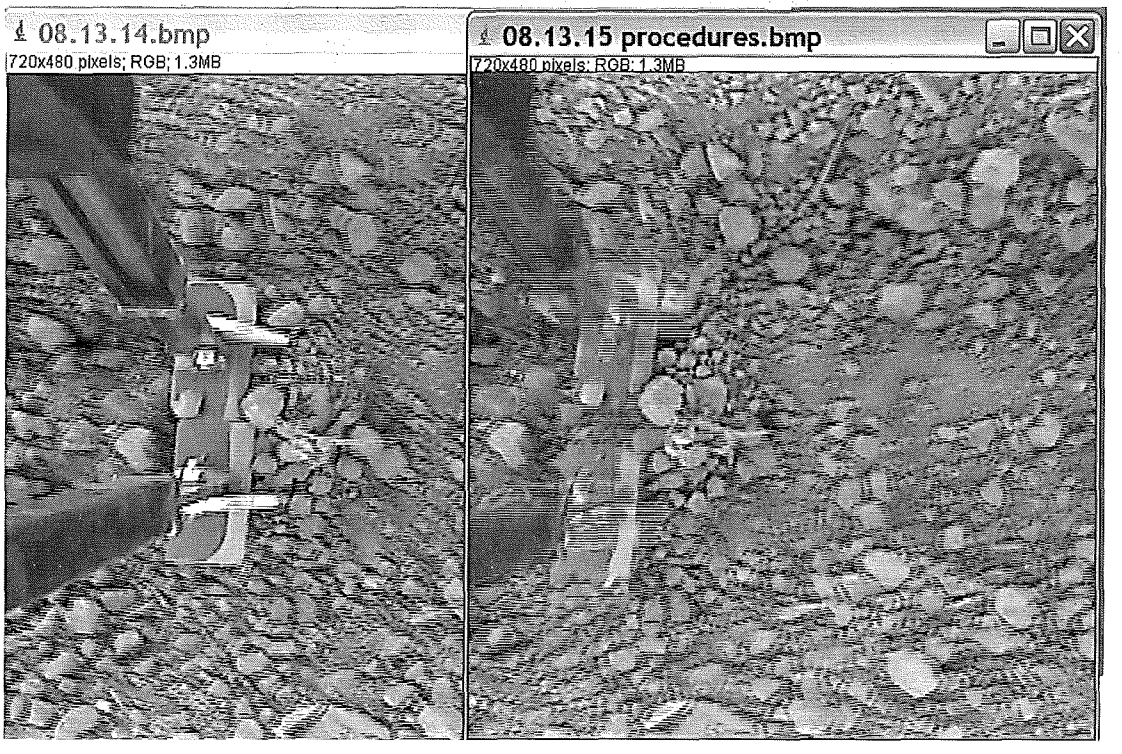


Figure 26. The frame on the right would be used to calculate the distance between the knives and the plant. The frame on the left represents the previous frame in which the knives have not yet started to open.


Figure 27. The frame on the right was used to calculate the distance between the knives and plant upon closing of the knives. The frame on the left represents the frame previous frame in which the knives are still in a position where they avoid plants.

***Determining the Location of the Knife when hidden Underground***

Thus far, data had been collected through visual means. However, this poses a problem when the knives are underground and are not visible. As a result, the location of each knife must be carefully estimated. The position of the knives within each frame will always be constant. As long as two reference points could be visualized, the estimated outline of the knives could be determined (dark shaded parallelogram in figure 28). In this study, the dashed line in figure 28 connects the same two reference points on the mechanical knives that were visible above ground. It was determined from visible images that the edge of the knife was exactly 65 pixels to the right of the midpoint of the

dashed line representing the reference points (represented by the solid line in figure 28). Once the edge of the knife was determined, a line was drawn at an angle of -8.7 degrees as shown by the double dashed line in figure 28 to determine the distance of the knives away from the plant (depicted by the dot in figure 28). The light colored parallelogram in figure 29 represents the theoretical location of the knives at the moment the leading edge would reach the plant if they did not open.

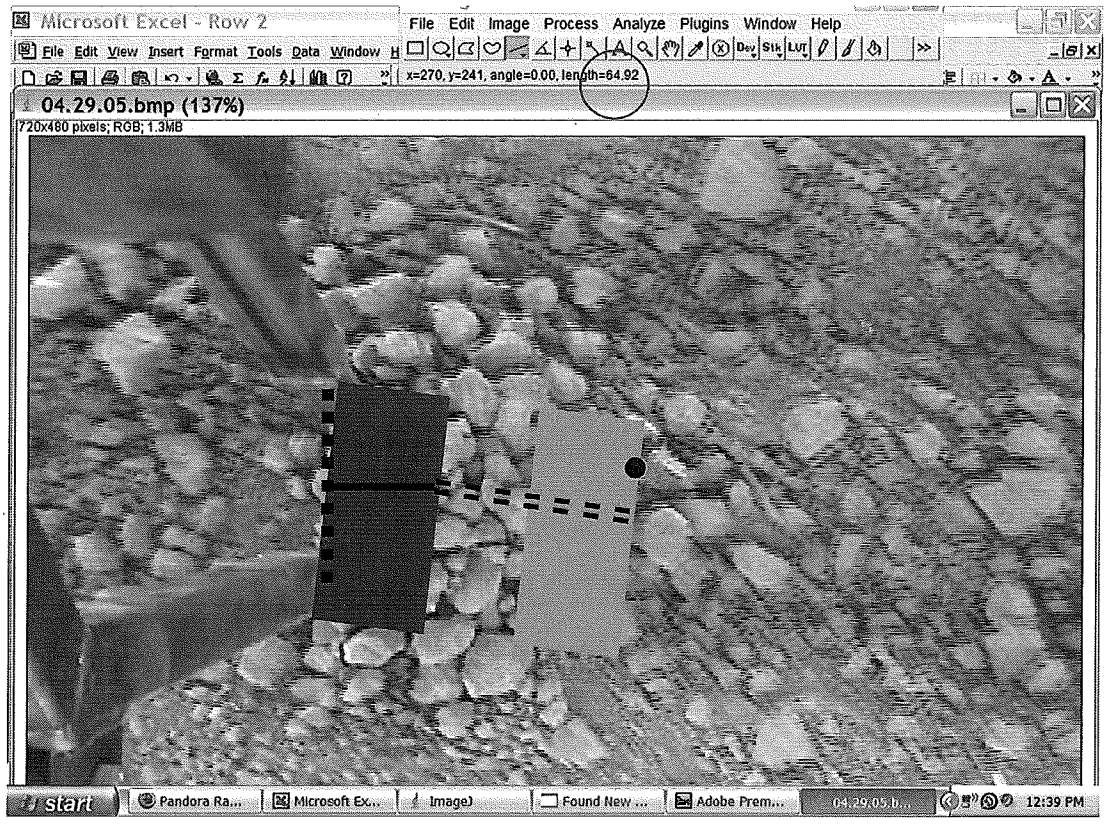


Figure 28. Estimation of distance between the edge of knives and plant when the knives were underground.

# Results and Discussion

## Sensor Calibration

### *Tilt Sensor*

Calibration results for the tilt sensor showed a highly linear relationship and good performance. Equation 5 relates the tilt sensor's voltage value to the pitch while equation 6 was used to relate the tilt sensor's voltage value to the roll. An $R^2$ value of 0.995 and 0.992 were achieved for the pitch and roll calibration, respectively, in this study.

(5)

Forward pitch displacement (meters) = 0.856 (meters/volt) X (pitch voltage) - 2.21 (meters)

(6)

Right roll displacement (meters) = -0.953 (meters/volt) X (roll voltage) + 2.50 (meters)

### *Micrometer*

Calibration results for the yaw level micrometer showed a highly linear relationship and good performance for GPS localization. Figure 29 shows the calibration used to relate the micrometer's voltage to the yaw correction. A positive deviation refers to the right side of the transplanter in the direction of travel.

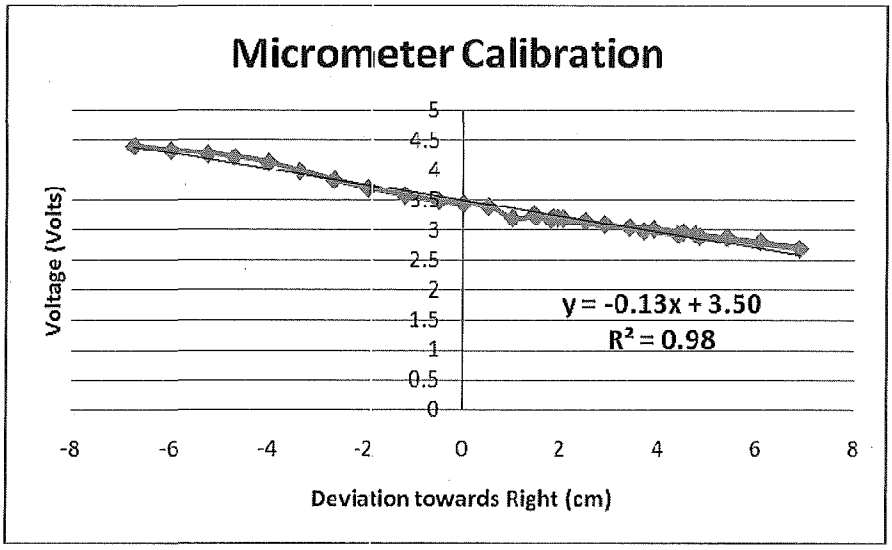


Figure 29. Calibration equation to for yaw correction. The $R^2$ value is shown as well.

***Pixel Width***

A summary of the results for calibration of the pixel resolution for the weeding video was tabulated. Table 1 indicates that the number of pixels correlating to a width of a centimeter on the video averaged 101.4 pixels/cm, with a standard deviation of 2.3 pixels/cm. The depth at which the sled dug into the ground resulted in the difference between each row.

Table 1. Data relating the number of pixels corresponding to the width of one centimeter in the video.

| Row | Pixels/cm |
|---|---|
| **1** | 104.2 |
| **2** | 104.7 |
| **3** | 101.7 |
| **4** | 99.1 |
| **5** | 100.6 |
| **6** | 100.8 |
| **7** | 98.7 |
| **Average** | 101.4 |
| **Stdev** | 2.3 |

**Plant Mapping**

In order to determine the accuracy of the map, the plant GPS locations were compared to the true location measured using the range pole. From the difference in Northing and Easting values, the cross track and along track errors were determined. Figure 30 describes these two types of errors.

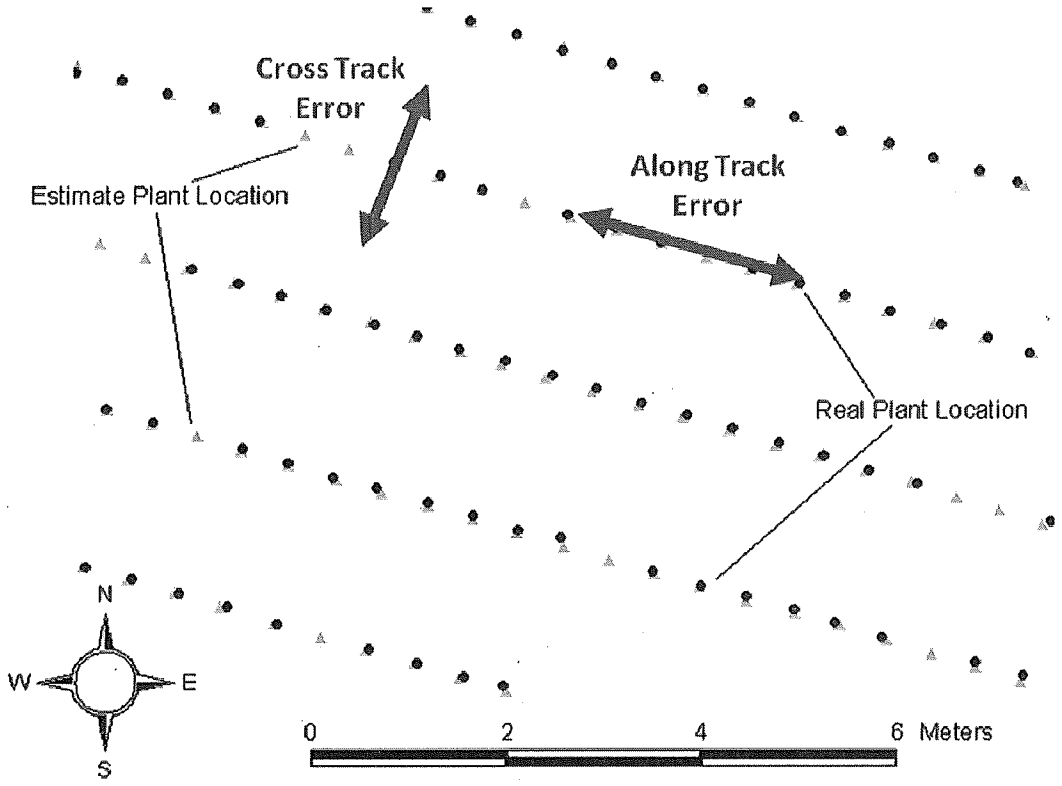


Figure 30. Graphical description of the difference between cross track error and along track error.

### *Map Creation Using Optical Sensor*

An evaluation of the plant map results using the optical sensor was conducted. The locations of 512 plants were determined by means of the range pole. The optical sensor was considerably less reliable than the planting wheel sensor at both sensing plants, and the accuracy at which it determined the position, generating both false positive and false negative errors. Selecting the optimal location for the optical sensor was challenging. Figure 31 illustrates the four different situations that resulted in a plant event (or lack of) by the light beam sensor in the mapping database: (a) the main stem of a plant was correctly detected; (b) failure to detect a plant by the optical sensor because it was planted at an angle or rooted too deep, causing it to pass below the sensor without breaking the light beam; (c) light beam sensor detecting dirt clods because the sensor was placed too low, and (d) one plant causing multiple light beam detections of stems and leaves. The optical (light beam) sensor detected a total of 491 objects, of which 249 (51%) corresponded to the main stems of the tomato plants. Depending upon the soil clod structure, the optical sensor should be placed at a height sufficient to pass above the majority of soil clods. However, to avoid detection of plant foliage or upper branch structures, the sensor must be positioned close to the soil to provide reliable detection of the main stem while avoiding other leaves and stems. In this study, a good position for the optical sensor proved elusive. The optical sensor was only able to successfully detect 48.6% of the transplants planted, with many plants having passed beneath the sensor without blocking the light beam. Additional research is required to develop an automated technique to extract the optical sensor event that corresponds to the main stem of the

transplant, and to distinguish between light beam interruptions due to soil, foliage and stems.

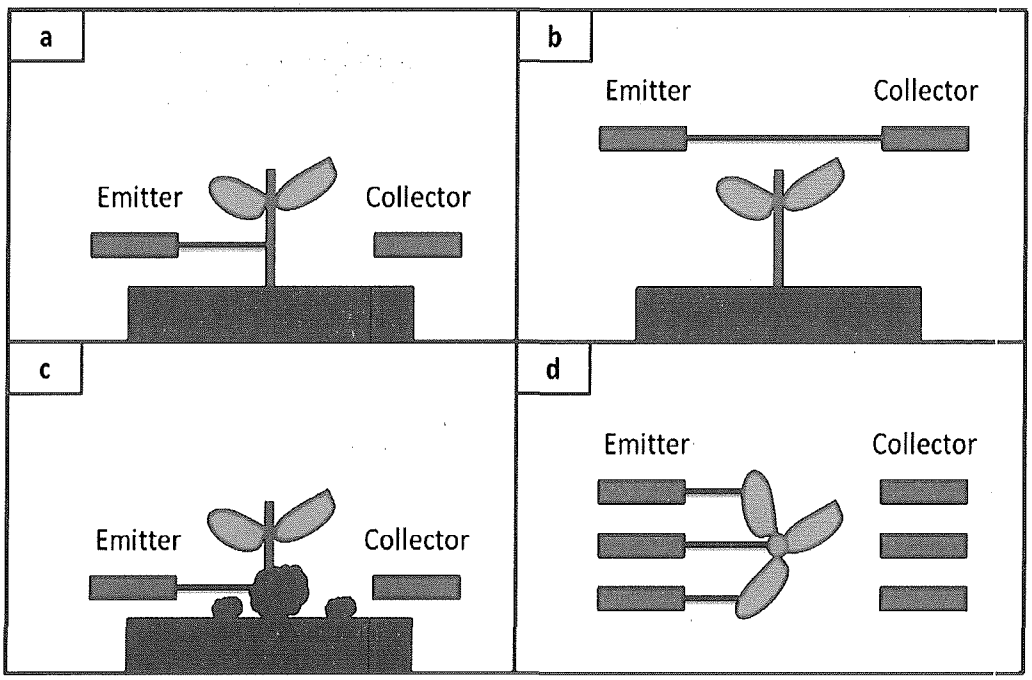


Figure 31. Different scenarios that can be detected by the light beam sensor. a) Shows the accurate detection of a transplant. b) plant was missed because the light beam sensor was too high. c) false detection of a dirt clod when the sensor was placed too low. d) multiple detection when the sensor is placed at a level where leaves in addition to the plant stem are detected.

### *Plant Wheel Sensor for Map Creation*

Using the absolute wheel encoder to determine when the planting wheel reached a planting location was a reliable method to detect when a transplant was placed in the ground. In total, 527 planting wheel events from 7 different rows were automatically logged as a part of the study. A false negative occurred when a plant died or if one was not placed into the planting fingers. The false negative error rate for the planting wheel sensor was a testament to the skill of the transplanting team during planting. In

commercial practice, experienced workers are used. Elimination of this type of error would require an additional sensor to confirm that a plant was actually placed in the planting arm. False negatives might also be a function of the transplant survival rate. Plant survival rate was not an issue in this study because the locations of each plant were surveyed immediately after planting. The planting wheel sensor proved to be generally reliable and produced no false positive errors during this study.

### *Mapping Data Using Transplanter GPS without Tilt Correction*

The transplant map showing the estimated plant locations automatically generated from the plant wheel sensor data were compared to the surveyed plant locations as shown in figure 32. The data in Table 2 shows the absolute difference between the surveyed plant positions and the estimates automatically generated using the transplanter GPS in combination with the plant wheel sensor (absolute encoder) and the optical sensor (light beam) for the 7 rows in the test plot when transplanter inclination is ignored.

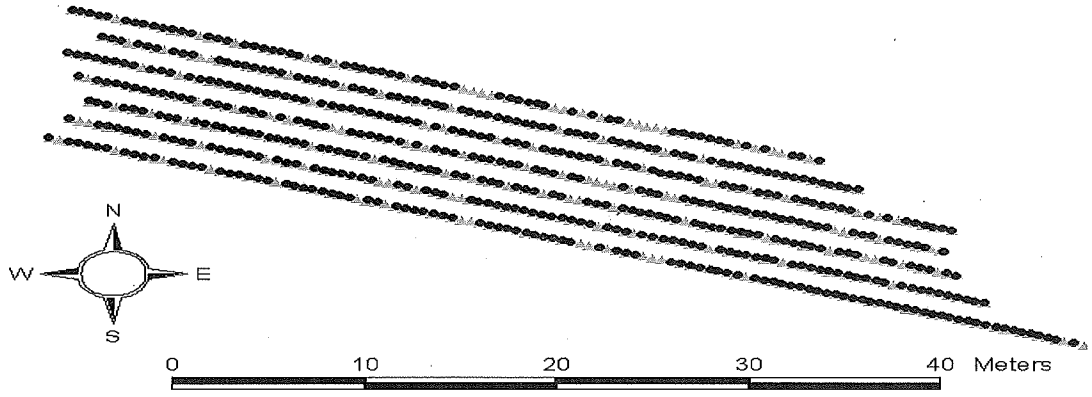


(a)

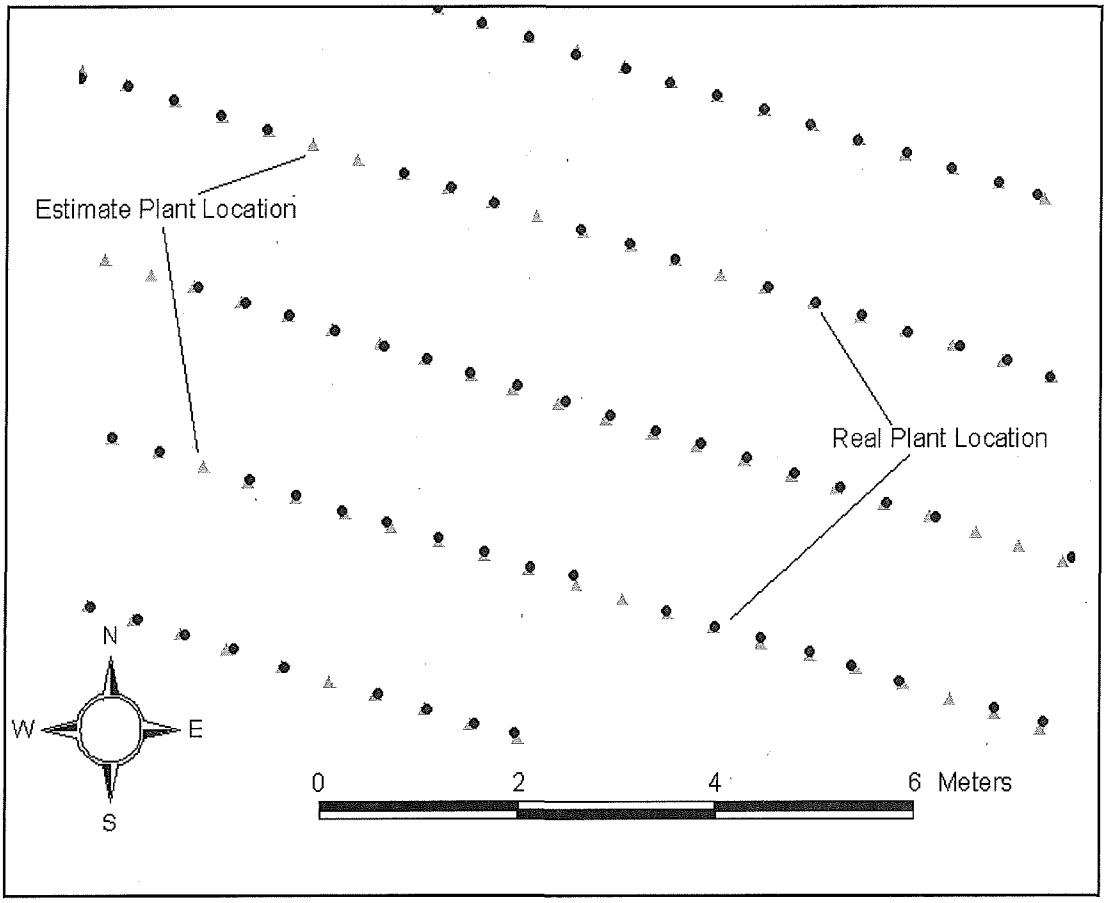


(b)

Figure 32. Map graphics created by Manuel Perez-Ruiz shows an example transplant location map. a) Plant location map for the 7 test rows using the RTK-GPS transplanter and the planting wheel sensor and b) view in detail of the surveyed plant location and estimated plant location using the planting wheel sensor.

Table 2. Geo-spatial mapping performance of plant wheel and optical plant sensors without pitch and roll correction.

| | Mean Absolute Deviation (cm) | | | | | | Std. Dev. (cm) | | | | | |
|---|---|---|---|---|---|---|---|---|---|---|---|---|
| | Absolute Encoder | | | Light Beam Sensor | | | Absolute Encoder | | | Light Beam Sensor | | |
| Rows Planting | Plants | Northing | Easting | Plants | Northing | Easting | Plants | Northing | Easting | Plants | Northing | Easting |
| 1 | 82 | 4.6 | 5.68 | 40 | 4.63 | 4 | 82 | 1.92 | 2.47 | 40 | 2.21 | 3.01 |
| 2 | 83 | 1.65 | 3.91 | 24 | 5.26 | 3.79 | 83 | 1.11 | 1.87 | 24 | 1.57 | 3.02 |
| 3 | 79 | 1.6 | 5.11 | 38 | 4.66 | 2.26 | 79 | 1.09 | 2.25 | 38 | 1.61 | 1.58 |
| 4 | 73 | 3.24 | 6.26 | 33 | 5.71 | 2.22 | 73 | 2.06 | 2.51 | 33 | 3.18 | 1.65 |
| 5 | 65 | 2 | 1.72 | 31 | 2.37 | 5.17 | 65 | 1.3 | 1.5 | 31 | 1.32 | 2.61 |
| 6 | 72 | 3.1 | 1.73 | 41 | 5.51 | 6.86 | 72 | 0.48 | 2.82 | 41 | 1.15 | 2.82 |
| 7 | 58 | 4.7 | 2.12 | 27 | 4.97 | 5.92 | 58 | 1.54 | 1.48 | 27 | 1.55 | 2.82 |
| Average | 73 | 2.98 | 3.79 | 33 | 4.73 | 4.32 | 73 | 1.36 | 2.13 | 33 | 1.80 | 2.50 |

***Mapping Data Using Transplanter GPS with Tilt Correction***

When tilt correction was considered in the map determination, accuracies improved. Table 3 shows the same set of data once tilt correction was taken into consideration. Since the rows were predominantly oriented in the East/West direction, the error in Northing values is dominated by inclination and GPS errors. The data show that correction for inclination is crucial when attempting to develop centimeter accuracy maps. For example, the absolute error in Northing dropped from an average of 3.0 cm to 1.2 cm for the plant wheel sensor when the GPS locations were corrected for transplanter inclination. A similar improvement in performance was observed for the optical sensor Northing values. These results concur with those observed by Norremark et al. (2003), where he found the RMS error of a stationary RTK GPS unit over the course of 24 hours to be 0.95 cm. He also demonstrated that inclination sensing is important for RTK GPS level accuracy when using a transplanter to generate plant maps.

The errors in the transplant map were also evaluated in the travel direction. The absolute error in Easting after correction for inclination was 3.0 cm for the plant wheel sensor, and 3.7 cm for the optical sensor. The error values in estimating Easting were considerably higher than those of Northing. However, this increase was expected due to the fact that the travel direction was aligned with the Easting direction - and errors associated with accurate determination of plant placement usually occur in the travel direction. The data show a small advantage in both accuracy and precision of the plant wheel sensor over the optical sensor. Coupled with the high false positive error rate (almost 50%) of the optical plant sensor, the data indicate that using an absolute encoder on the transplanting wheel shaft resulted in superior performance.

The errors between the seven rows for the plant wheel sensor map ranged from 0.8 to 2.1 cm in the Northing direction, and 1.6 to 3.8 cm in the Easting direction. These levels of performance are similar to those obtained by Ehsani et al. (2004), and Griepentrog et al. (2005) in their work on automatic RTK GPS mapping of seeds during planting. Given the GPS error in the reference (survey) method, these results are reasonably good and demonstrate the feasibility of developing a RTK GPS enabled transplanter for the automatic generation of centimeter accuracy planting maps for transplanted crops.

Table 3. Geo-spatial mapping performance of plant wheel and optical plant sensors with pitch and roll correction.

| | Mean Absolute (cm) | | | | | | Std. Dev. (cm) | | | | | |
|---|---|---|---|---|---|---|---|---|---|---|---|---|
| | Absolute Encoder | | | Light Beam Sensor | | | Absolute Encoder | | | Light Beam Sensor | | |
| Rows Planting | Plants | Northing | Easting | Plants | Northing | Easting | Plants | Northing | Easting | Plants | Northing | Easting |
| 1 | 82 | 0.83 | 3.83 | 40 | 1.59 | 3.03 | 82 | 0.77 | 2.21 | 40 | 1.05 | 1.74 |
| 2 | 83 | 0.86 | 2.31 | 24 | 3.82 | 2.93 | 83 | 0.7 | 1.61 | 24 | 1.65 | 2.24 |
| 3 | 79 | 2.12 | 2.56 | 38 | 2.4 | 3.74 | 79 | 1.34 | 2.25 | 38 | 1.51 | 2.9 |
| 4 | 73 | 1.72 | 3.76 | 33 | 1.58 | 3.48 | 73 | 1.18 | 2.69 | 33 | 0.83 | 2.43 |
| 5 | 65 | 0.73 | 1.57 | 31 | 1.11 | 3.36 | 65 | 0.25 | 0.81 | 31 | 1.07 | 2.31 |
| 6 | 72 | 1.01 | 3.53 | 41 | 1.11 | 4.45 | 72 | 0.79 | 1.82 | 41 | 0.87 | 2.18 |
| 7 | 58 | 1.13 | 3.54 | 27 | 1.15 | 4.85 | 58 | 0.78 | 1.55 | 27 | 0.98 | 2.07 |
| Average | 73 | 1.20 | 3.01 | 33 | 1.82 | 3.69 | 73 | 0.83 | 1.85 | 33 | 1.14 | 2.27 |

### *Map Creation Using Tractor GPS*

GPS transplant maps were also created using the RTK-GPS system mounted on the tractor and the results compared to the map created with the transplanter GPS. The tractor GPS outputs coordinates that are already corrected for tilt, however, since the tractor GPS estimated a GPS position that was under the tractor and not directly under the transplanter itself, it was not as accurate as the transplanter GPS at creating an accurate map. Table 4 demonstrates the mapping error using the absolute encoder in plant detection and the tractor GPS as the location identifier. On the other hand, Table 5 shows the mapping error using the light beam sensor and the tractor GPS as the location

identifier. It should be noted that using the absolute encoder once again proved superior to the light beam sensor when determining the plant map. Upon close examination of light beam sensor errors, it appears that each row has shifted in the Northing direction by about 20 cm. A portion of this error can be attributed to the inaccurate measurement of the distance between the light beam sensor and the tractor GPS. In addition to this, the same datum was shared between the range pole and the transplanter GPS - while the tractor GPS used an alternate datum, resulting in additional errors in this study. In the Easting direction, the differences in error between the 7 rows were much larger than in the Northing direction. This was likely the case because the tractor traveled primarily in the Easting direction. We would thus expect a larger difference in error for the Easting direction.

Figures 33 and 34 show the comparison of the Northing and Easting errors between the transplanter GPS and the tractor GPS using the absolute encoder respectively. It was hypothesized that the average and standard deviation of the error was lower in both the Northing and Easting directions when the transplanter GPS was used because it was positioned directly above the location of the plant drop, while the tractor GPS was shifted 259 cm from this location. The change in relative position of the tractor GPS to the plant release location likely caused this rise in error. Figures 35 and 36 show the comparison of the Easting and Northing error between the transplanter GPS and the tractor GPS using the light beam sensor. The error in the Northing direction was particularly poor when using the light beam sensor respectively, most likely due to the inaccurate offset determination between the tractor GPS and the plant location. When the error from row 1 was used to correct for this inaccuracy, the error for 5 of the remaining

six rows improved greatly. Despite the correction, the transplanter GPS performed better in this study. Row 3 data were very different from the other rows. This could be due to a major failure in the use of the light beam sensor or a mistake when collecting or analyzing the data.

Table 4. Error of Tractor GPS using ABS Encoder for plant detection. (cm)

| GPS Tractor- Absolute Encoder-Row 1 | | | | |
|---|---|---|---|---|
| | Northing | Easting | ABS Northing | ABS Easting |
| Average | -0.84 | -0.98 | 2.55 | 2.60 |
| Stdev | 3.13 | 3.10 | 1.98 | 1.95 |
| **GPS Tractor- Absolute Encoder-Row 2** | | | | |
| | Northing | Easting | ABS Northing | ABS Easting |
| Average | 0.93 | -1.30 | 2.83 | 2.69 |
| Stdev | 3.40 | 3.19 | 2.08 | 2.13 |
| **GPS Tractor- Absolute Encoder-Row 3** | | | | |
| | Northing | Easting | ABS Northing | ABS Easting |
| Average | 3.40 | 2.02 | 3.92 | 2.45 |
| Stdev | 3.20 | 2.66 | 2.53 | 2.26 |
| **GPS Tractor- Absolute Encoder-Row 4** | | | | |
| | Northing | Easting | ABS Northing | ABS Easting |
| Average | 0.29 | -7.40 | 2.49 | 7.44 |
| Stdev | 3.12 | 4.07 | 1.88 | 3.98 |
| **GPS Tractor- Absolute Encoder-Row 5** | | | | |
| | Northing | Easting | ABS Northing | ABS Easting |
| Average | 0.86 | -0.82 | 2.24 | 2.16 |
| Stdev | 2.60 | 2.79 | 1.55 | 1.94 |
| **GPS Tractor- Absolute Encoder-Row 6** | | | | |
| | Northing | Easting | ABS Northing | ABS Easting |
| Average | 1.60 | 5.49 | 2.59 | 5.61 |
| Stdev | 2.73 | 3.41 | 1.81 | 3.20 |
| **GPS Tractor- Absolute Encoder-Row 7** | | | | |
| | Northing | Easting | ABS Northing | Easting |
| Average | 0.17 | 5.10 | 2.41 | 5.42 |
| Stdev | 3.19 | 4.33 | 2.07 | 3.91 |
| **Combined Average** | | | | |
| | Northing | Easting | ABS Northing | ABS Easting |
| Average | 0.91 | 0.30 | 2.72 | 4.05 |
| Stdev | 3.05 | 3.36 | 1.99 | 2.77 |

Table 5. Error of Tractor GPS using LB Sensor for plant detection. (cm)

| GPS Tractor- Light Beam Sensor-Row 1 | | | | |
|---|---|---|---|---|
| | Northing | Easting | ABS Northing | ABS Easting |
| Average | -23.93 | 28.82 | 23.93 | 28.82 |
| Stdev | 3.89 | 2.96 | 3.89 | 2.96 |
| **GPS Tractor- Light Beam Sensor-Row 2** | | | | |
| | Northing | Easting | ABS Northing | ABS Easting |
| Average | -20.08 | -6.33 | 20.08 | 6.38 |
| Stdev | 3.60 | 3.62 | 3.60 | 3.53 |
| **GPS Tractor- Light Beam Sensor-Row 3** | | | | |
| | Northing | Easting | ABS Northing | ABS Easting |
| Average | -6.53 | -18.71 | 6.67 | 18.71 |
| Stdev | 3.58 | 3.92 | 3.30 | 3.92 |
| **GPS Tractor- Light Beam Sensor-Row 4** | | | | |
| | Northing | Easting | ABS Northing | ABS Easting |
| Average | -22.12 | -6.72 | 22.12 | 7.04 |
| Stdev | 4.09 | 4.76 | 4.09 | 4.24 |
| **GPS Tractor- Light Beam Sensor-Row 5** | | | | |
| | Northing | Easting | ABS Northing | ABS Easting |
| Average | -21.97 | 0.91 | 22.68 | 2.93 |
| Stdev | 5.46 | 3.80 | 3.76 | 2.54 |
| **GPS Tractor- Light Beam Sensor-Row 6** | | | | |
| | Northing | Easting | ABS Northing | ABS Easting |
| Average | -21.63 | 6.44 | 21.63 | 6.44 |
| Stdev | 3.62 | 3.09 | 3.62 | 3.09 |
| **GPS Tractor- Light Beam Sensor-Row 7** | | | | |
| | Northing | Easting | ABS Northing | ABS Easting |
| Average | -23.09 | 7.23 | 23.09 | 7.24 |
| Stdev | 3.94 | 4.51 | 3.94 | 4.50 |
| **Combined Average** | | | | |
| | Northing | Easting | ABS Northing | ABS Easting |
| Average | -19.91 | 1.66 | 20.03 | 11.08 |
| Stdev | 4.03 | 3.81 | 3.74 | 3.54 |

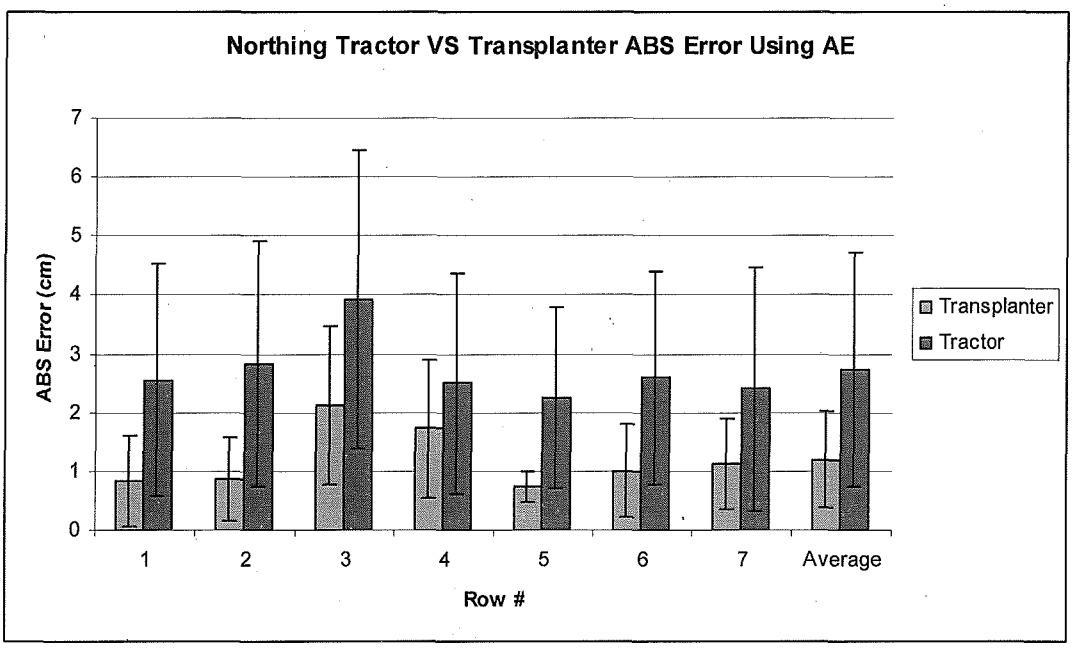


Figure 33. ABS mapping error comparison in the Northing direction of the Tractor versus Transplanter GPS using Absolute Encoder.

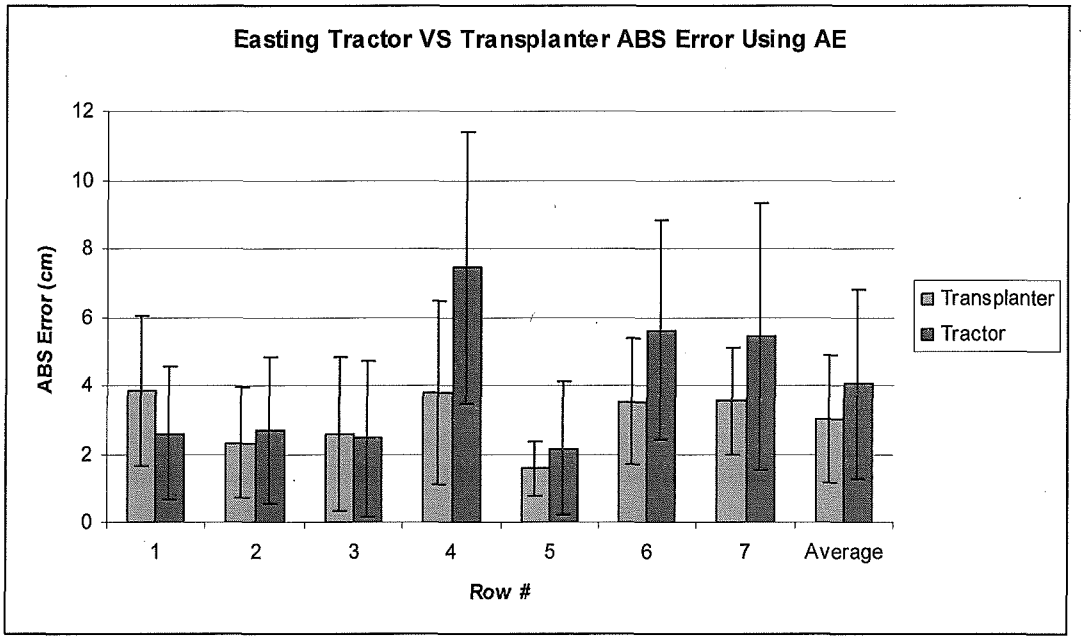


Figure 34. ABS mapping error comparison in the Easting direction of the Tractor versus Transplanter GPS using Absolute Encoder.

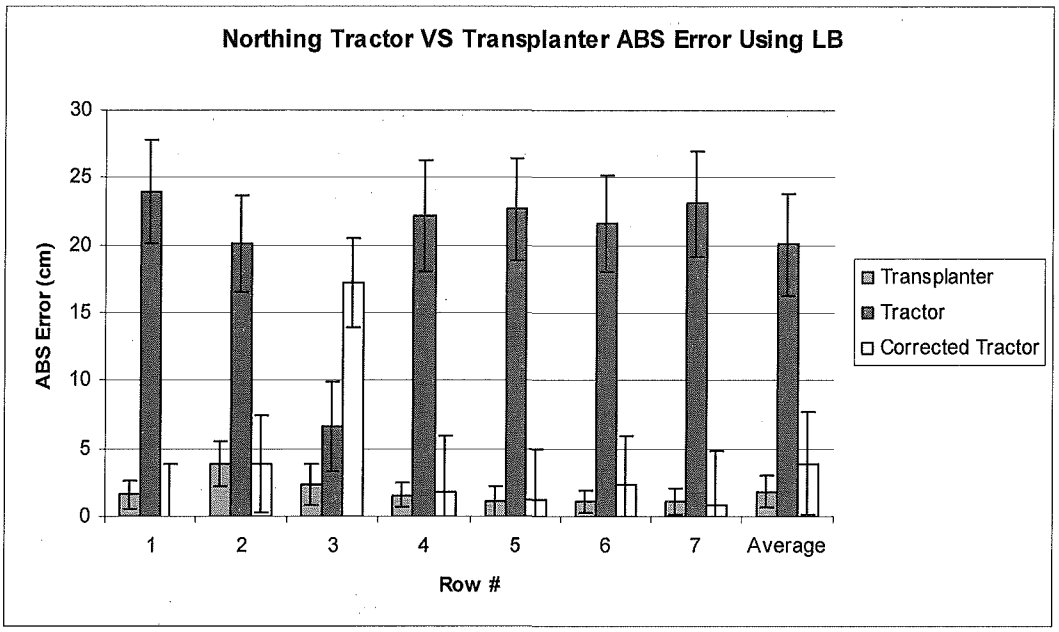


Figure 35. ABS mapping error comparison in the Northing direction of the Tractor versus Transplanter GPS using Light Beam Sensor. The error of the tractor GPS was corrected using the average first row error (white bar).

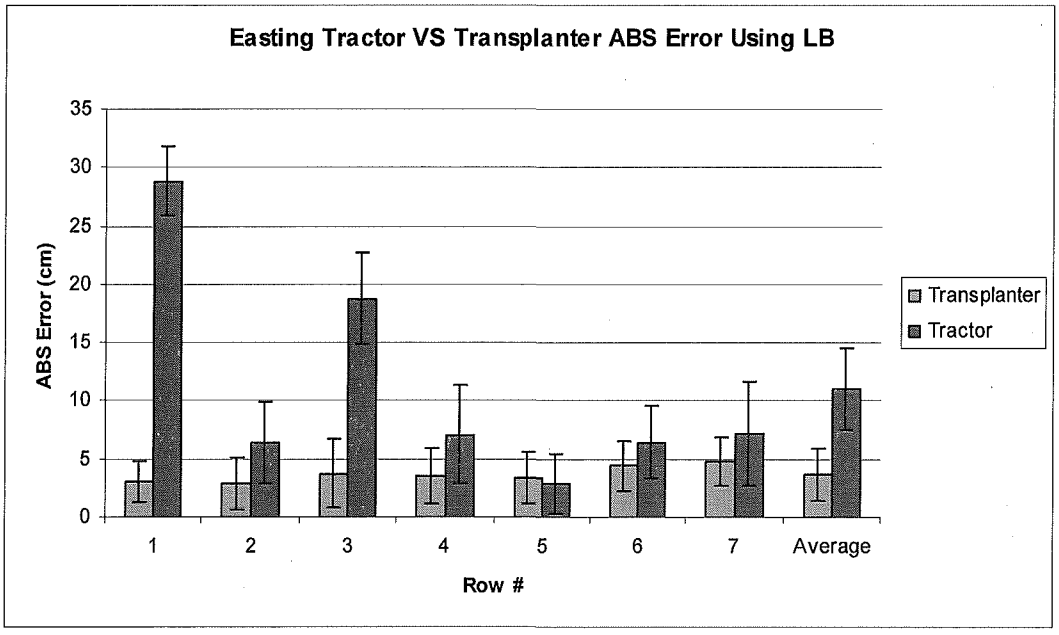


Figure 36. ABS mapping error comparison in the Easting direction of the Tractor versus Transplanter GPS using Light Beam Sensor.

***Other Sources of Error***

Table 6 shows the $R^2$ relationship between time and odometry value at each PPS. The high $R^2$ value indicates that time and odometry were highly linearly related and that overall the odometry sensor worked well. Furthermore, if the first few PPS points were ignored - the $R^2$ value of all 7 rows would be equal to 1. However, errors can occur if the tractor changes speed or stops during the mapping. In this scenario, odometry-based mapping would prove more beneficial.

The error for each plant within a row was analyzed. Figure 37 is a sample graph with a linear regression line relating the error to the plant number within a row. Table 7 is a summary of the slope, y-intercept and $R^2$ of the linear best fit line for rows 1 through 7. The slope of the best fit line is an indicator of a potential relationship between error and plant number. The slope of the Easting line ranged from -0.0002 to 0.0001 meters/plant# while the slope of the Northing line ranged from -0.00005 to 0.0005 meters/plant #. Moreover, the $R^2$ value of the regression line considers both slope and error to give a numerical representation of the relationship between error and plant number. The Northing and Easting lines had maximum $R^2$ values of 0.1041 and 0.1927, respectively. The low slope and $R^2$ values indicate a weak linear relationship between error and plant number in each row. Even rows were planted in one direction while odd rows were planted in the reverse travel direction. If the travel direction was taken into consideration, there is still no strong correlation between error and plant number in the row indicating GPS error and other factors such as soil moisture level, dirt clod size, sensor error and ground wheel slip did not play a role in the error from one end of the row to the other.

Table 6. $R^2$ relationship of Time VS Odometry based map determination.

| Row # | $R^2$ |
|---|---|
| 1 | 0.9994 |
| 2 | 0.9999 |
| 3 | 0.9999 |
| 4 | 1.0000 |
| 5 | 1.0000 |
| 6 | 0.9999 |
| 7 | 0.9999 |
| **Average** | **0.99986** |

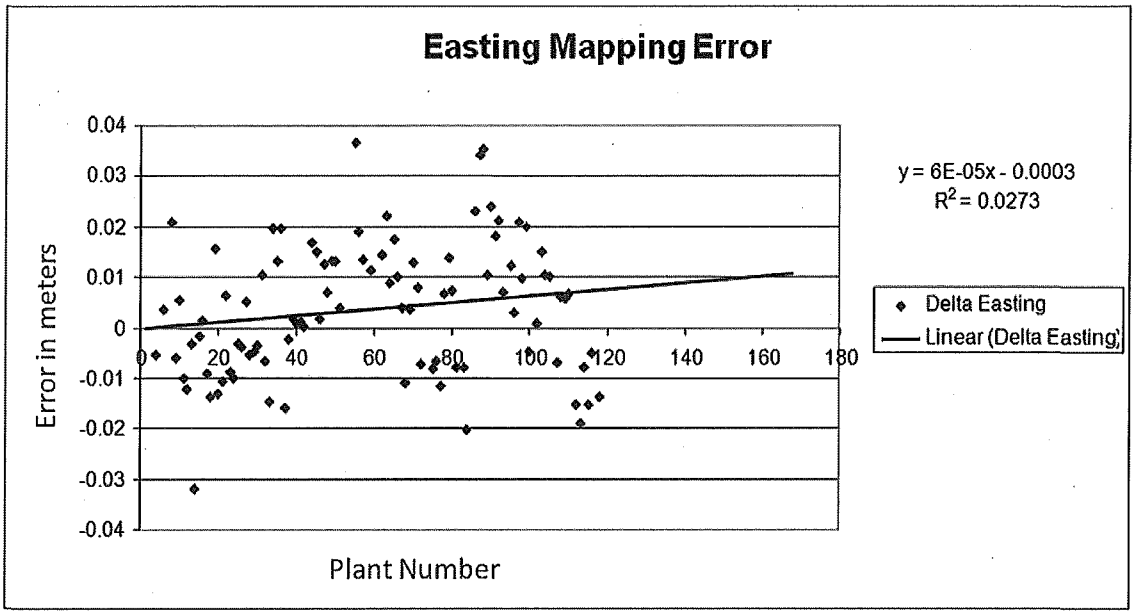


Figure 37. Sample linear regression line of error along a row (#1) using transplanter GPS.

Table 7. Slope, Y-Intercept and $R^2$ value of the regression line for error along each planted row using transplanter GPS. Units of Slope in meters/plant# and units of Y-Int in meters.

| Easting | | | | Northing | | | |
|---|---|---|---|---|---|---|---|
| **Row** | **Slope** | **Y-int** | **R^2** | **Row** | **Slope** | **Y-int** | **R^2** |
| **1** | 0.00006 | -0.00030 | 0.02730 | **1** | -0.00005 | -0.01280 | 0.00260 |
| **2** | 0.00002 | -0.00460 | 0.00200 | **2** | 0.00020 | -0.01860 | 0.05430 |
| **3** | -0.00004 | -0.01620 | 0.00350 | **3** | 0.00030 | -0.00220 | 0.09400 |
| **4** | 0.00010 | -0.02180 | 0.04750 | **4** | 0.00050 | -0.06260 | 0.19270 |
| **5** | 0.00002 | -0.00240 | 0.00200 | **5** | 0.00030 | -0.01810 | 0.16720 |
| **6** | -0.00006 | 0.00370 | 0.01290 | **6** | -0.00005 | -0.03150 | 0.00350 |
| **7** | -0.00020 | 0.01280 | 0.10410 | **7** | 0.00003 | -0.03450 | 0.00120 |
| **Avg** | -0.00001 | -0.00411 | 0.02847 | **Avg** | 0.00018 | -0.02576 | 0.07364 |
| **Stdev** | 0.00010 | 0.01172 | 0.03731 | **Stdev** | 0.00021 | 0.01958 | 0.08055 |

## Weeding

### *Plant Identification Rate*

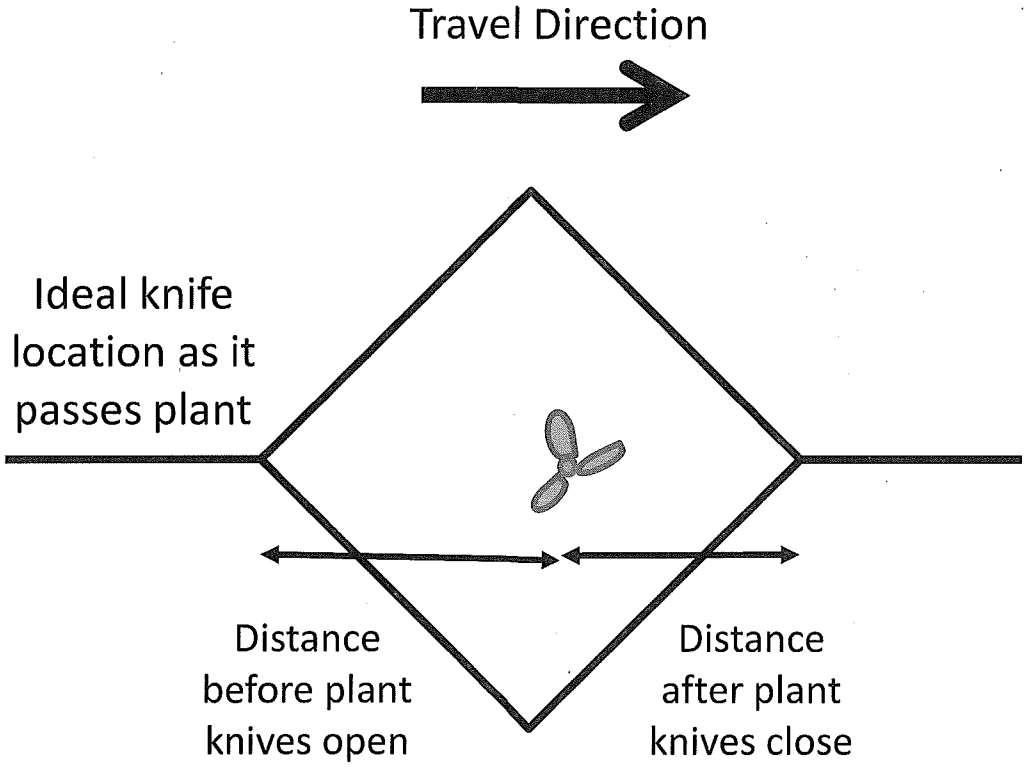


(a)

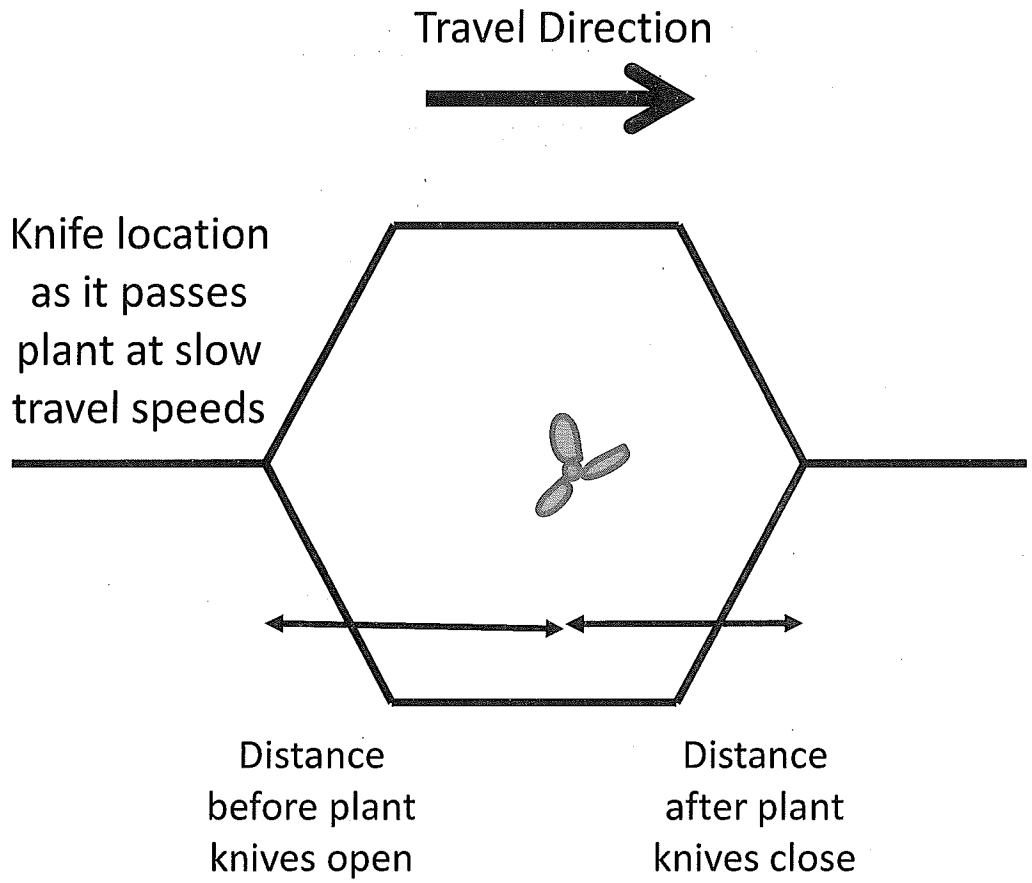


(b)

Figure 38. Depiction of how the distance the knives open before the plant and the distance the knives close behind the plant are measured in order to determine the accuracy of the weeding system. (a) Safe zone under ideal situations. (b) Safe zone at slow travel speeds.

Video analysis of the weeding study was conducted to assess weed knife performance. Figure 38 above shows the diamond representing the "safe zone." Accuracy of the weeding system is determined by measuring the distance from the plant to the two horizontal corners which represent the distance the knives open before the plant and the distance the knives close behind the plant. Although 667 plants were saved,

only 503 plants could be correctly identified in the weeding video as shown in Table 8 below. A plant was expected every 46 cm, and when it could not be located in the video - no data were obtained. There were a total of 164 plants that were not located in the video. Possible explanations include: transplant was not placed in the planting arm or short stems that were buried. Table 8 also shows that overall, plants were successfully identified 75.4 percent of the time. The detection rate steadily increased, peaking at 83.3 percent for row 5. However, the detection rate drastically decreased for the last 2 rows. Nonetheless, this statistic was anticipated - as the operator became more efficient at transplanting as the testing continued through the day. The plants with the skinniest, shortest and most tilted stems were sorted for the end hence the percentage of plants identified drastically decreased for the last two rows. By the time rows 6 and 7 were planted, the transplants had such short stems that they were planted below the soil line. This resulted in a 62.2% visualization rate for row 7.

Table 8. Planting and Weeding Efficiency.

| Row | Total Planting Locations | Plants Visualized | Missed Plants | Dead Plants | % Successful Plant Location | Plant Survival Rate (%) |
|---|---|---|---|---|---|---|
| **1** | 110 | 84 | 26 | 1 | 76.4 | 98.8 |
| **2** | 100 | 78 | 22 | 4 | 78.0 | 94.9 |
| **3** | 98 | 74 | 24 | 2 | 75.5 | 97.3 |
| **4** | 96 | 75 | 21 | 3 | 78.1 | 96.0 |
| **5** | 96 | 80 | 16 | 0 | 83.3 | 100.0 |
| **6** | 85 | 61 | 24 | 2 | 71.8 | 96.7 |
| **7** | 82 | 51 | 31 | 11 | 62.2 | 78.4 |
| **Total** | 667 | 503 | 164 | 23 | 75.4 | 95.4 |

*Accuracy of Knives Openings*

Of the 503 plants with which knife data were calculated, 23 were killed for an overall survival rate of 95.4%. A plant was categorized as "killed" if one of the following 3 scenarios occurred: (a) the knives opened and closed before it reached the plant; (b) the knives opened and closed after it passed the plant; (c) the knives did not open at all. Once again, row 5 displayed the highest survival rates (100%), while row 7 held the lowest (78.4%). Should row 7 data be omitted, the survival rate would improve to 97.3%. Row 7 had the highest kill rate because the distance in which the knives opened from the plant was by far the closest. That, compounded with a large standard deviation, resulted in the death of 11 plants.

Table 9 shows the average and standard deviation of the distance away from the plant the knives opened and closed. Row 2 total was 1.48 cm too small while Row 6 total was 1.08 cm too large. The discrepancy could be due to a software bug or analysis mistake that was made in these rows. The distance was also totaled to show the distance the knives stayed in the open position – an average of 12.33 cm. On average, the knives opened 4.5 cm before they reached the plant, and closed 7.82 cm after they passed the plant. This suggests that there was a systematic error in the calibration that determined the knives mounting location with respect to the GPS projection that was shifted by 1.66 cm toward the front of the instrument. In other words, the knives should have opened earlier at a time corresponding to a distance of 1.66 cm. If the safe zone was expanded by 0.97 cm on either side for example, the number of dead plants would have been reduced from 22 to 17.

***Sources of Error***

Theoretically, the distance the knives stayed in open position should be consistent for each plant. Any errors may be caused by a combination of wheel slip, the update of the wheel encoder calibration value from refreshed GPS error data, software bugs or operator error to turn on dynamic wheel calibration.

Table 9 also suggests the delay in opening increased considerably throughout the trial. One factor could be a failure to correctly implement the dynamic wheel encoder calibration value or counts to meters. A second factor that could explain this phenomenon is that the 7 rows were all watered with one row of rotating sprinklers during bed preparation to break up the dirt clods. As a result, each had different water saturation levels. As the sled traveled along the row, the different soil moisture levels would result in different heights in which the knives dug into the dirt - and thus the average size of the dirt clods in the bed. Perchance knives were buried deeper in the ground, or if the dirt clods were larger - there would be more resistance to slow the opening of the knives. Subsequent studies however do not indicate this is the source of error.

Table 9. Average and Standard Deviation of knife opening distances in cm.

| | Average (cm) | | | Stdev (cm) | | |
|---|---|---|---|---|---|---|
| **Row** | **Open** | **Close** | **Total** | **Open** | **Close** | **Total** |
| **1** | 7.02 | 5.01 | 12.03 | 1.91 | 2.02 | 1.21 |
| **2** | 5.07 | 5.79 | 10.85 | 3.14 | 2.68 | 1.84 |
| **3** | 4.53 | 8.11 | 12.64 | 2.25 | 1.99 | 1.04 |
| **4** | 3.82 | 8.91 | 12.73 | 2.76 | 2.46 | 1.25 |
| **5** | 3.73 | 9.07 | 12.80 | 1.94 | 1.72 | 0.96 |
| **6** | 3.81 | 9.60 | 13.41 | 1.90 | 1.94 | 1.08 |
| **7** | 2.48 | 9.48 | 11.96 | 2.68 | 3.03 | 1.96 |
| **Average** | 4.50 | 7.82 | 12.33 | 2.73 | 2.85 | 1.55 |

Although an RTK quality signal was maintained throughout the test, the correction value could have drifted as the testing progressed from row 1 to row 7. The standard deviation of the distance between the plant and knives upon opening and closing were 2.73 cm and 2.85 cm respectively, similar to the error found during mapping. This suggests that the difference in error between the rows was largely due to field conditions, rather than GPS error. Figure 39 is a graphical representation of these data. Figure 40 shows the standard deviation of the open and close value for each row. In this case, there does not seem to be a row-to-row trend, suggesting the variation was likely caused by disparities in GPS accuracy.

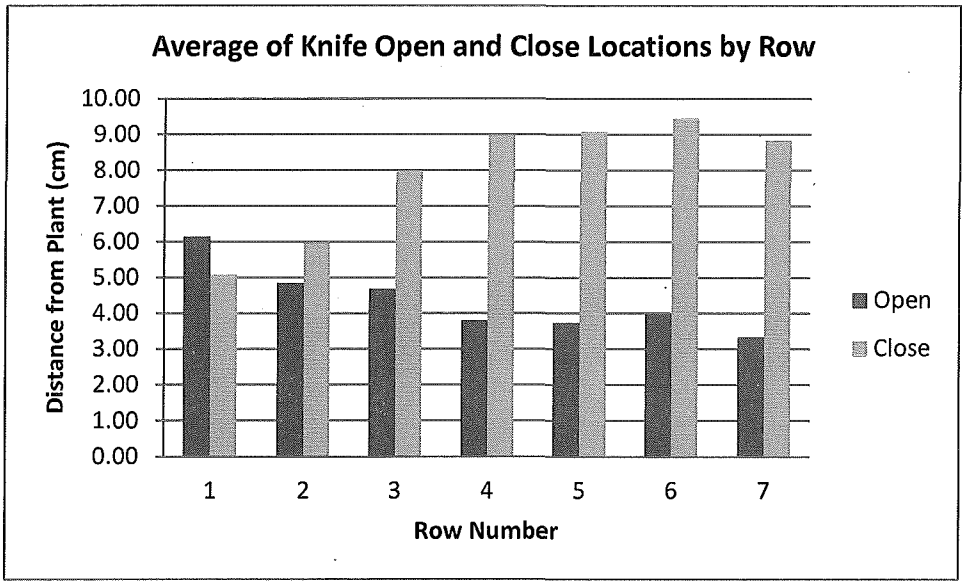


Figure 39. Average opening and closing locations of the weed knives for each row. As the row number increased, the location of the diamond moved forward.

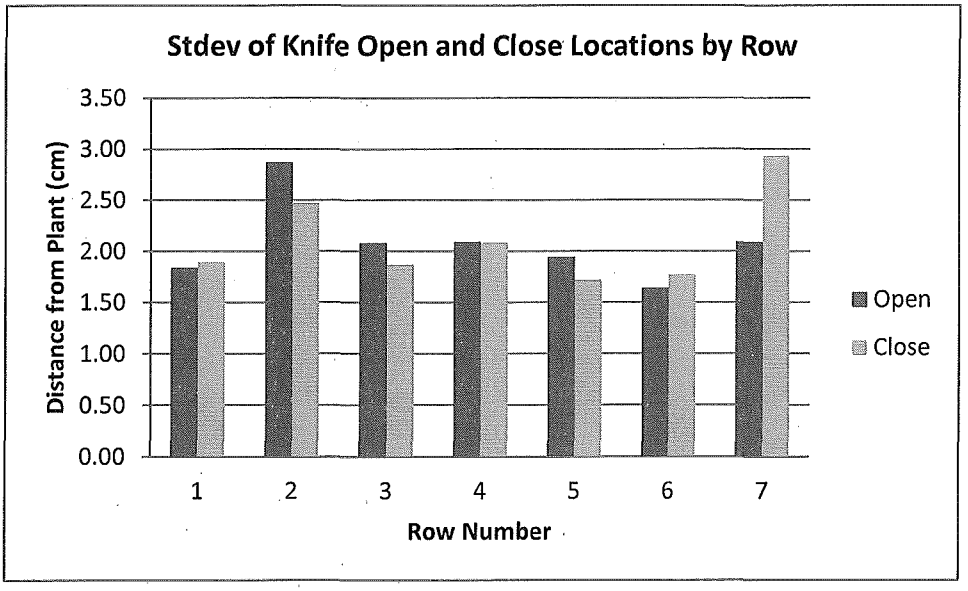


Figure 40. Average standard deviations of the knives open and close locations by row. The bar describes the variability in the distance away from the plant that the knives were in the open position. There is no discernible trend in standard deviation as the tractor progressed from row to row.

The knives were expected to be open for a distance of 12.8 cm, though the test results showed that they stayed open for an average of 12.33 cm. One contributing factor to this error is the accuracy of the calibration relating the number of pixels in the width of an inch. Differences in soil moisture and the digging of the transplanter sleds into the row can change the height of the camera in relation to the bed.

In figures 41-47 below, the vertical lines depict the range the knives stayed open for each plant in the row. The solid line represents the distance between the centers of the safe zone to the plants while the dotted line represents the best linear fit line for the error. The low $R^2$ values in rows 1 to 6 indicates there was little linear correlation between the accuracy of the knives' open and close locations and plant number across the whole row. Row 7 shows a slight slope potentially attributed to a change in soil moisture level.

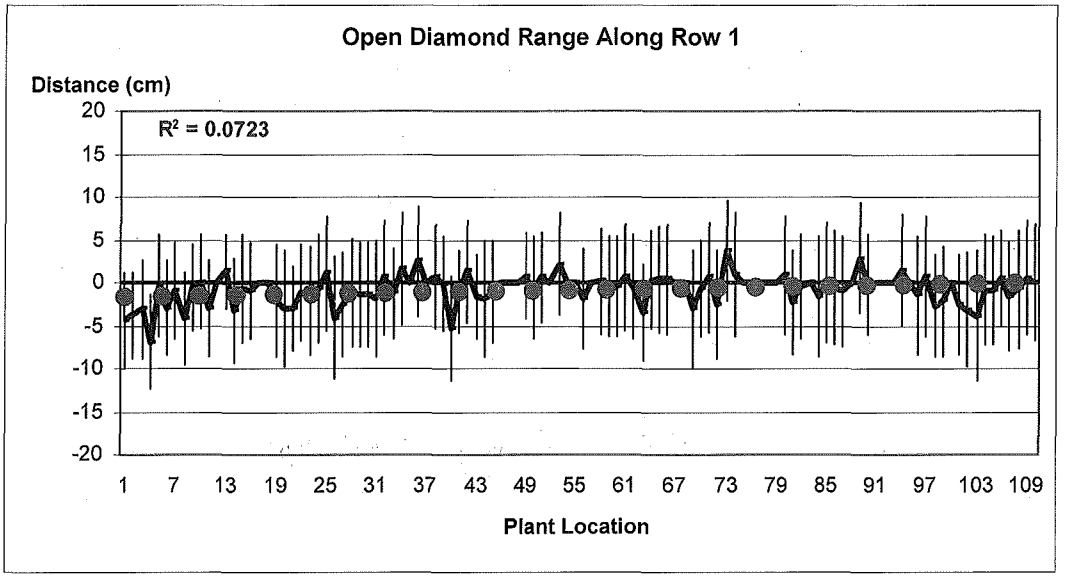


Figure 41. Open diamond range along row 1. The solid line represents the distance between the centers of the safe zone to the plants while the dotted line represents the best linear fit line for the error.

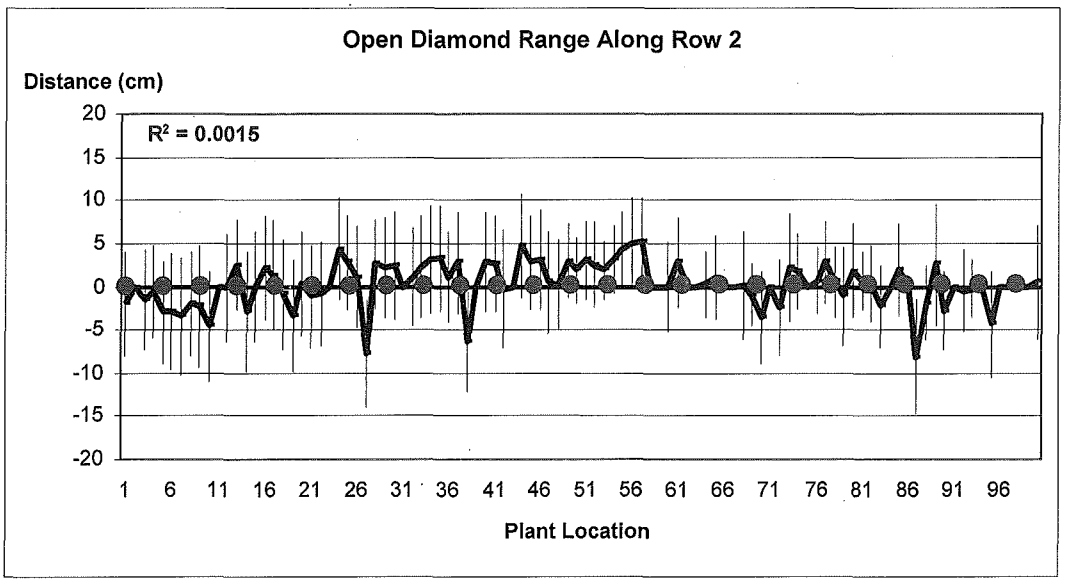


Figure 42. Open diamond range along row 2. The solid line represents the distance between the centers of the safe zone to the plants while the dotted line represents the best linear fit line for the error.

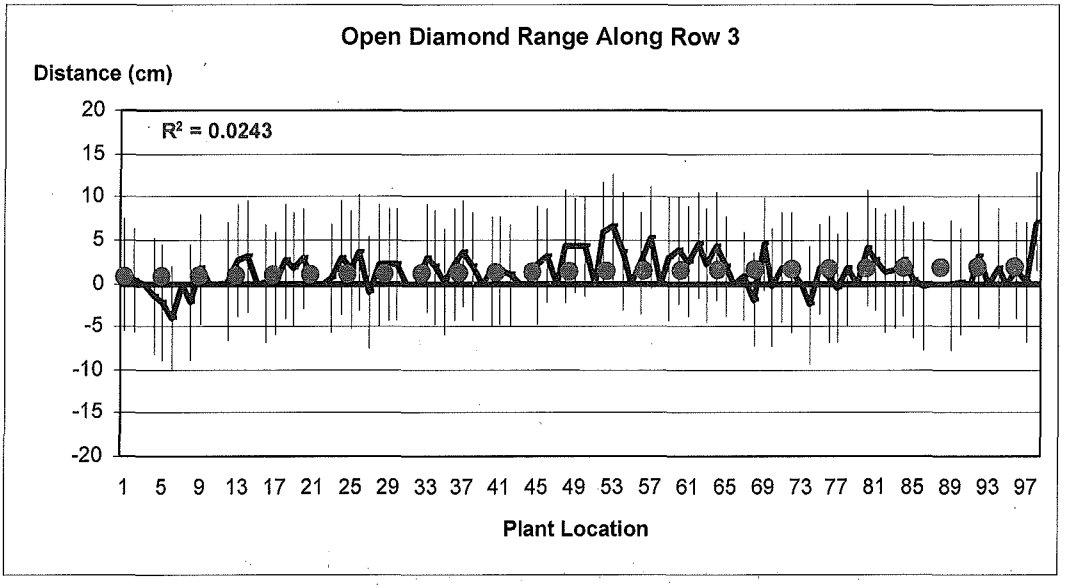


Figure 43. Open diamond range along row 3. The solid line represents the distance between the centers of the safe zone to the plants while the dotted line represents the best linear fit line for the error.

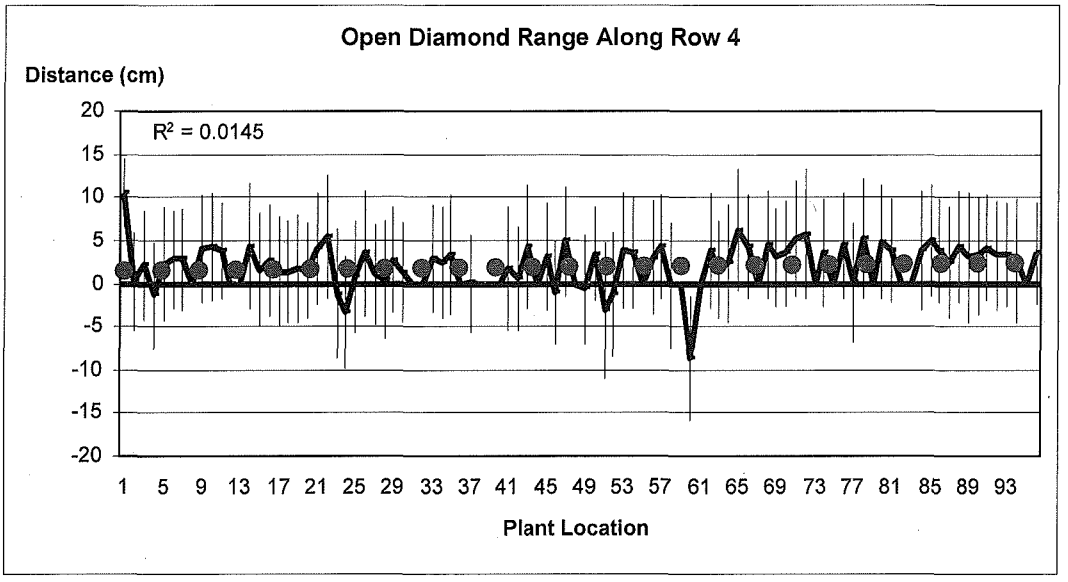


Figure 44. Open diamond range along row 4. The solid line represents the distance between the centers of the safe zone to the plants while the dotted line represents the best linear fit line for the error.

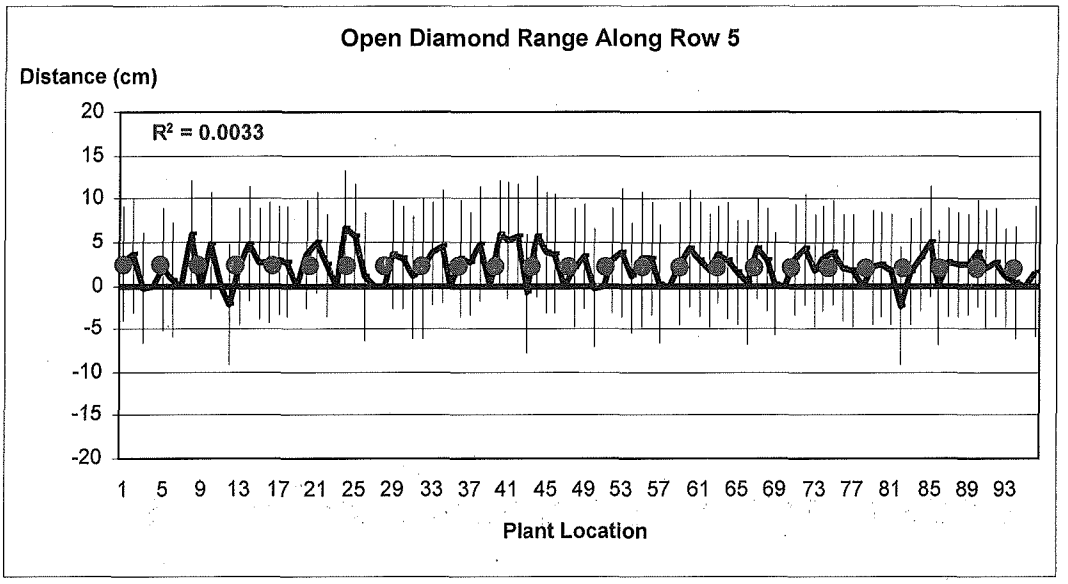


Figure 45. Open diamond range along row 5. The solid line represents the distance between the centers of the safe zone to the plants while the dotted line represents the best linear fit line for the error.

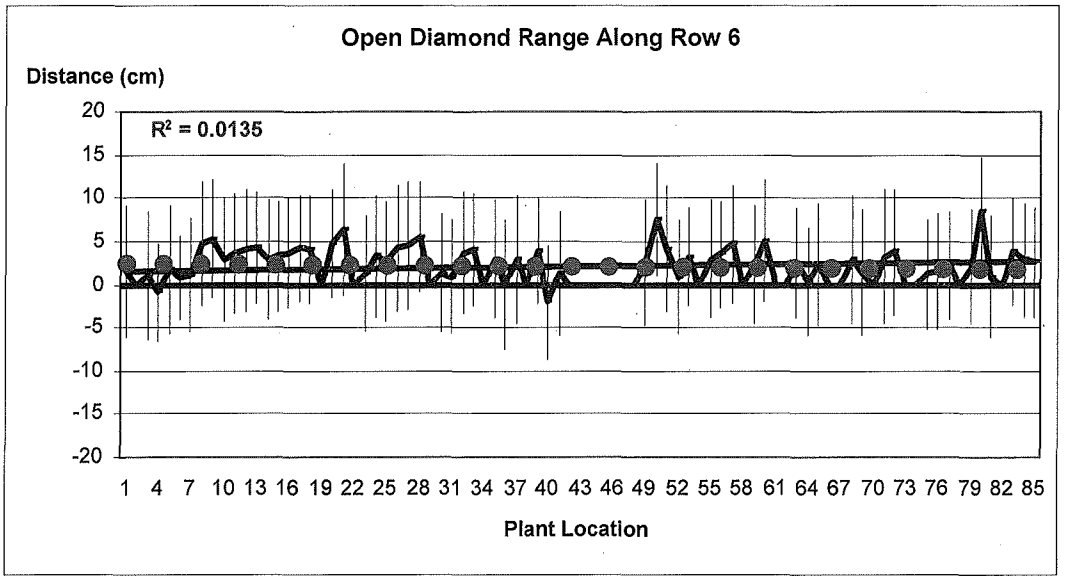


Figure 46. Open diamond range along row 6. The solid line represents the distance between the centers of the safe zone to the plants while the dotted line represents the best linear fit line for the error.

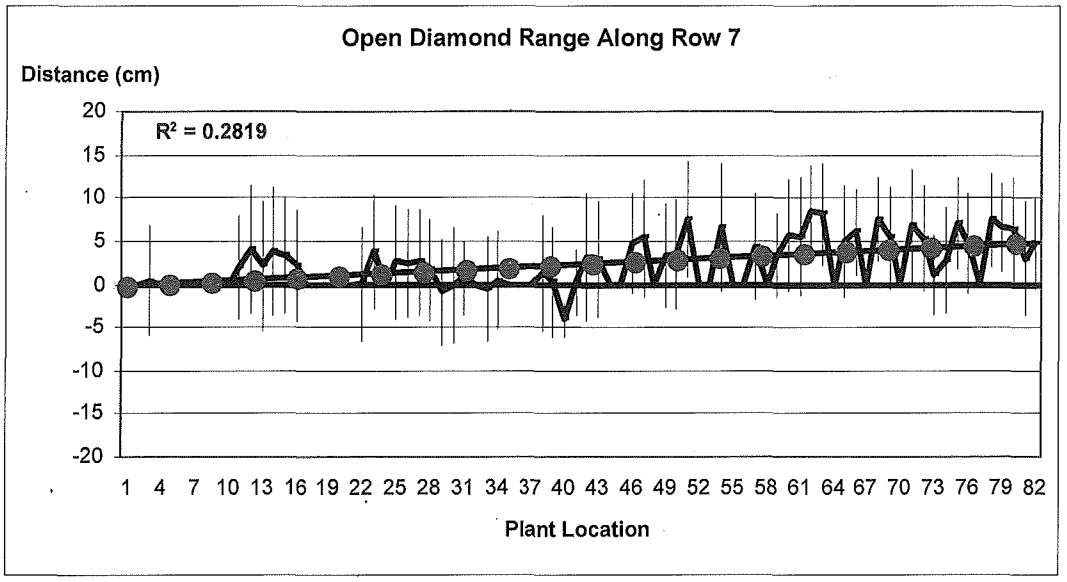


Figure 47. Open diamond range along row 7. The solid line represents the distance between the centers of the safe zone to the plants while the dotted line represents the best linear fit line for the error.

### *Size of Safe Zone Versus Plant Survival Rate*

There is a tradeoff between minimizing the size of the safe zone around the crop plant (thereby maximizing weed kill) and maximizing the plant survival rate. Many plants could have been spared if the knives were kept open over a wider distance. Table 10 and figure 48 show the correlation between the width of the safe zone and the overall plant survival rate. An increase in knife open width from 12.33 to 16.2 cm would have resulted in improved survival rates from 95.4% to 99%, however, widening the diamond would also mean more weeds would have remained in the close-to-crop area. The histogram shown in Figure 48 does not appear to be Normally distributed as expected but is skewed to the right. It was determined that the flat shape to the distribution for diamond widths below 8.6 cm was due to the use of the Euclidian distance as the basis for determining the real-time distance between the weed knife and the plant stem and a

problem with the tilt sensor, which together caused the knife controller to overestimate the distance between the knife and the plant resulting in a high proportion of small safe zone widths.

Table 10. Histogram of the size of the safe zone width (Diamond width).

| *Size of safe zone width (cm)* | *Frequency* | *Survival %** |
|---|---|---|
| 0.0 | 1 | 0.20% |
| 1.0 | 57 | 11.53% |
| 1.9 | 44 | 20.28% |
| 2.9 | 50 | 30.22% |
| 3.8 | 43 | 38.77% |
| 4.8 | 46 | 47.91% |
| 5.7 | 49 | 57.65% |
| 6.7 | 61 | 69.78% |
| 7.6 | 40 | 77.73% |
| 8.6 | 30 | 83.70% |
| 9.5 | 25 | 88.67% |
| 10.5 | 17 | 92.05% |
| 11.5 | 12 | 94.43% |
| 12.4 | 6 | 95.63% |
| 13.4 | 7 | 97.02% |
| 14.3 | 4 | 97.81% |
| 15.3 | 4 | 98.61% |
| 16.2 | 2 | 99.01% |
| 17.2 | 3 | 99.60% |
| 18.1 | 1 | 99.80% |
| 19.1 | 0 | 99.80% |
| 20.0 | 0 | 99.80% |
| More | 1 | 100.00% |

*In addition this table also shows a relationship between the width of the diamond and the overall plant survival rate.

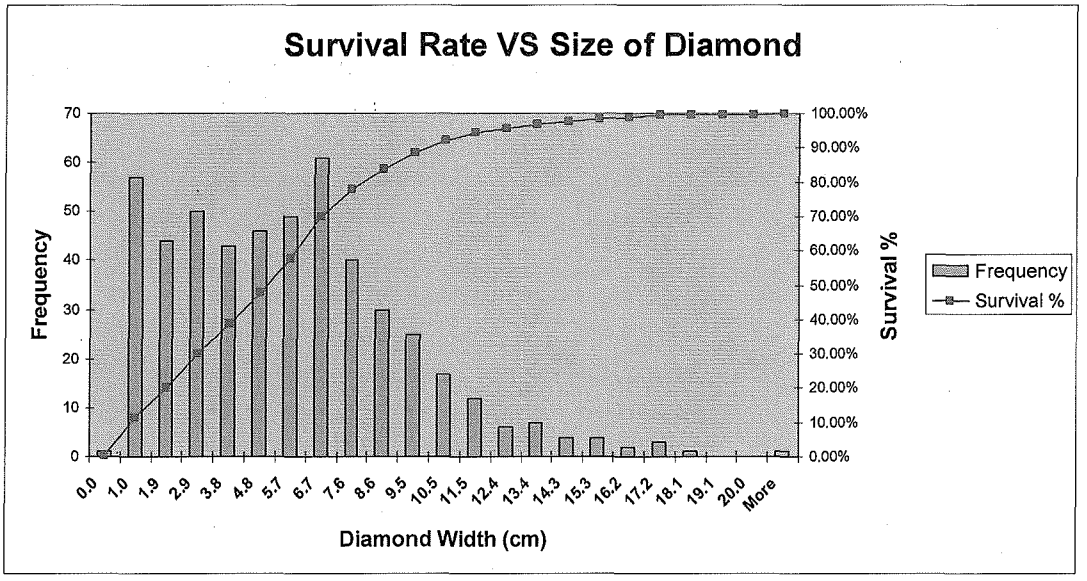


Figure 48. Histogram of the size of the safe zone width (Diamond width). In addition, this graph also shows a relationship between the width of the diamond and the overall plant survival rate.

# Conclusions

## Study Results

As a result of this study, the following conclusions were reached:

1. A vegetable crop transplanter can be successfully modified to allow automatic data logging of RTK Fixed quality GPS data and transplant odometry.
2. Using an off-line interpolation method based upon linear regression, a plant map can be automatically created with a greater degree of centimeter-level accuracy as compared to plant positions determined manually by an RTK GPS survey.
3. A plant map generated by means of plant detection using a light beam sensor towards the rear of the implement is not as accurate as a plant map generated using an absolute shaft encoder mounted on the planting wheel.
4. The size of dirt clods resulting from low soil moisture results in higher errors in weeding.
5. Using transplants with thicker and longer stems results in significantly improved performance.
6. With a kill rate averaging 95.4%, automated weeding using RTK GPS can be a robust solution that does not have the drawbacks of machine visions systems.

## Suggestions for Future work

**Based on observations during this study following suggestions are offered for future explorations:**

1. Instead of using a counter algorithm to detect the number of rising edges of the light beam sensor, future studies could include an algorithm that examines the time in which the light beam sensor was blocked. In this manner, any time the

light beam sensor is blocked for a period longer or shorter than the width of a typical main stem - that value can be labeled as a false reading.

2. A better filtering algorithm for the tilt sensor so to remove any high frequency noise could be developed and applied.
3. Better filtering of the micrometer sensor could be conducted.
4. A mechanism could be added to the ground wheel assembly to control the amount of pressure on the ground wheel.
5. More care in test field preparations can be taken in order to reduce the number of dirt clods, and ensure soil moisture is controlled and taken into consideration.
6. The knife opening and closing control algorithm should base actuation events upon the distance between the plant and the knife in the direction of travel rather than the Euclidian distance. This will potentially eliminate errors in maintaining the desired safe zone size when the tractor guidance fails to keep the tractor centered above the seedline.

## References

Abidine, A.Z., Heidman, B.C., Upadhyaya, S.K., Hills, D.J., 2004. Autoguidance system operated at high speed causes almost no tomato damage. Calif. Agric. 58 (1), 44–47.

Andersen, H.J., Ring, L., Kirk, K., 2005. Geometric plant properties by relaxed stereo vision using simulated annealing. Comput. Electron. Agric. 49, 219-242.

Ascard, J., 1998. Comparison of flaming and infrared radiation techniques for thermal weed control. Weed Res. 38, 69–76.

A˚ strand, B., 2005. Vision based perception or mechatronic weed control. Doctor of Philosophy Thesis, Chalmers and Halmstad Universities, Sweden.

A˚ strand, B., Baerveldt, A.-J., 2002. An agricultural mobile robot with vision-based perception for mechanical weed control. Auton. Rob. 13, 21–35.

Bainer, Roy. The Engineering of Abundance an Oral History Memoir of Roy Bainer. Regents of the University of California. 1975, pp. 273.

Bak, T., Jakobsen, H., 2004. Agricultural robotic platform with four wheel steering for weed detection. Biosyst. Eng. 87 (2), 125–136.

Backer, T., (2009), An Autonomous Robot for Weed Control: Design, Navigation and Control, PhD Dissertation, Wageningen University.

Bakker, T., Asselt K.V., Bontsema, J., Müller, J., Straten, G.V., Autonomous navigation using a robot platform in a sugar beet field, Biosystems Engineering, Volume 109, Issue 4, August 2011, Pages 357-368.

Blasco, J., Aleixos, N., Roger, J.M., Rabatel, G., Molt´ o, E., 2002. Robotic weed control using machine vision. Biosyst. Eng. 83 (2), 149–157.

Bochtis, D.D., Sorensen, C.G., Jorgensen, R.N., Norremark, M., Hameed, I.A., Swain, K.C., Robotic Weed Monitoring. Acta Agriculturae Scandinavica Section B - Soil and Plant Science, 2011; 61: 202-208.

Bowditch, N., "The American Practical Navigator," Bicentennial Edition, *NIMA*, Pub. No. 9, 2002. CD-ROM.

CDPR. (2007). Analyses of Pesticide Use Trends. Retrieved February 25, 2008, from California Department of Pesticide Regulation (CDPR): http://www.cdpr.ca.gov/docs/pur/pur06rep/trends06.pdf

Chandler, J.M., Cooke, F.T., 1992. Economics of cotton losses caused by weeds. In: McWhorter, C.G., Abernathy, J.R. (Eds.), Weeds of Cotton: Characterization and Control. The Cotton Foundation, Memphis, TN, pp. 85–116.

Chi, Y.T., Chien, C.F., Lin, T.T., 2002. Leaf shape modeling and analysis using geometric descriptors derived from Bezier curves. Trans. ASAE 46 (1), 175–185.

Christensen, S., Sogaard, H. T., Kudsk, P., Norremark, M., Lund, I., Nadimi, E. S. and Jorgensen, R. (2009), Site-specific weed control technologies. Weed Research, 49: 233–241.

Comba, L., Gay, P., Piccarolo, P., Ricauda Aimonino, D. Robotics and automation for crop management: trends and perspective, International Conference on "Work Safety and Risk Prevention in Agro-food and Forest Systems", Ragusa, Italy, 2010.

Concurrent Solutions, 2004. An Ultralight Autonomous Robot for Weed Control. Final Report, Phase I Proposal Number 00128, USDA 2003 SBIR Program, USDA CSREES, Washington, D.C.

Daar, S., 1994. New technology harnesses hot water to kill weeds. IPM Pract. 16, 1–5.

Daniell, J.W., Chapell, W.E., Couch, H.B., 1969. Effect of sublethal and lethal temperature on plant cells. Plant Physiol. 44, 1684–1689.

Diprose, M.F., Benson, F.A., 1984. Electrical methods of killing plants. J. Agric. Eng. Res. 30 (3), 197–209.

Downey, D., Giles, D.K., Slaughter, D.C., 2004a. Pulsed jet micro-spray applications for high spatial resolution of deposition on biological targets. Atomizat. Sprays 14, 93–109.

Downey, D., Giles, D.K., Slaughter, D.C., 2004b. Weeds accurately mapped using DGPS and ground-based vision identification. Calif. Agric. 58, 218–221.

Dreezens E., Martijn C., TenbultP., Kok G., Vries N. 2005.Food and values: an examination of values underlying attitudes toward genetically modified- and organically grown food products. Appetite 44:115–22.

Ehsani, M.R., Upadhyaya, S.K., Mattson, M.L., 2004. Seed location mapping using RTK GPS. Trans. ASAE 47 (3), 909–914.

El-Rabbany, A., *The Effect of Physical Correlations on the Ambiguity Resolution and Accuracy Estimation in GPS Differential Positioning*, Technical Report No. 170, Department of Geodesy and Geomatics Engineering, Federicton, New Brunswick, Canada: University of New Brunswick, 1994.

El-Rabbany, Ahmed, *Introduction to GPS the Global Positioning System*, 2nd edition, MA: Artech House, 2006.

Fathallah, F.A., Musculoskeletal disorders in labor-intensive agriculture, Applied Ergonomics, Volume 41, Issue 6, October 2010, Pages 738-743.

Fennimore, S.A., Tourte, L., Rachuy, J.S., Smith, R.F., George, C., 2010. Evaluation and economics of a machine-vision guided cultivation program in broccoli and lettuce. Weed Technol. 24, 33–38.

Fraden, Jacob, *Handbook of Modern Sensors*, 4th edition, NY: Springer, 2010.

Franz, E., Gebhardt, M.R., Unklesbay, K.B., 1991a. Shape description of completely visible and partially occluded leaves for identifying plants in digital images. Trans. ASAE 34 (2), 673–681.

Franz, E., Gebhardt, M.R., Unklesbay, K.B., 1991b. The use of local spectral properties of leaves as an aid for identifying weed seedlings in digital images. Trans. ASAE 34 (2), 682–687.

FRP, U.S. Federal Radio navigation Plan, 2001.

Garrett, R.E., 1966a. Development of a synchronous thinner. J. Am. Soc. Sugar Beet Technol. 14 (5), 206–213.

Garrett, R.E., 1966b. Device designed for synchronous thinning of plants. Agric. Eng. 47 (12), 652–653.

Georgiadou, Y., and K. D. Doucet, "The Issue of Selective Availability," *GPS World*, Vol. 1, No. 5, September/October 1990, pp. 53-56.

Giles, D.K., Downey, D., Slaughter, D.C., Brevis-Acuna, J.C., Lanini, W.T., 2004. Herbicide micro-dosing for weed control in field grown processing tomatoes. Appl. Eng. Agric. 20 (6), 735–743.

Giles, D.K., Lanini, W.T., Slaughter, D.C., 2005. Precision weed control for organic and conventional specialty crops. Buy California Crop lock Grant Program Final Report. California Department of Food and Agriculture, Sacramento, CA, pp. 9.

Gobor Z (2007) Development of a novel mechatronic system for mechanical weed control of the intra-row area in row crops based on detection of single palnts and adequate controlling of the hoeing tool in real-time. PhD thesis University of Bonn, Bonn

GopalaPillai, S., Tian, L., Zhang, J., 1990. Evaluation of a flow control system for site-specific herbicide applications. Trans. ASAE 42 (4), 863-870.

Griepentrog, H.W., Nørremark, M., Nielsen, H., Blackmore, B.S., 2005. Seed mapping of sugar beet. Precis. Agric. 6, 157–165.

Griepentrog HW, Noerremark M, Nielsen J (2006) Autonomous intra-row rotor weeding based on GPS. In: CIGR World Congress Agricultural Engineering for a Better World. Bonn, 3–7th September, pp 1–7

Griepentrog H W, Gulhom-Hansen T, Nielsen J (2007) First field results from intra-row rotor weeding. Proceedings of 7th european weed research society workshop on physical and cultural weed control. Salem, Germany

Guo, H. R., Tanaka, S., Halperin, W. E., & Cameron, L. L. (1999). Back pain prevalence in US industry and estimates of lost workdays. *Am J Public Health, 89*(7), 1029-1035.

Hodgson, J.M., 1968. The nature, ecology, and control of Canada thistle. In: Tech. Bull. 1386. U.S. Department of Agriculture, Agricultural Research Service, Washington, D.C.

Hoffmann-Wellenhof, B., H. Lichtenegger, and J. Collins, *Global Positioning System: Theory and Practice*, 5th revised edition, New York: Springer-Verlag, 2001.

Hough, P.V.C., 1962. Method and means for recognizing complex patterns. US Patent 3,069,654.

ILO, 2003. Facts on Agriculture. Retrieved August 25, 2007, from: http://www.ilo.org.

Inman, J.W., 1968. Precision planting—a reality for vegetables. Agric. Eng. 49 (6), 344–345.

Kaplan, E. D. and C. J. Hegarty (Eds.), *Understanding GPS: Principles and Applications*, 2nd Edition, Norwood, MA: Artech House, 2006.

Kise, M., Noguchi, N., Ishii, K., Terao, H., 2002. The development of the autonomous tractor with steering controller applied by optimal control. In: Zhang, Q. (Ed.), Automation Technology for Off-Road Equipment, Proceedings of the July 26–27, 2002 Conference (Chicago, Illinois, USA) ASAE Publication Number 701P0502, pp. 367–373.

Kishore C. Swain, Michael Nørremark, Rasmus N. Jørgensen, Henrik S. Midtiby, Ole Green, Weed identification using an automated active shape matching (AASM) technique, Biosystems Engineering, Volume 110, Issue 4, December 2011, Pages 450-457.

Kleusberg, A., and R. B. Langley, "The Limitations of GPS," *GPS World*, Vol. 1, No. 2, March/April 1990, pp. 50-52.

Kouba, J., "A Guide to Using International GPS Service (IGS)," 2003, http://igscb.jpl.nasa.gov/igscb/resource/pubs/Guideto UsingIGSProducts.pdf.

Lagu¨ e, C., Gill, J., P´eloquin, G., 2001. Thermal control in plant protection. In: Fleurat-Lessard, F., Panneton, B., Vincent, C. (Eds.), Physical Control Methods in Plant Protection. Springer-Verlag, Berlin, Germany, pp. 35–46.

Lamm, R.D., Slaughter, D.C., Giles, D.K., 2002. Precision weed control system for cotton. Trans. ASAE 45 (1), 231–238.

Langley, R.B., "Mathematics of Attitude Determination with GPS," *GPS World*, Vol. 2, No. 7, July/August 1991a, pp. 45-50.

Langley, R. B., "Time, Clocks, and GPS," *GPS World*, Vol. 2, No. 10, November/December 1991b, pp.38-42.

Langley, R.B., "RTK GPS Observables," *GPS World*, Vol. 4, No. 4, April 1993, pp. 52-59.

Lanini, W.T., Le Strange, M., 1991. Low-input management of weeds in vegetable fields. Calif. Agric. 45 (1), 11–13.

Lee, W.S., 1998. Robotic weed control system for tomatoes. Ph.D. dissertation, University of California, Davis, p. 287.

Lee, W.S., Slaughter, D.C., Giles, D.K., 1999. Robotic weed control system for tomatoes. Precis. Agric. 1, 95–113.

Leer, S., Lowenberg-DeBoer, J., 2004. Purdue study drives home benefits of GPS auto guidance, http://news.uns.purdue.edu/UNS/html4ever/2004/040413.Lowenberg.gps.html.

Leick, A., *GPS Satellite Surveying*. 3rd Ed., New Jersey: John Wiley & Sons, 2004.

Levitt, J., 1980. Responses of plants to environmental stresses. Chilling, Freezing, and High Temperature Stresses, vol. I., 2nd ed. Academic Press, New York, USA.

Linyuan X., "Multipath in GPS Navigation and Positioning," GPS Solutions, Vol. 8, 2004, pp. 49-50. Kepner, R.A., Bainer, R., Barger, E.L., 1978. Selective Mechanical or chemical thinning. In: Principles of Farm Machinery. Section 11.22. AVI Publishing company, Inc., Westport, Connecticut, USA, pp. 237–257.

Loghavi, M., Behzadi Mackvandi, B., 2008. Development of a target oriented weed control system. Computers and Electronics in Agric. 63, 112-118.

Marchant, J.A., Brivot, R., 1995. Real-time tracking of plant rows using a Hough transform. Real-time Imaging 1, 363–371.

Marchant, J.A., Hague, T., Tillett, N.D., 1997. Row-following accuracy of an autonomous vision-guided agricultural vehicle. Comput. Electron. Agric. 16, 165–175.

Marks, R.S., Ward, J.R., 1993. Nutrients and pesticide threats to water quality. In: Robert, P.C., Rust, R.H., Larson, W.E., Madison (Eds.), Proceedings of the Soil Specific Crop Management Workshop. ASA-CSSA-SSSA, WI, pp. 293-299.

McCurdy, S.A., Samuels, S.J., Carroll, D.J., Beaumont, J.J., Morrin, L.A., 2003. Agricultural injury in California migrant Hispanic farm workers. Am. J. Ind. Med. 44 (3), 225e235.

McLean, K.A., 1969. Chemical thinning of sugar beet. J. Agric. Eng. Res. 14 (2), 147–153.

Melander B (2006) Current achievements and future directions of physical weed control in Europe. AFPP 3rd International conference on non-chemical crop protection methods, Lille, 13–15 March. Orgprints. http://orgprints.org/9998. Accessed on 27 February 2012. 49–58

Mobed, K., Gold, E. B., Schenker, M. B. (1992). Occupational Health Among Migrant And Seasonal Farm Workers. Western Journal of Medicine, 157(3): 367–373.

AFPP 3rd International conference on non-chemical crop protection methods, Lille, 13–15 March. Orgprints. http://orgprints.org/9998. Accessed on 04 January 2009. 49–58

Monaco, T.J., Grayson, A.S., Sanders, D.C., 1981. Influence of four weed species on the growth, yield, and quality of direct seeded tomatoes (*Lycopersicon esculentum*). Weed Sci. 29 (4), 394–397.

Nagasaka, Y., Umeda, N., Kanetai, Y., Taniwaki, K., Sasaki, Y., 2004. Autonomous guidance for rice transplanting using global positioning and gyroscopes. Comput. Electron. Agric. 43, 223–234.

NASS, N. A. S. S. (2008). 2007 Census of Agriculture. from United States Department of Agriculture: http://www.nass.usda.gov/Census_of_Agriculture/index.asp

NASS, N. A. S. S. (2011). 2010 Census of Agriculture. from United States Department of Agriculture: http://usda.mannlib.cornell.edu/MannUsda/viewDocumentInfo.do?documentID=1066

Nordmeyer, H., Hausler, A., Niemann, P., 1997. Patchy weed control as an approach in precision farming. In: Stafford, J.V. (Ed.), Precision Agricultural 97, vol. 1. Silsoe Research Institute, UK, pp. 307-314.

Norremark, M., Griepentrog, H.W., Nielson, J., Sogaard, H.T., Blackmore, B.S., 2003. A method for high accuracy geo-referencing of data from field operations. In: Stafford,

J.V., Werner, A. (Eds.), Proceedings of the 4th European Conference on Precision Agriculture. Berlin, Germany.

Norremark, M., Griepentrog, H.W., Nielson, J., Sogaard, H.T., 2008. The development and assessment of the accuracy of an autonomous GPS-based system for intra-row mechanical weed control in row crops. Biosystems Eng. 101, 396-410.

Norremark, M., Sogaard, H.T., Griepentrog, H.W., Nielson, H., 2007. Instrumentation and method for high accuracy geo-referencing of sugar beet plants. Comp. and Elect. In Agric. 56, 130-146.

Perez-Ruiz, M., Slaughter, D.C., Gliever, C., Upadhyaya, S.K., Tractor-based Real-time Kinematic-Global Positioning System (RTK-GPS) guidance system for geospatial mapping of row crop transplant, Biosystems Engineering, Volume 111, Issue 1, January 2012, Pages 64-7.

Roberts, H.A., Hewson, R.T., Ricketts, M.A., 1977. Weed competition in drilled summer lettuce. Hortic. Res. 17, 39–45.

Shaw, M., K. Sandhoo, and D. Turner, "Modernization of Global Positioning System," *GPS World*, Vol. 11, No. 9, September 2000, pp. 36-44.

Shrefler, J.W., Stall, W.M., Dusky, J.A., 1996. Spiny amaranth (*Amaranthus spinosus* L.) a serious competitor to crisphead lettuce (*Lactuca sativa* L.). Hortic. Sci. 31, 347–348.

Siderer Y., Maquet A., Anklam E. 2005. Need for research to support consumer confidence in the growing organic food market. Trends Food Sci Tech 16:332–43

Slaughter, D.C., Chen, P., Curley, R.G., 1999. Vision guided precision cultivation. Precis. Agric. 1 (2), 199–216.

Slaughter, D.C., Curley, R.G., Chen, P., Giles, D.K., 1996. Robotic cultivator. U.S. Patent 5,442,553. Washington D.C. U.S. Patent and Trademark Office.

Slaughter, D.C., Lanini, W.T., Giles, D.K., 2004. Discriminating weeds from processing tomato plants using visible and near-infrared spectroscopy. Trans. ASAE 47 (6), 1907–1911.

Slaughter, D.C., Giles, D.K., Fennimore, S.A., Smith, R.F., Multispectral Machine Vision Identification of Lettuce and Weed Seedlings for Automated Weed Control. Weed Technology. 2008. 20:378-384.

Søgaard, H.T., 2005. Weed classification by active shape models. Biosyst. Eng. 91 (3), 271–281.

Søgaard, H.T., Nørremark, M., 2004. Robotic localisation of sugar beets by use of RTK-GPS, computer vision and seed maps. In: Engineering the Future, AgEng2004 International Conference on Agricultural Engineering in Leuven, Belgium, 12–16 September.

Staab, E.S., Slaughter, D.C., Zhang, Y., Giles, D.K., 2009. Hyperspectral Imaging System for Precision Weed Control in Processing Tomato. ASABE Paper No. 096635, St. Joseph, MI.

Stoll, A., Kutzbach, H.D., 2000. Guidance of a forage harvester with GPS. Precis. Agric. 2, 281–291.

Sun, H., Slaughter, D. C., Perez-Ruiz, M., Gliever, C., Upadhyaya, S. K., & Smith, R. F. (2010). RTK GPS mapping of transplanted row crops, 2010. Computers and Electronics in Agriculture, 71, 32e37.

Tillett and Hague Technology LtD., Robocrop Vision Guidance, Tillet and Hague Technology Ltd., <http://www.thtechnology.co.uk/Robocrop.html> (accessed 23 February 2012).

Tillett, N.D., Hague, T., Grundy, A.C., Dedousis, A.P., 2008. Mechanical within-row weed control for transplanted crops using computer vision. Biosystems Eng. 99, 171-178.

Trimble, 2010, GPS Tutorial. Trimble Navigation, Sunnyvale, CA http://www.trimble.com/gps/index.shtml (accessed 15 November 2010)

Upadhyaya, S., 2003, Method and Apparatus for Ultra Precision GPS-Based Mapping of Seeds or Vegetation During Planting. US Patent 6,516,271

Upadhyaya, S., Ehsani, M., Mattson, M.L., 2003. Method and apparatus for ultra precise GPS-based mapping of seeds or vegetation during planting. US Patents 6,553,312, and 6,941,225. Washington D.C. U.S. Patent and Trademark Office.

USDA, 2007. Agricultural chemical usage 2006 vegetables summary. National Agricultural Statistics Service, United States Department of Agriculture, Washington, DC.
<http://usda.mannlib.cornell.edu/MannUsda/viewDocumentInfo.do?documentID=1561> (accessed 22 February 2012).

Van der Weide RY, Bleeker PO, Machten VTJ et al. (2008) Innovation in mechanical weed control in row crops. Weed Res 48:215–224

Vargas, R., Fischer, W.B., Kempen, H.M., Wright, S.D., 1996. Cotton weed management. In: Johnson, M.S., Kerby, T.A., Hake, K.D. (Eds.), Cotton Production. UC DANR Pub 3352, Oakland, CA, pp. 187–202.

Villarejo, D., 1998. Occupational injury rates among hired farm workers. J. Agric. Saf. Health (1), 39e46 (special issue).

Villarejo, D., Baron, S.L., 1999. The occupational health status of hired farm workers. Occup. Med. 14 (3), 613e635.

Whole Foods Market. 2005. 2005 Whole Foods Market organic trend tracker. Austin, Tex.: Whole Foods Market.

Winter CK, Davis SF. Organic foods. J Food Sci 2006;71:R117–24.

Woebbecke, D.M., Meyer, G.E., Von Bargen, K., Mortensen, D.A., 1995a. Color indices for weed identification under various soil, residue, and lighting conditions. Trans. ASAE 38 (1), 259–269.

Woebbecke, D.M., Meyer, G.E., Von Bargen, K., Mortensen, D.A., 1995b. Shape features for identifying young weeds using image analysis. Trans. ASAE 38 (1), 271–281.

Yonekawa, S., Sakai, N., Kitani, O., 1996. Identification of idealized leaf types using simple dimensionless shape features by image analysis. Trans. ASAE 39 (4), 1525–1533.

Young. S.L., Weed Control in Organic Cropping Systems, 2010. West Central Research and Extension Center North Platte, Paper 12.

Zhang, Y., Staab, E. S., Slaughter, D. C., Giles, D. K., & Downey, D. (2009). Precision automated weed control using hyperspectral vision identification and heated oil. Paper No. 1009313 The 2009 ASABE Annual International Meeting.

Zhang, Y., Slaughter, D.C., Hyperspectral species mapping for automatic weed control in tomato under thermal environmental stress, Computers and Electronics in Agriculture, Volume 77, Issue 1, June 2011, Pages 95-104.

Zhang, Y., Slaughter, D.C., Influence of solar irradiance on hyperspectral imaging-based plant recognition for autonomous weed control, Biosystems Engineering, Volume 110, Issue 3, November 2011, Pages 330-339.

Zwiggelaar, R., 1998. A review of spectral properties of plants and their potential use for crop/weed discrimination in row-crops. Crop Protect. 17 (3), 189–206.